2020

Substandard antimicrobial drugs: detection methods and their contributions to antibiotic resistance

BOSTON UNIVERSITY

SCHOOL OF MEDICINE

Dissertation

SUBSTANDARD ANTIMICROBIAL DRUGS: DETECTION METHODS AND THEIR CONTRIBUTIONS TO ANTIBIOTIC RESISTANCE

by

ZOHAR BAT-EL WEINSTEIN

B.S., Northeastern University, 2008

Submitted in partial fulfillment of the

requirements for the degree of

Doctor of Philosophy

2018

Approved by

First Reader

Muhammad H. Zaman, Ph.D.
Professor of Biomedical Engineering

Second Reader

Susan E. Leeman, Ph.D.
Professor of Pharmacology

ACKNOWLEDGMENTS

This work would not be possible without the enthusiastic support of my research advisor, Muhammad Zaman, who encouraged me to branch out into novel topics of research for the lab, and fostered a creative environment to advance in my independent studies. I also wish to thank my dissertation advisory committee members; Ben Wolozin, Chris Gill, Eric Rubin and Susan Leeman for lending their diverse expertise in pharmacology, global health and infectious diseases. I am also grateful to my rotation advisors, Jim Collins and Mo Khalil for their role in my training, and continued mentorship throughout my graduate studies.

Carol Walsh, John Schwartz, Steven Borkan and Vickery Trinkaus-Randall provided instrumental guidance in preparing research presentations and general guidance during my pursuit of an MD/PhD dual degree. The administrative support of Millie Agosto, Christina Cherel, Sara Johnson, Wanda Roberts and Nadiyah Shaheed has been a great help as well.

I would also like to thank my colleagues that I have collaborated with during my graduate studies; Darash Desai, Nga Ho, Szilvia Kiriakov, Atena Shemirani and Fabian Spill, and benefited from through lab meeting discussions; Andrew Acevedo, Alex Bloom, Katie Clifford, Jacopo Ferruzzi, Jessica Kim, Dan Reynolds, RJ Seager, Yasha Sharma, Meng Sun, and Diego Vargas.

Finally, I would like to thank my family for their encouragement throughout my ongoing endeavors in education. Research would not be as much fun without this amazing reservoir of support.

SUBSTANDARD ANTIMICROBIAL DRUGS: DETECTION METHODS AND THEIR CONTRIBUTIONS TO ANTIBIOTIC RESISTANCE

ZOHAR BAT-EL WEINSTEIN

Boston University School of Medicine, 2018

Ph.D. requirements completed in 2018

Dual M.D./Ph.D. degrees expected in 2020

Major Professor: Muhammad H. Zaman, Ph.D. Professor of Biomedical Engineering

ABSTRACT

Substandard and counterfeit medicines are major obstacles to the treatment of infectious diseases. Substandard medicines vary from standard drugs in terms of dose, bioavailability, or the presence of impurities. Current methods to identify substandard and counterfeit antimicrobial drugs are either resource intensive or have poor specificity. This dissertation examined two issues related to poor quality antimicrobial medicines: 1) Methods to detect and prevent the consumption of substandard drugs. 2) The relationship between substandard medicines and the evolution of rifampicin resistance. This dissertation advanced two technologies that may aid in the detection of substandard medicines: aptamers and biosensors. Oligonucleotide aptamers may be adapted for drug detection by coupling binding events to changes in fluorescence, luminescence or colorimetric signals. A computational model was developed to discover experimental factors that increase the probability of selecting a high affinity aptamer. Among them are: micromolar drug target concentration, high affinity substrate to partition aptamers, and high aptamer library affinity distribution. Random losses of aptamers due to experimental

noise greatly decreased the probability of selecting an aptamer. Experimental parameters to optimize the process of aptamer discovery for small molecules are discussed. Bacterial biosensors are an alternative strategy for the detection of active pharmaceutical ingredients. Here, luciferase-expressing *Escherichia coli* were used to create profiles of drug interactions for anti-mycobacterial drugs. Drug interactions were tested by the Loewe additivity model. A novel method to differentiate rifamycin drugs from the drug degradation product rifampicin quinone was developed by analyzing each drug's unique interactions.

While subinhibitory drug doses are known to select for antimicrobial resistance *in vitro*, the role of substandard anti-mycobacterial medicines in the development of rifampicin resistance remains poorly understood. The role of the drug degradation product rifampicin quinone on rifamycin resistance was assessed through *in vitro* studies of bacteria. Wild type *Escherichia coli* and *Mycobacterium smegmatis* cultured in the presence of rifampicin quinone acquired high levels of resistance to rifamycin drugs. Resistance was associated with genetic mutations in the rifampicin resistance cluster of the rpoB gene. The studies presented here demonstrate that substandard medicines can contribute towards rifamycin resistance, and offer methodologies to identify substandard medicines.

TABLE OF CONTENTS

LIST OF TABLES

LIST OF FIGURES

LIST OF ABBREVIATIONS

API……. ..... Active pharmaceutical ingredient

CHL.....Chloramphenicol

DAP .....Dapsone

DNA ..... Deoxyribonucleic acid

ERG.....Ergosterol

ERY..... Erythromycin

GFP .....Green fluorescent protein

HPLC .....High performance liquid chromatography

IC.....Inhibitory concentration

K_D..... Dissociation constant

LMIC.....Low and middle income countries

M .....Molar

MIC ..... Minimal inhibitory concentration

mRNA .....Messenger ribonucleic acid

MUP .....Mupirocin

NAL .....Nalidixic acid

NIT ..... Nitrofurantoin

NMR ..... Nuclear magnetic resonance

OXA .....Oxacillin

PCR ..... Polymerase chain reaction

RFB ..... Rifabutin

RFP ..... Rifapentine

RFQ ..... Rifampicin quinone

RFQ-res ..... Rifampicin quinone resistant

RIF ..... Rifampicin

RIF-res ..... Rifampicin resistant

RNA ..... Ribonucleic acid

SELEX ..... Systematic evolution of ligands by exponential enrichment

STR ..... Streptomycin

TB ..... Tuberculosis

TET ..... Tetracycline

CHAPTER 1: Introduction

Prevalence of substandard and counterfeit anti-mycobacterial drugs

Substandard and counterfeit medicines are major obstacles to the treatment of infectious diseases in the developing world. Counterfeit medicines are illicit copies of genuine medicines that are unlikely to contain active pharmaceutical ingredients (1). Besides lacking their stated active ingredients, counterfeit medicines may contain other drugs, or toxic impurities (2). Substandard medicines vary from standard drugs in terms of dose, bioavailability, or the presence of synthetic byproducts, degradation products or impurities (3). Substandard medicines may arise due to poor formulations or due to post manufacturing issues such as drug expiry and improper storage conditions (4). Chemical instability of drugs may lead to substantial loss of active pharmaceutical ingredients, especially under poor storage conditions (5).

Antimicrobial agents are among the most prevalent drugs to be counterfeit or substandard (4). Approximately 25% of medicines in low and middle- income countries are counterfeit or substandard, the majority of which are antimicrobial agents (6). Among antimicrobial agents, anti-tuberculosis drugs have a very high impact on global health given the annual incidence of tuberculosis is approximately ten million cases (7, 8). Counterfeit and substandard medicines are more prevalent in the regions of the world most plagued by infectious diseases (9).

A recent meta-analysis of reports of substandard medicines found that 28 countries had reports of substandard of counterfeit anti-tuberculosis drugs, the majority of which were in Africa and Southeast Asia (10). In a study of over 700 anti-mycobacterial

samples that were analyzed in this region, 9% of registered products had inadequate dose or bioavailability, the failure rate went up to 29% for unregistered products as measured by disintegration (11). The failure rate ranged from 4% in middle income countries to 10% in India and 17% in Africa. Approximately half of the failed products were falsified medicines and the remainder contained subtherapeutic doses of drugs.

The frequency of poor drug quality may vary depending on formulation as well as location. A study of the quality of anti-mycobacterial medicines in Tamil Nadu India showed that the rate of substandard rifampicin from 8% in 150 mg tablets to 20% in in 450 mg tablets (12). A World Health Organization study of anti-mycobacterial drugs in former Soviet Union states found that rifampicin containing tablets had the greatest quality failure rate of 28% (13). In a Botswana convenience sample, 31% of fixed dose combination therapies containing rifampicin failed quality testing by thin layer chromatography (14). A study of drugs from Nigerian pharmacies found that nearly half of tested antimicrobial drugs were not within British Pharmacopeia standards, and one third of the tested rifampicin capsules had the wrong dose of active ingredient (15).

Substandard antimicrobials and clinical outcomes

Poor quality antimicrobial drugs undermine the treatment of infectious disease, and may thereby lead to patient level and population level poor health outcomes (6). Drug degradation products may partially or fully replace the standard active pharmaceutical ingredient, resulting in a diminished dose to patients (16). One study identified a case of 'false' chloroquine resistance, wherein drug sensitive plasmodia appeared resistant due to the failed treatment with poor quality anti-malarial drugs (17).

Depending on their therapeutic range, substandard drugs may or may not impact individual treatment. Illnesses such as malnutrition can exacerbate the problem of low dose medicines, due to its role in reduction of drug bioavailability (18). Rifampicin is considered to have a narrow therapeutic index due to the relatively small range between therapeutic doses and toxicity inducing doses (19). Rifampicin is a strong inducer of cytochrome p450, and an inhibitor of oat drug transporter and thereby mediates many adverse drug interactions (20). Rifampicin is therefore an especially risky drug, whether present in poor quality medicines in abnormally high or low doses.

In addition to potential treatment failures and toxicity on the individual treatment level, substandard medicines may also contribute to antibiotic resistance worldwide. Under-dosing is a known contributor to the selection of antibiotic resistant microbes *in vitro* (21). Countries with a high level of drug resistant microbes coincide with regions with poor quality antimicrobial drugs (22, 23). A meta-analysis of four cohort studies had insufficient data to assess the impact of drug quality on the development of MDR-TB (24). Therefore, additional studies are required to determine the influence the impact of substandard rifampicin on the development of antibiotic resistant mycobacteria.

Use of rifampicin as a broad-spectrum antibiotic

Rifampicin is a semisynthetic drug in the rifamycin class. Rifampicin works by binding the DNA dependent RNA polymerase, and thereby prevents elongation of mRNA transcripts (25). Given the extent to which the DNA dependent RNA polymerase is conserved within bacteria, rifampicin is a broad spectrum antibiotic. Hundreds of millions of rifampicin containing tablets are used each year for the treatment of

tuberculosis (26). Rifampicin may be used as a prophylaxis against staphylococcal and meningococcal infections, and has efficacy against *E. coli* and pseudomonas (27, 28).

The use of rifampicin as an effective antibacterial agent is threatened by the development of drug resistant microbes. There are many factors that are associated with drug resistance in mycobacteria, ranging from host determinants such as immune status and adherence, and population factors such as HIV rate, host-pathogen sympatry and local efforts to control disease (29). Substandard medicines contribute to these factors by hindering efforts to control disease, and undermining patient trust in the medical system that may materialize in poor adherence and decreased tendency to seek professional care (30).

Another large factor in the development of drug resistance in mycobacteria is the influence of treatment on the bacteria. Clinical treatment of active tuberculosis is associated with a biphasic decrease in bacteria number; the initial decrease due to the reduction in drug sensitive bacteria, leaving a residual population of persister cells (31). Drug treatments can result in changes to bacterial transcription, metabolism, and cell wall components and may select for resistance conferring mutations (29).

Spontaneous mutations occur in *Mycobacterium tuberculosis* at the rate of 10^{-10} for dormant populations and up to 1 order of magnitude more frequently in actively dividing populations (32). The vast majority of rifampicin resistance in *Mycobacterium tuberculosis* is associated with mutations in the rpoB gene, which encodes the Beta subunit of the DNA dependent RNA polymerase (33). Rifampicin has a close complementary fit to the binding pocket of DNA dependent RNA polymerase, as

assessed by X-ray crystallography (25). Mutations in the rpoB gene disrupt this binding site, thereby decreasing the affinity of rifampicin to its target. An 81 base pair span of the gene is particularly enriched for resistance conferring mutations and is thereby deemed a 'resistance cluster'. Two other resistance clusters also reside in the rpoB gene. Amino acids 516, 526 and 531 of the rpoB gene (using *E. coli* gene mapping notation) have a particularly high co-occurrence with rifampicin resistance in Mycobacteria (33).

Depending on the specific rpoB mutant alleles, rifampicin resistant Mycobacteria have variable levels of resistance to rifabutin and rifapentine, which are other rifamycin-derived drugs (34). The phenomenon of cross-resistance occurs when bacteria gain resistance to an antibiotic it has not been exposed to after gaining resistance to another antibiotic (34). Cross-resistance is common among antibiotics from similar classes (35). Competition experiments with radiolabeled drugs in *E. coli* demonstrate that rifampicin, rifabutin and rifapentine all share a common binding site on RNA polymerase (36).

Rifampicin degradation to rifampicin quinone

Rifampicin's main degradation product occurs from non-enzymatic auto-oxidation to form rifampicin quinone (37). Besides rifampicin quinone, degradation of rifampicin may also produce rifampin n-oxide, 5-desacetyl rifampicin, and rifampin SV. Rifampicin quinone was the most common degradation product found by HPLC analysis of substandard medicines found in the former Soviet Union territories of Armenia, Azerbaijan, Belarus, Kazakhstan, Ukraine, and Uzbekistan (13).

Rifampicin is the least stable component of fixed dose combinations that also contain isoniazid, pyrazinamide and ethambutol (38). Environmental conditions such as

heat, humidity and buffer choice all influence the rate of degradation. Rifampicin undergoes rapid auto-oxidation in the presence of Tris buffers, which is a limit to some experimental studies using rifampicin (39). In forced degradation studies with .1M hydrochloric acid treatment, 25-33% of rifampicin content was lost from mono and combination tablets, as measured by HPLC. Another study of forced degradation under 1M hydrochloric acid or 1M sodium hydroxide found rifampicin primarily converted to rifampicin quinone and rifampin SV (40). In non-oxidative environments, rifamycin SV is more likely to form, while in oxidative environment, rifampicin quinone is the more prevalent degradation product (41).

The International Council for Harmonisation of Technical Requirements for Pharmaceuticals for Human Use describes accelerated degradation conditions as temperatures of 40 degrees Celsius and 75% humidity or greater. This environment has indeed been shown to accelerate the degradation of anti-mycobacterials such as rifampicin and isoniazid (42). A study of medicine quality in India found that light exacerbates drug degradation, based on rifampicin content evaluated by HPLC. In ambient temperatures, there was less than 10% loss of active ingredient over 3 months. However, with heat, humidity and light exposure over the same period of time, up to 85% of the rifampicin degraded (43). Proper packaging can attenuate the degradation conditions; another study found only 15% loss of rifampicin over several months for 6 different drug formulations (44). The presence of isoniazid in fixed dose combinations is also associated with accelerated rifampicin decomposition (23, 45).

Many rifampicin-related compounds have some antimicrobial activity, though their affinity to RNA polymerase may vary widely (25). Rifampicin quinone is bioactive and inhibits RNA polymerase, with a K_D of approximately 1 uM (39). Rifampicin quinone may have deleterious *in vivo* effects, as it has shown immunosuppression in animal models (46). Rifampicin quinone is also thought to underlie some of the toxicity and adverse drug interactions commonly associated with rifampicin (47, 48).

Biochemical methodologies for active pharmaceutical ingredient detection

High performance liquid chromatography (HPLC) is a gold standard method to verify the concentration of active ingredients of pharmaceuticals. HPLC is a resource intensive process requiring customization of solvents, columns and elution time for varying tablet formulations. Acetonitrile and methanol are common toxic reagents that are used in the process of HPLC, which may be of poor accessibility and leave an environmental impact in low and middle-income countries. An adaptation of US Pharmacopeia HPLC guidelines allowed for resolution of rifampicin from its degradation products with a half hour run time for each tablet (38). An expedited version of the methodology cut the elution time to 11 minutes in order to differentiate rifampicin from rifampicin quinone and rifampin SV (40). NMR is another methodology that provides quantitative data regarding drug tablet content. NMR can distinguish between varying rifamycin drugs as well as formulation variations that may underlie differences in drug bioavailability (49, 50).

Thin layer chromatography is a semi-quantitative method used to assess drug quality. The global pharma health fund MiniLab is currently in supply to about 90 countries as a measure to detect counterfeit and substandard drugs by thin layer chromatography. They advise screening based on tablet appearance, disintegration and performance on thin layer chromatography (51). This methodology can only detect absolute fake drugs and grossly substandard medicines that have less than 80% the stated active ingredient (52). A study of antimalarials in Gabon found that 2 artemesinin-based drugs that failed the MiniLab test had no active ingredient as confirmed by HPLC testing (53). Thin layer chromatography identified many low dose rifampicin-containing drugs in a convenience sample on combination tuberculosis medicines, but was unable to identify tablets with high doses of drugs (14). High performance thin layer chromatography is capable of resolving rifampicin from rifampicin quinone, in a methodology that is less time and resource intensive than HPLC , but less sensitive (45, 54). However, these assays are not broadly accessible in the developing world.

Colorimetric assays are a simple, if not highly specific means to identify counterfeit drugs (55). As they do not provide quantitative data, colorimetric assays are not sensitive enough to distinguish substandard medicines from standard. The recently developed paper analytic device had 85% sensitivity. This device identifies rifampicin through a reaction with iron(III), and may be of use in low resource settings to identify grossly poor quality medicines (56).

Nucleic acid aptamers for active pharmaceutical ingredient detection

Experimental devices utilize signaling molecules to identify substandard and counterfeit drugs. These devices require specific signaling molecules to probe for the presence of drug products. As most antimicrobial agents are small molecules, novel approaches to detection are required, as antibodies cannot typically be utilized for such compounds. Given the immense experimental challenges in the discovery of novel probes for small molecules, we generated a computational model to optimize experimental parameters for this process.

Nucleic acids are a potential alternative to antibodies for sensitive and specific detection of small molecule drugs. Nucleic acids that bind specifically to other molecules have been coined aptamers (57). The first aptamers to be discovered were composed of RNA. RNA aptamers are desirable for their great range of conformation and potential catalytic activity (58), while DNA aptamers have preferable stability (59, 60).

Aptamers for small molecules may be adapted for the detection of drugs via the conjugation of fluorescence markers or the modification of chemiluminescence assays, while some aptamers enhance fluorescence of other molecules (61). One such example is the detection of the environmental toxin acetamaprid at concentrations as low as 62 pM with peroxide and luminol on gold nanoparticles with bound aptamers providing a chemiluminescence signal (62). An aptamer for tetracycline was adapted for a colorimetric assay to detect tetracycline (63, 64).

Aptamers are selected through the iterative screening of random libraries containing 10^{10} to 10^{15} random sequences. Systematic Evolution of Ligands by

EXponential Enrichment describes the methodology used to select aptamers with high affinity to ligands from an initial library of nucleic acid sequences of unknown affinity to the ligand (65). Ligands are incubated with the target, and those that exhibit preferential binding are amplified for the next round of selection. Through 10-20 rounds of selection, an initial library can be reduced to a handful of high-affinity aptamers (66). Aptamers typically contain conserved sequences for amplification, and random regions for binding to the ligand of interest. While many aptamer selection methods utilize immobilized ligand, this is not feasible for small molecule targets. Aptamer candidates may be immobilized on a substrate material such as graphene oxide or via docking sequences on streptavidin beads to facilitate separation of target-bound and unbound ligands (67).

Many variables of the aptamer selection process influence the likelihood of successfully identifying an aptamer with affinity to a ligand of interest. The length of docking sequences, primer binding sites and length and number of random regions in the aptamer library may all affect selection outcome (68). After selection, the truncation of aptamers can affect affinity to the ligand (69). Experimental parameters such as ligand concentration, binding substrate of choice, wash stringency and amplification protocols can all impact whether an aptamer survives to the next round of selection or becomes mutated or lost in process (70-72).

Bacterial biosensors for active pharmaceutical ingredient detection

Biosensors use living systems to transduce an environmental signal into a change in phenotype. Cells may be modified by incorporation of colorimetric, luminescence or fluorescence markers for use as whole cell bioreactors or detectors that couple detection

of a molecule with a measurable response (73). Bacteria based biosensors are inherently reproducible and are low cost to maintain and propagate.

Biosensors have been developed for the detection of environmental toxins using *E. coli*. *E. coli* carrying a tetracycline inducible plasmid with 3 different reports can provide different signals (colorimetric, fluorescent or luminescence) depending on the concentration of tetracycline in milk (74). A suite of *E. coli* biosensors with a luminescence reporter can detect heavy metal contaminants such as mercury, zinc, cadmium and lead, copper (75). Some of the reporters were promiscuous for multiple heavy metals while others were specific to a single toxin. Other organisms such as *Proteus mirabilis* and *Bacilus subtilis* are also adaptable for small molecule detection systems (76, 77).

Using reporters for specific drug mechanisms of action, bacteria may be adapted to detect antimicrobial drugs. RecA coupled to green fluorescent protein (GFP) has been used for the detection of inhibitors of DNA metabolism in bacteria (78). The strength of fluorescence output was useful to differentiate gyrase inhibitors from ligase inhibitors. A pharmaceutical company was able to classify drugs based on their stimulation of several luminescence-coupled promoters in *B. subtilis* (77). DNA damaging agents were identified by luminescence of the yorB promoter, RNA targeting agents identified by the yvgS promoter, protein synthesis inhibitors associated with luminescence of the yheI promoter. Cell wall inhibitors and fatty acids synthesis inhibitors were associated with induction of the ypuA and fabHB promoters, respectively. Another research group

studying drugs targeting RNA polymerase further validated this methodology, comparing drugs with known and unknown mechanism of action (79).

Drug interaction testing for antimicrobial detection

Recent studies suggest that drug interaction profiles (the drug interaction scores for a particular drug against a panel of other drugs) are unique even for drugs with the same mechanism of action and may therefore be harnessed to identify antimicrobial compounds (80, 81). Drug interactions are defined by a combined effect that is different than expected. A drug interaction score may be computed based on the comparison of the expected vs. the observed phenotype for the drug combination [$\log_2$(observed/expected)]. For the growth inhibition phenotype, the interaction score is 0 when the observed growth equals expected, negative when observed growth is less than expected and positive when observed growth is greater than expected.

The expected phenotype of drug combinations varies based on model. According to the Bliss independence model, the relative effect of a drug is independent of the other drug's activity (82). For the growth phenotype, if two drugs each inhibit cellular growth by 50% each (IC50), their expected combined effect is 75% growth inhibition (1 - 0.5*0.5). Experimentally, drug interactions may be tested using the Bliss independence model in a simple 2x2 setup of drug 1, drug 2, drug 1 + drug 2, and a drug free control.

According to the Loewe additivity model of drug interactions, a drug is not expected to interact with itself (83). Drug interactions are classically tested in an 8x8 checkerboard assay of dose combinations, with each of the 2 drugs increasing on each axis. For drugs tested against themselves in this experimental setup, isophenotypic

contours for growth are expected to have 0 concavity for any given inhibitory concentration level and high correlation of growth across the symmetry axis. Isophenotypic contour concavity with deviation from 0 therefore indicates that an unknown drug is not equivalent to the known drug. Under the Loewe additivity model, drug interactions may also be determined using a sampling of the checkerboard, by comparing the dose response of the drug combination to the individual dose responses of the individual drug components. The Loewe additivity model is more stringent for identifying negative interactions. For example, the expected growth inhibition for the combination of 2 drugs at IC50 is complete inhibition, in comparison with the 75% inhibition expected under the Bliss model.

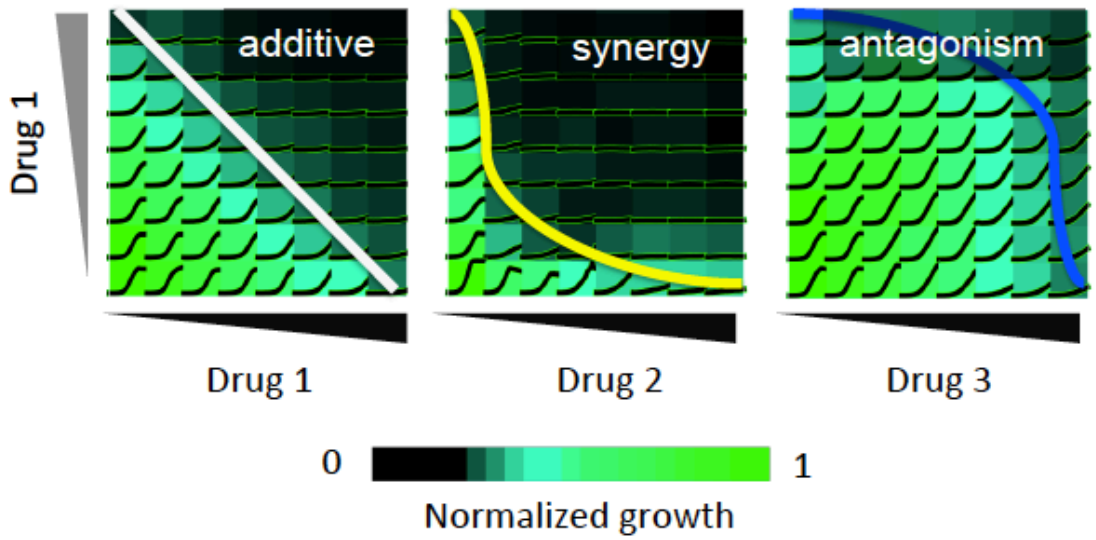

Figure 1.1: Classification of drug interactions.

Displayed are representative interaction experiments with growth curves superimposed on a heat map for normalized growth level (0 at minimal inhibitory concentration, 1 at drug-free condition). According to the Loewe additivity model of drug interactions, the concavity of isophenotypic curves for growth level is expected to be significantly less than or greater than linear for synergistic and antagonistic drug interactions, respectively. 'Self-self' experiments, in which the same drug is increased on each axis, define the experimental assay variability and define the 95% confidence interval for additive drug interactions. At the left is the self-self experiment of drug 1+drug 1 combined with itself; note the straight isophenotypic curve. At middle is drug 1+drug 2, the negative isophenotypic curve indicating a synergistic relationship. At right, drug 1+drug 3, the positive isophenotypic curve indicating an antagonistic relationship.

Yeh et al. conducted one of the largest systematic screens of drug combinations in *E. coli* and assessed all pairwise interactions of 21 antibacterial drugs using the Bliss independence model (80). Inspection of the data indicates that drug interaction profiles (drug interaction scores for a particular drug against a panel of other drugs) are unique. For example, doxycycline and tetracycline are both 30S ribosome protein synthesis inhibitors in *E. coli*, yet they have varying interaction scores with ampicillin and the majority of the other twenty drugs. Large arrays of drug interactions may therefore create a fingerprint for the purpose of identifying active pharmaceutical ingredients.

Dissertation Research Specific Aims

Due to the significant impact of substandard drugs on global health, and the limitations of current technologies for use in low-resource settings, there is interest in developing new technologies that could be particularly useful in field settings in resource poor countries. This led to investigations into the selection process for aptamers for small molecule drugs (Chapter 2). Thematically linked to this issue, was interest in creating accurate yet simpler methods for identifying drugs and drug degradation products using a bioassay (Chapter 3). Lastly, data are presented regarding the consequences of substandard drugs using an *in vitro* model that maps the acquisition of resistance to rifampicin due to exposure to its primary oxidative degradation product, rifampicin quinone (Chapter 4). These data validate concerns that substandard drugs could lead to higher rates of drug resistance to the primary compound, and contribute to treatment failures and adverse health outcomes.

Specific Aim 1: To assess selection strategies for DNA aptamers for small molecule drug detection.

Hypothesis: Experimental parameters including target concentration, library affinity distributions and random events can influence the successful enrichment of DNA aptamers to small molecule targets.

Approach: The capture-SELEX method served as the basis of our computational model of selection dynamics. An aptamer library containing ~10^{15} unique sequences was incubated with a substrate and allowed to equilibrate with a small molecule target ligand. There was therefore competition between the substrate and small molecule for binding to aptamer candidates. Aptamers that were unbound due to ligand binding or random events from the substrate were partitioned, amplified and prepared for additional rounds of selection. The affinity of the aptamers to the small molecule target was expected to increase with each selection cycle. Our model analyzed the influence of the initial aptamer affinity distribution and target concentration on the probability of selecting high affinity aptamer through the capture-SELEX method.

Specific Aim 2: To determine whether anti-mycobacterial drugs may be identified based on drug interaction profiles in *E. coli*.

Hypothesis: Drug interactions between rifamycin compounds and other drugs can be used to create a unique drug interaction fingerprint for drug quality assurance.

Approach: Wild-type *E. coli* with a luciferase expressing plasmid were cultured *in vitro* with combinations of 13 antibiotics with 4 rifamycin drugs or the drug degradation product rifampicin quinone to create profiles of drug interactions. Drug interactions were

tested by comparing shifts in dose response for drug combinations versus single drug effects. Dose response were assessed for each single drug and combination (a one to one mixture) with linear dilutions. Drug combinations were an equal mixture of single agents containing approximately one half minimal inhibitory concentration of each single agent. Dose-response curves were generated based on the area under the luminescence curve, standardized to the drug free condition, over a one-hour interval. All doses were adjusted to fraction of minimal inhibitory concentration from zero to one. The drug interaction score was approximated by the fractional inhibitory concentration index, using the Loewe additivity model, which assumes that a drug cannot interact with itself. Drug interaction profiles were composed of arrays of drug interaction scores for each rifamycin drug or degradation product tested with other antibiotic compounds. All experiments were done in replicate. Drug identification was based on similarity of a query drug interaction profile to the known drug interaction profiles.

Specific Aim 3: To determine whether exposure to rifampicin degradation products induces resistance to the standard antimicrobial rifampicin *E. coli* and *M. smegmatis.*

Hypothesis: Exposure to rifampicin quinone will select for the evolution of antimicrobial resistance to rifampicin in *E. coli* and *M. smegmatis*.

Approach: Wild-type *E. coli* and *M. smegmatis* were cultured *in vitro* with the drug degradation product rifampicin quinone or subtherapeutic doses of rifampicin until a thirty fold change in minimal inhibitory concentration (MIC) was observed. Cells were monitored for changes in MIC over time. A resistance score was computed comparing the

MIC of treated cells to controls: $\log_2(MIC_{resistant}/MIC_{parental})$. Representative colonies from each population were isolated, sequenced and assessed for single nucleotide polymorphisms, insertion and deletions in the rifampicin resistance clusters of the rpoB gene, which allowed us to propose mechanistic causes of antimicrobial resistance and identify features of resistance induced by standard medicines versus degraded drugs. Cross-resistance to additional rifamycin antibiotics was assessed to evaluate cross-resistance patterns of standard drugs versus impurities.

The studies presented aimed to test the broader notion that substandard medicines contribute towards antimicrobial resistance, and proposed methodologies to identify substandard medicines.

Chapter 1 References

1. Pecoul B, Chirac P, Trouiller P & Pinel J (1999) Access to essential drugs in poor countries: A lost battle?. *JAMA* 281(4): 361-367.

2. Kelesidis T & Falagas ME (2015) Substandard/counterfeit antimicrobial drugs. *Clinical Microbiology Reviews* 28(2): 443-464.

3. van Crevel R*, et al* (2004) Bioavailability of rifampicin in Indonesian subjects: A comparison of different local drug manufacturers. *International Journal of Tuberculosis and Lung Disease* 8(4): 500-503.

4. Johnston A & Holt DW (2014) Substandard drugs: A potential crisis for public health. *British Journal of Clinical Pharmacology* 78(2): 218-243.

5. Ballereau F*, et al* (1997) Stability of essential drugs in the field: Results of a study conducted over a two-year period in Burkina Faso. *American Journal of Tropical Medicine and Hygiene* 57(1): 31-36.

6. Pincock S (2003) WHO tries to tackle problem of counterfeit medicines in Asia. *British Medical Journal* 327(7424): 1126.

7. World Health Organization (2017) *Global tuberculosis report 2017,* (World Health Organization, Geneva, Switzerland).

8. World Health Organization (2014) Companion handbook to the WHO guidelines for the programmatic management of drug-resistant tuberculosis.

9. Roger B & Boateng K (2007) Bad medicine in the market. *World Hospitals and Health Services* 43(3): 17-21.

10. Kelesidis T & Falagas ME (2015) Substandard/counterfeit antimicrobial drugs. *Clinical Microbiology Reviews* 28(2): 443-464.

11. Bate R, Jensen P, Hess K, Mooney L & Milligan J (2013) Substandard and falsified anti-tuberculosis drugs: A preliminary field analysis. *International Journal of Tuberculosis and Lung Disease* 17(3): 308-311.

12. Ramachandran G*, et al* (2013) Estimation of content of anti-TB drugs supplied at centres of the revised national TB control programme in Tamil Nadu, India. *Tropical Medicine and International Health* 18(9): 1141-1144.

13. World Health Organization (2011) Survey of the quality of anti-tuberculosis medicines circulating in selected newly independent states of the former Soviet Union

14. Kenyon TA*, et al* (1999) Detection of substandard fixed-dose combination tuberculosis drugs using thin-layer chromatography. *International Journal of Tuberculosis and Lung Disease*3(11): 347-350.

15. Taylor RB*, et al* (2001) Pharmacopoeial quality of drugs supplied by Nigerian pharmacies. *Lancet* 357(9272): 1933-1936.

16. Hall Z, Allan EL, van Schalkwyk DA, van Wyk A & Kaur H (2016) Degradation of artemisinin-based combination therapies under tropical conditions. *American Journal of Tropical Medicine and Hygiene* 94(5): 993-1001.

17. Basco LK, Ringwald P, Manene AB & Chandenier J (1997) False chloroquine resistance in Africa. *Lancet* 350(9072): 224-6736(05)62397-5.

18. Okeke IN, Lamikanra A & Edelman R (1999) Socioeconomic and behavioral factors leading to acquired bacterial resistance to antibiotics in developing countries. *Emerging Infectious Diseases* 5(1): 18-27.

19. Blix HS, Viktil KK, Moger TA & Reikvam A (2010) Drugs with narrow therapeutic index as indicators in the risk management of hospitalised patients. *Pharmacy Practice (Granada)* 8(1): 50-55.

20. Asaumi R*, et al* (2018) Comprehensive PBPK model of rifampicin for quantitative prediction of complex drug-drug interactions: CYP3A/2C9 induction and OATP inhibition effects. *CPT Pharmacometrics Systems Pharmacology*

21. Kohanski MA, DePristo MA & Collins JJ (2010) Sublethal antibiotic treatment leads to multidrug resistance via radical-induced mutagenesis. *Molecular Cell* 37(3): 311-320.

22. Shakoor O, Taylor RB & Behrens RH (1997) Assessment of the incidence of substandard drugs in developing countries. *Tropical Medicine and International Health* 2(9): 839-845.

23. Laserson KF, Kenyon AS, Kenyon TA, Layloff T & Binkin NJ (2001) Substandard tuberculosis drugs on the global market and their simple detection. *International Journal of Tuberculosis and Lung Disease* 5(5): 448-454.

24. van der Werf MJ, Langendam MW, Huitric E & Manissero D (2012) Multidrug resistance after inappropriate tuberculosis treatment: A meta-analysis. *European Respiratory Journal* 39(6): 1511-1519.

25. Campbell EA, *et al* (2001) Structural mechanism for rifampicin inhibition of bacterial rna polymerase. *Cell* 104(6): 901-912.

26. Norval PY, Blomberg B, Kitler ME, Dye C & Spinaci S (1999) Estimate of the global market for rifampicin-containing fixed-dose combination tablets. *International Journal of Tuberculosis and Lung Disease* 3(11): 292-300.

27. Kruse AJ, Peerdeman SM, Bet PM & Debets-Ossenkopp YJ (2006) Successful treatment with linezolid and rifampicin of meningitis due to methicillin-resistant staphylococcus epidermidis refractory to vancomycin treatment. *European Journal of Clinical Microbiology and Infectious Diseases* 25(2): 135-137.

28. Mikalauskas A, Parkins MD & Poole K (2017) Rifampicin potentiation of aminoglycoside activity against cystic fibrosis isolates of pseudomonas aeruginosa. *Journal of Antimicrobial Chemotherapy* 72(12): 3349-3352.

29. Koch A, Mizrahi V & Warner DF (2014) The impact of drug resistance on mycobacterium tuberculosis physiology: What can we learn from rifampicin?. *Emerging Microbes and Infections* 3(3): e17.

30. Arnold A, *et al* (2017) Drug resistant TB: UK multicentre study (DRUMS): Treatment, management and outcomes in London and West Midlands 2008-2014. *Journal of Infections* 74(3): 260-271.

31. Horsburgh CR,Jr, Barry CE,3rd & Lange C (2015) Treatment of tuberculosis. *New England Journal of Medicine* 373(22): 2149-2160.

32. David HL (1970) Probability distribution of drug-resistant mutants in unselected populations of mycobacterium tuberculosis. *Applied Microbiology* 20(5): 810-814.

33. Castan P*, et al* (2014) Point-of-care system for detection of mycobacterium tuberculosis and rifampin resistance in sputum samples. *Journal of Clinical Microbiology* 52(2): 502-507.

34. Williams DL*, et al* (1998) Contribution of rpoB mutations to development of rifamycin cross-resistance in mycobacterium tuberculosis. *Antimicrobial Agents and Chemotherapy* 42(7): 1853-1857.

35. Oz T*, et al* (2014) Strength of selection pressure is an important parameter contributing to the complexity of antibiotic resistance evolution. *Molecular Biology and Evolution* 31(9): 2387-2401.

36. Xu M, Zhou YN, Goldstein BP & Jin DJ (2005) Cross-resistance of Escherichia coli RNA polymerases conferring rifampin resistance to different antibiotics. *Journal of Bacteriology* 187(8): 2783-2792.

37. Bolt HM & Remmer H (1976) Implication of rifampicin-quinone in the irreversible binding of rifampicin to macromolecules. *Xenobiotica* 6(1): 21-32.

38. Mohan B, Sharda N & Singh S (2003) Evaluation of the recently reported USP gradient HPLC method for analysis of anti-tuberculosis drugs for its ability to resolve degradation products of rifampicin. *Journal of Pharmaceutical and Biomedical Analysis* 31(3): 607-612.

39. Reisbig, Richard R., Woody, A. Young M., Woody,Robert W., (1982) Rifampicin as a spectroscopic probe of the mechanism of RNA polymerase from E. coli. *Biochemistry* 21(1): 196-200.

40. Liu J, Sun J, Zhang W, Gao K & He Z (2008) HPLC determination of rifampicin and related compounds in pharmaceuticals using monolithic column. . *Journal of Pharmaceutical and Biomedical Analysis* 46(2): 405-409.

41. Prankerd, Richard J., Walters, John M., Parnes,Joel H., (1992) Kinetics for degradation of rifampicin, an azomethine-containing drug which exhibits reversible hydrolysis in acidic solutions. *International Journal of Pharmaceutics* 78(1): 59-67.

42. Bhutani H, Singh S, Jindal KC & Chakraborti AK (2005) Mechanistic explanation to the catalysis by pyrazinamide and ethambutol of reaction between rifampicin and isoniazid in anti-TB FDCs. *Journal of Pharmaceutical and Biomedical Analysis* 39(5): 892-899.

43. Bhutani H, Mariappan TT & Singh S (2004) The physical and chemical stability of anti-tuberculosis fixed-dose combination products under accelerated climatic conditions. *International Journal of Tuberculosis and Lung Disease* 8(9): 1073-1080.

44. Ashokraj Y, Kohli G, Kaul CL & Panchagnula R (2005) Quality control of anti-tuberculosis FDC formulations in the global market: Part II-accelerated stability studies. *International Journal of Tuberculosis and Lung Disease* 9(11): 1266-1272.

45. Shishoo CJ, Shah SA, Rathod IS, Savale SS & Vora MJ (2001) Impaired bioavailability of rifampicin in presence of isoniazid from fixed dose combination (FDC) formulation. *International Journal of Pharmacology* 228(1-2): 53-67.

46. Konrad P & Stenberg P (1988) Rifampicin quinone is an immunosuppressant, but not rifampicin itself. *Clinical Immunology and Immunopathology* 46(1): 162-166.

47. Piriou A, Jacqueson A, Warnet JM & Claude JR (1983) Enzyme induction with high doses of rifampicin in wistar rats. *Toxicology Letters* 17(3-4): 301-306.

48. Shi F, Li X, Pan H & Ding L (2017) NQO1 and CYP450 reductase decrease the systemic exposure of rifampicin-quinone and mediate its redox cycle in rats. *Journal of Pharmaceutical and Biomedical Analysis* 132: 17-23.

49. Santos L*, et al* (2001) NMR studies of some rifamycins. *Journal of Molecular Structure* 563-564: 61-78.

50. Agrawal S, Ashokraj Y, Bharatam PV, Pillai O & Panchagnula R (2004) Solid-state characterization of rifampicin samples and its biopharmaceutic relevance. *European Journal of Pharmaceutical Sciences* 22(2-3): 127-144.

51. Jähnke R & Dwornik K (2018) *A concise quality control guide on essential drugs and other medicines: Supplement 2018 to Volume II on thin layer chromatography tests,* (GPHF, Frankfurt am Main, Germany).

52. Risha PG*, et al* (2008) The use of minilabs to improve the testing capacity of regulatory authorities in resource limited settings: Tanzanian experience. *Health Policy* 87(2): 217-222.

53. Visser BJ*, et al* (2015) Assessing the quality of anti-malarial drugs from gabonese pharmacies using the MiniLab(R): A field study. *Malaria Journal* 14: 273-015-0795-z.

54. Shewiyo DH*, et al* (2012) Optimization of a reversed-phase-high-performance thin-layer chromatography method for the separation of isoniazid, ethambutol, rifampicin and pyrazinamide in fixed-dose combination antituberculosis tablets. *Journal of Chromatography A* 1260: 232-238.

55. Mariappan TT, Jindal KC & Singh S (2004) Overestimation of rifampicin during colorimetric analysis of anti-tuberculosis products containing isoniazid due to formation of isonicotinyl hydrazone. *Journal of Pharmaceutical and Biomedical Analysis* 36(4): 905-908.

56. Weaver AA, *et al* (2013) Paper analytical devices for fast field screening of beta lactam antibiotics and antituberculosis pharmaceuticals. *Analytical Chemistry* 85(13): 6453-6460.

57. Ellington AD & Szostak JW (1990) In vitro selection of RNA molecules that bind specific ligands. *Nature* 346(6287): 818-822.

58. Sassanfar M & Szostak JW (1993) An RNA motif that binds ATP. *Nature* 364(6437): 550-553.

59. Smirnov I & Shafer RH (2000) Effect of loop sequence and size on DNA aptamer stability. *Biochemistry* 39(6): 1462-1468.

60. Williams KP, *et al* (1997) Bioactive and nuclease-resistant L-DNA ligand of vasopressin. *Proceedings of the National Academy of Sciences* 94(21): 11285-11290.

61. Gotrik M, *et al* (2018) Direct selection of fluorescence-enhancing RNA aptamers. *Journal of the American Chemical Society* 140(10): 3583-3591.

62. Qi Y, Xiu FR, Zheng M & Li B (2016) A simple and rapid chemiluminescence aptasensor for acetamiprid in contaminated samples: Sensitivity, selectivity and mechanism. *Biosensors and Bioelectronics* 83: 243-249.

63. Berens C, Thain A & Schroeder R (2001) A tetracycline-binding RNA aptamer. *Bioorganic Medicinal Chemistry* 9(10): 2549-2556.

64. Kim YS, *et al* (2010) A novel colorimetric aptasensor using gold nanoparticle for a highly sensitive and specific detection of oxytetracycline. *Biosensors and Bioelectronics* 26(4): 1644-1649.

65. Tuerk C, MacDougal S & Gold L (1992) RNA pseudoknots that inhibit human immunodeficiency virus type 1 reverse transcriptase. *Proceedings of the National Academy of Sciences* 89(15): 6988-6992.

66. Spill F, *et al* (2016) Controlling uncertainty in aptamer selection. *Proceedings of the National Academy of Sciences* 113(43): 12076-12081.

67. Nguyen VT, Kwon YS, Kim JH & Gu MB (2014) Multiple GO-SELEX for efficient screening of flexible aptamers. *Chemical Communications* 50(72): 10513-10516.

68. Zhou Q, Xia X, Luo Z, Liang H & Shakhnovich E (2015) Searching the sequence space for potent aptamers using SELEX in silico. *Journal of Chemical Theory Computing* 11(12): 5939-5946.

69. Frost NR, McKeague M, Falcioni D & DeRosa MC (2015) An in solution assay for interrogation of affinity and rational minimer design for small molecule-binding aptamers. *Analyst* 140(19): 6643-6651.

70. Chen C & Kuo T (2007) Simulations of SELEX against complex receptors with a condensed statistical model. *Computers \& Chemical Engineering* 31(9): 1007-1019.

71. Cherney LT, Obrecht NM & Krylov SN (2013) Theoretical modeling of masking DNA application in aptamer-facilitated biomarker discovery. *Analytical Chemistry* 85(8): 4157-4164.

72. Seo Y, Nilsen-Hamilton M & Levine HA (2014) A computational study of alternate SELEX. *Bulletin of Mathematical Biology* 76(7): 1455-1521.

73. Webb AJ, Kelwick R & Freemont PS (2017) Opportunities for applying whole-cell bioreporters towards parasite detection. *Microbial Biotechnology* 10(2): 244-249.

74. Hansen LH & Sorensen SJ (2000) Detection and quantification of tetracyclines by whole cell biosensors. *FEMS Microbiolog Letters* 190(2): 273-278.

75. Ivask A, Rolova T & Kahru A (2009) A suite of recombinant luminescent bacterial strains for the quantification of bioavailable heavy metals and toxicity testing. *BMC Biotechnology* 9: 41-6750-9-41.

76. Coker C, Zhao H & Mobley HL (2002) Green fluorescent protein urea sensors. uropathogenic proteus mirabilis. *Methods in Molecular Biology* 183: 287-293.

77. Urban A*, et al* (2007) Novel whole-cell antibiotic biosensors for compound discovery. *Applied Environmental Microbiology* 73(20): 6436-6443.

78. Fan J*, et al* (2014) A novel high-throughput cell-based assay aimed at identifying inhibitors of DNA metabolism in bacteria. *Antimicrobial Agents and Chemotherapy* 58(12): 7264-7272.

79. Mariner KR, Ooi N, Roebuck D, O'Neill AJ & Chopra I (2011) Further characterization of bacillus subtilis antibiotic biosensors and their use for antibacterial mode-of-action studies. *Antimicrobial Agents and Chemotherapu* 55(4): 1784-1786.

80. Yeh P, Tschumi AI & Kishony R (2006) Functional classification of drugs by properties of their pairwise interactions. *Nature Genetics* 38(4): 489-494.

81. Cokol M*, et al* (2011) Systematic exploration of synergistic drug pairs. *Molecular Systems Biology* 7: 544.

82. Zhao W*, et al* (2014) A new bliss independence model to analyze drug combination data. *Journal of Biomolecular Screening* 19(5): 817-821.

83. Greco WR, Bravo G & Parsons JC (1995) The search for synergy: A critical review from a response surface perspective. *Pharmacological Reviews* 47(2): 331-385.

CHAPTER 2: Controlling uncertainty in aptamer selection

Published in the following manuscript:
Spill, F., Weinstein, Z.B., Irani Shemirani, A., Ho, N., Desai, D. & Zaman, M.H. 2016, "Controlling uncertainty in aptamer selection", *Proceedings of the National Academy of Sciences of the United States of America,* vol. 113, no. 43, pp. 12076-12081.

Abstract

Oligonucleotide aptamers have increasing applications as a class of molecules that bind with high affinity and specificity to a target. Aptamers are typically selected from a large pool of random candidate nucleic acid libraries through competition for the target. Using a stochastic hybrid model, we are able to study the combined impact of important evolutionary success factors such as competition, randomness, and changes in the environment. Whereas the environment may be tuned with experimental parameters such as target concentration, competition varies with differences in the initial distribution of aptamer–target binding affinities, and random events can eliminate even the ligands with the highest affinity. The search for high-affinity aptamers for targets such as proteins, small molecules, or cancer cells remains a formidable endeavor. Systematic Evolution of Ligands by EXponential Enrichment (SELEX) offers an iterative process to discover these aptamers through evolutionary selection of high-affinity candidates from a highly diverse random pool. This randomness dictates an unknown population distribution of fitness parameters, encoded by the binding affinities, toward SELEX targets. Adding to this uncertainty, repeating SELEX under identical conditions may lead to variable outcomes. These uncertainties pose a challenge when tuning selection pressures to isolate

high-affinity ligands. Here, we present a stochastic hybrid model that describes the evolutionary selection of aptamers to explore the impact of these unknowns. To our surprise, we find that even single copies of high-affinity ligands in a pool of billions can strongly influence population dynamics, yet their survival is highly dependent on chance. We perform Monte Carlo simulations to explore the impact of environmental parameters, such as the target concentration, on selection efficiency in SELEX and identify strategies to control these uncertainties to ultimately improve the outcome and speed of this time- and resource-intensive process.

Introduction

Understanding and exploiting target–ligand binding are bedrocks of the biomedical sciences and support a host of applications ranging from diagnostics, therapeutics, and drug discovery to biosensing, imaging, and gene regulation. Antibodies and rational design provide a constructive playground to develop these applications, yet there generally remains a paucity of strong and specific binders for the innumerable viral, protein, and small-molecule targets under investigation.

Aptamers offer an alternative to antibodies, yet despite their growth (1–4), the discovery of high-affinity aptamers remains a challenge, especially for small-molecule targets (5, 6). Systematic Evolution of Ligands by EXponential Enrichment (SELEX) (7, 8) is the premier framework for aptamer development and isolates high-affinity ligands from an initial library similar to how advantageous traits are enriched in a biological population through Darwinian selection. In a cyclic process, ligands are incubated with the target, and those that exhibit preferential binding are amplified and survive to the next

round. Target molecules are typically immobilized on a substrate material to facilitate easy separation of target-bound and unbound ligands. Through numerous rounds of selection, an initial library can be reduced to a handful of high-affinity aptamers. Nucleic acids comprise the vast majority of libraries used in SELEX, where sequence regions are randomized to generate tremendous structural diversity. Whereas this diversity underpins the evolutionary nature of SELEX, numerous works suggest that initial library design is a significant contributor to its overall success (9).

Although conceptually simple, the practical application of SELEX is plagued by uncertainty. Despite the impact of library design, the initial affinity distribution for any library toward a specific target remains a priori unknown. Target immobilization further complicates the procedure, particularly for small molecules. In comparison with large molecular weight targets such as proteins (10), viruses (11), and whole cells (12, 13), the immobilization of small molecules eliminates ligand binding sites and is thus impractical. Newer approaches instead bind the library itself to a substrate material using noncovalent equilibrium binding, but this introduces the opportunity for competitive losses of high-affinity ligands that are initially present in extremely low numbers. Wash steps and other experimental procedures may lead to further random losses, whereas nonspecific selection of ligands can counter environmental pressures and stall selection. In short, these uncertainties may quickly compound to apply tremendous risk toward the guarantee of successful selection.

Mathematical modeling therefore has great potential to help understand the uncertainties of aptamer selection and devise strategies to optimize environmental

parameters and improve selection outcomes. Previous models have explored SELEX for protein targets, considering parameters such as target concentration (14–16), separation efficiency of target-bound and unbound ligand (17), nonspecific binding of DNA to target (18), and negative selection steps (19). These studies predict that, despite its experimental complexity, the evolutionary nature of SELEX guarantees selection of the highest affinity ligand from the initial library. However, these works focus primarily on the use of deterministic equilibrium equations (14), whereas the presence of ligands in low copy numbers and the role of other experimental uncertainties suggest the use of more fundamental stochastic models rather than deterministic approximations. Mathematically, the chemical master equation provides a framework to test this hypothesis and generalize the above-mentioned deterministic models to include intrinsic stochasticity (20). Whereas this approach could be applied toward a purely stochastic model for SELEX, the result cannot currently be solved analytically or simulated by conventional techniques such as the Gillespie algorithm (21), due to the large number of molecules present. These limitations are common for many stochastic multiscale problems in biology, chemistry, and physics; the development of novel analytic approximations or numerical techniques to address this problem is an important ongoing research topic (22).

Using these ideas as our foundation, we introduce a hybrid model for aptamer selection that builds on the chemical master equation to introduce stochastic uncertainty in SELEX modeling. Here, ligands are separated into two categories of high and low copy number. In the former case, the master equation is simplified toward a deterministic

equilibrium system, whereas in the latter it can be approximately solved analytically. Unlike previous efforts to incorporate stochasticity into aptamer modeling (23, 24), our framework allows us to simultaneously investigate the impact of low copy number ligands and their competitive binding to target molecules and immobilization substrates among the presence of high copy number ligands. Most importantly, this approach can capture total loss of individual ligands, which can strongly contribute to protocol outcome. Such events have not previously been investigated and cannot be captured by other approximations of the master equation such as the Langevin approximation, which rely on the presence of sufficiently high numbers of molecules and thereby diminish the possibility of extinction events (25).

Using this framework, we investigate unexplored sources of uncertainty in SELEX, beginning with a systematic analysis of the role the initial library affinity distribution plays in selection. We further challenge the assumption that this distribution is continuous at its tails and evaluate the impact of adding noise at these extremes. We find that introducing as few as 20 additional ligands outside the bulk distribution of 10^{15} molecules can strongly affect the outcome of selection. In light of these results, we revisit the topic of optimizing target concentration as discussed in previous works (14–16), and show that the assumed initial K_D distribution strongly influences protocol optimizations. We also provide additional insights regarding noncovalent ligand immobilization to support more recent efforts to develop robust protocols for small-molecule SELEX (26–28). Integrating these ideas, we show that simultaneously lowering the target

concentration and the substrate binding dissociation constant over the SELEX cycles can lead to improved selection outcomes for a wide range of initial conditions.

Materials and Methods

Computational model of selection dynamics

The original SELEX protocol (7, 8) serves as the basis for our model, with additional modifications to accommodate small-molecule targets as described in ref. 26. Whereas this marks a model that specifically considers small-molecule targets, the main ideas and conclusions derived from this work remain applicable to other targets and selection schemes. The main steps of our approach are summarized in Fig. 2.1. We begin with a library of $A^{\sim tot}_i$ ligands of type i, where $i=\{1,\ldots,M^A\}$ and M^A is the total number of unique ligands. The ligands are then noncovalently immobilized using $S^{\sim tot}$ substrate molecules, where K_S is the ligand–substrate dissociation constant. These complexes are then subjected to wash steps to remove unbound ligands, from which $A^{\sim I}_i$ ligands of type i survive. Surviving ligands are then incubated with $T^{\sim tot}$ target molecules, where a ligand of type i binds to the target with a dissociation constant $K_{D,i}$. Ligands that are bound to a target or have unbound from the substrate are partitioned from those that remain bound to the substrate. Finally, the partitioned ligands are amplified via PCR, modeled as a constant factor increase of α_{PCR}, and used to begin the next cycle. The proceeding sections highlight the notable details of our hybrid approach, whereas a more thorough description and derivation of the model can be found in the Supplementary Information

(SI). Throughout these sections, quantities that refer to an absolute number of molecules are denoted with a tilde, whereas those without represent concentrations.

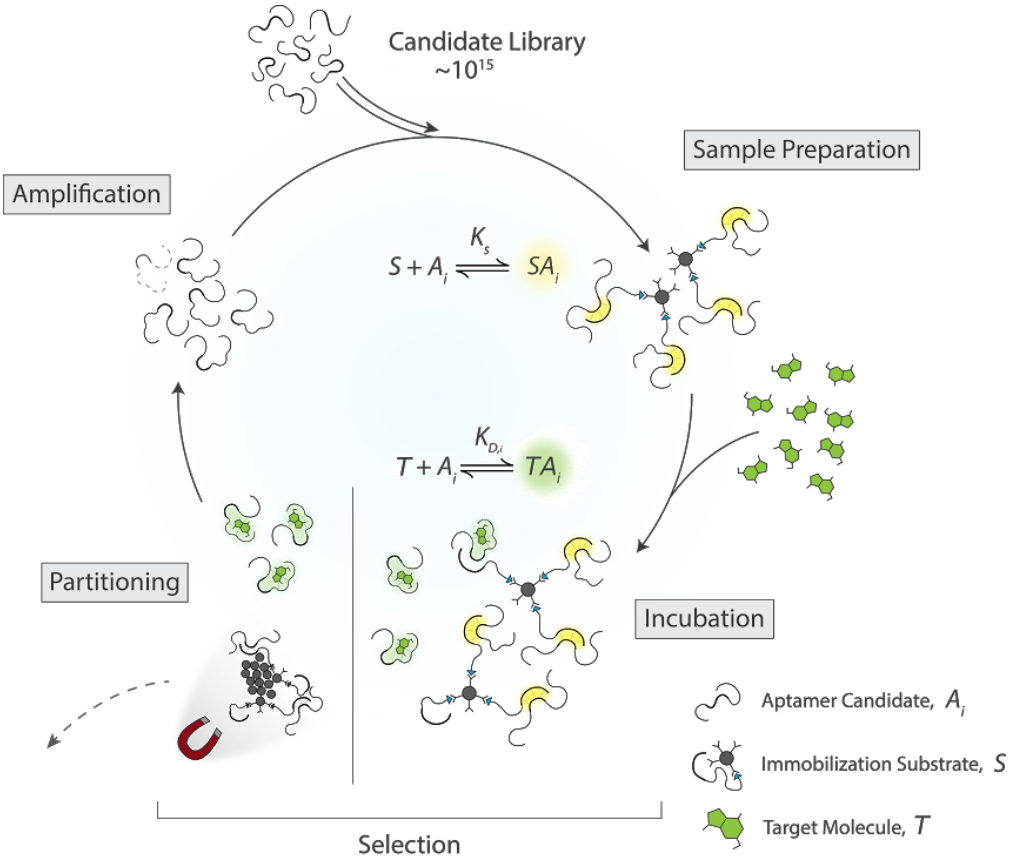

Figure 2.1: Capture SELEX Schematic

Sample candidate library of ligands Ai is prepared by letting the ligands bind to a substrate S. Then, the target is added, leading to competitive binding between the different aptamers for substrate and target molecules T. The ligands still bound to the substrate are then separated from those that are either bound to a target, or have randomly unbound from the substrate. The latter two are subsequently amplified and taken into the next cycle.

Deterministic model of ligand binding

Earlier works use equilibrium conditions to characterize ligand–target interactions during selection (14–17), focusing on changes in bulk properties, such as the mean dissociation constant, to study the enrichment of a single best candidate. We instead monitor the full ligand affinity distribution in an effort to better understand how parameters such as the initial SD also impact selection dynamics. Because modeling each of the $M^A \approx 10^{15}$ unique ligands is computationally intractable, we discretize the initial distribution of M^A unique ligands into M^B bins, each containing $A^{\sim}_i$ ligands of dissociation constant $K_{D,i}$, where $i=\{1,\ldots,M^B\}$. We choose M^B to be large enough that the results do not depend on the binning, and small enough to optimize simulation performance. We further build on this analysis by introducing additional equilibrium conditions for nonspecific ligand–substrate interactions represented by a dissociation constant K_S. In ref. 26, substrate–ligand binding is accomplished through DNA base pairing using a fixed sequence, and is thus constant. Altering the length of this fixed sequence is a means to tune K_S. Moreover, different immobilization techniques, such as the use of graphene oxide (27, 28), will lead to variations of K_S within a given pool, but we do not consider such cases here and instead treat K_S to be constant throughout a single cycle of SELEX. Combining ligand–target and ligand–substrate binding, the full system of steady-state equilibrium binding conditions can be described by the set of equations:

$$[SA_i]=1/K_S(A^I_i-[SA_i]-[TA_i])S^{free},\ i=1,\ldots,M^B,$$

$$[TA_i]=1K_{D,i}\,((A^I_i-[SA_i]-[TA_i])T^{free},\ i=1,\ldots,M^B,$$

$$S^{tot}=\sum i=1{:}M^B\,[SA_i]+S^{free},\ T^{tot}=\sum i=1{:}M^B[TA_i]+T^{free}. \quad [1]$$

Here, $[SA_i]$ and $[TA_i]$ denote the concentration of ligand–substrate and ligand–target complexes, representing $2M^B$independent variables that are solved for; the quantities T^{tot},T^{free} and S^{tot},S^{free} denote the concentrations of total and free target and substrate, respectively. From these results, we determine the concentration of ligands which survive selection, denoted by $A^{S,D}_i$, and are amplified by PCR for the next cycle. The superscripts denote that this number is obtained after selection and using the deterministic model defined by Eq. 1. This concentration is simply the sum of free- and target-bound ligands, and is hence given by

$$A^{S,D}_i=[TA_i]+A^{free}_i= A^I_i-[SA_i]. \quad [2]$$

Stochastic model of ligand selection

Chemical reactions are fundamentally stochastic in nature, with forward and backward reactions occurring constantly. Whereas powerful and simple, Eq. 1 is based on real-valued concentrations which require sufficiently high molecular copy numbers to make discreteness and random fluctuations negligible. This is challenged at the tails of the K_D distribution, where appropriate binning results in few ligands per bin. To address this, a hybrid approach is used where additional stochastic analysis is applied when Eq. 1 predicts A~S,Di to be below a threshold Θ. To distinguish these quantities for stochastic analysis, we denote them as A~S,Dψ, where ψ represents the subset of indices i that satisfy the condition A~S,Di<Θ. Results exploring the choice for Θ are provided in SI, Fig. 2.S6. We then calculate the probability for selecting A~S,Sψ ligands, p(A~S,Sψ); the superscripts denotes that the number is obtained after selection and using the

stochastic model. As described in the SI Appendix, we find that by starting with the chemical master equation, p(A~S,Sψ) is well-approximated by a binomial distribution:

p(A~S,Sψ)=⎛⎝⎜⎜A~totψA~S,Sψ⎞⎠⎟⎟pA~S,Sψψ(1−pψ)A~totψ−A~S,Sψ,forA~S,Sψ=0,…,A~totψ. [3]

Here, the quantity pψ represents the probability that a single ligand is selected out of A~totψ ligands of type ψ. To provide the most accurate description, we account for stochastic contributions from both the immobilization and incubation steps. The contribution from immobilization is approximately the same for all candidates, and is given by $A^{\tilde{}I}/A^{\tilde{}tot}$, the fraction of remaining immobilized ligands after wash steps over those present before immobilization, where A~I=∑MBi=1A~Ii and A~tot=∑MBi=1A~totiA. The contribution from incubation is calculated as the fraction of predicted ligands, A~S,Dψ, out of an initial number of A~Iψ. Using these contributions, the total probability that a ligand in bin ψ survives is given by pψ=A~IAS,DψA~totAIψ. [4]

Finally, Eq. 3 requires A~totψ to be integer-valued, as it denotes a number of molecules. However, the deterministic equations yield real-valued concentrations that must be renormalized to an integer. We separate A~totψ into its integer and fractional parts, A~totψ=A~totψ,ℕ+A~totψ,fA, and then interpret 0≤A~totψ,f<10≤A~ψ,ftot<1 as the probability to have an extra molecule present. We then draw a uniformly distributed random number 0≤r≤1, and set A~totψ=A~totψ,ℕ+1A~ψtot=A~ψ,ℕtot+1 if r<A~totψ,

and A~totψ=A~totψ,ℕA otherwise. Following this renormalization, we finally draw a random variate distributed according to Eq. 3 to simulate the set of ligands A~S,Sψ that remain after both immobilization and selection.

Results

Using a hybrid computational approach, our model provides a generalized framework that can be used to analyze both deterministic and stochastic effects in SELEX. We use the model to deconstruct two main forms of uncertainties in aptamer selection. The first is parameter uncertainty, including the unknown initial K_D distribution as well as the experimentally tunable quantities K_s and T_{tot}. These are analyzed using a parameter study that observes the impact of these factors on SELEX dynamics. The second is stochastic uncertainty associated with low copy number binding phenomena. As this form of uncertainty is random in nature, we use Monte Carlo simulations to observe the variability in outcomes between repeated SELEX procedures and extract conclusions, which are robust with respect to stochastic fluctuations. Unless mentioned otherwise, the parameters from Table 2.S1 are used in all simulations.

Effect of K_D distribution on selection efficiency

Gaussian distributions describing the initial ligand pool dominate SELEX models in literature (16), yet we are not aware of any prior systematic approach to study the impact of various distributions on the outcome of SELEX. Whereas strong justifications have been made for the assumption of a log-normal Gaussian description (29), we explore various Gaussian as well as non-Gaussian distributions and their impact on

selection. Our convention for log-normal K_D distributions is such that a Gaussian $N(\mu,\sigma)$ with mean μ and SD σ in log-space translates to a mean of 10μ in K_D space; we do not shift the mean by $(1/2)\sigma 2$ as is customary in Ito calculus. Fig. 2.2 highlights the dramatic difference observed for just two different assumed distributions, and demonstrates the significant role the initial K_D distribution plays in SELEX. This point is further accentuated by the fact that different selection targets may significantly alter the initial K_D distribution for any given library. SI, Fig. 2.S1 confirms that for a variety of other distributions, including non-Gaussians, distribution shape has a dramatic impact on selection dynamics.

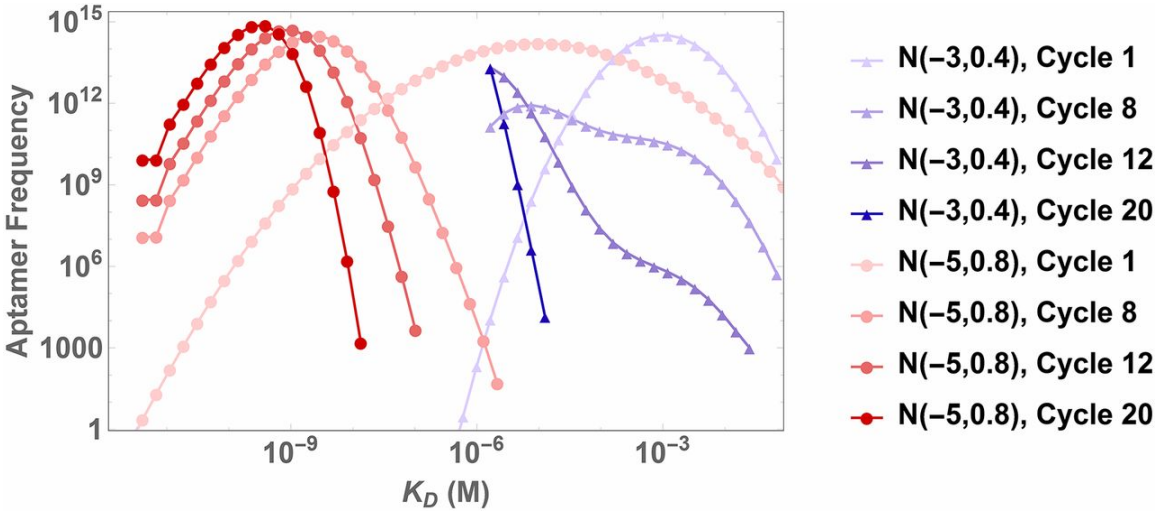

Figure 2.2: Initial distribution affects SELEX dynamics.

We plot the distribution of ligand binding affinities with increasing SELEX cycles for the same experimental parameters and two different assumed Gaussian distributions at cycle 1, N(−3,0.4) (blue triangles) and N(−5,0.8) (red dots). The dynamics of the two cases are totally different. For N(−5,0.8), the distribution shifts to the left and becomes considerably narrower, while for N(−3,0.4), the distribution additionally skews to the left, such that after cycle 12 the highest affinity binders have outcompeted the rest of the distribution.

In addition to shape, we also explore the assumption that the K_D distribution is continuous everywhere. Whereas this assumption is credible near the distribution mean where the frequency of molecules is sufficiently high, we expect it to fail at the extreme tails where stochastic effects dominate and highly specific sequences can create gaps in the affinity distribution. Indeed, it is well-known that even single base-pair changes in DNA can dramatically impact binding (30). Ligands in this regime are highly prized, but may also be at highest risk to be lost to stochastic effects due to low copy numbers.

We investigate this risk by using an initial $N(-4,0.4)$ distribution and adding a fixed noise component that is randomly sampled from a uniform distribution in log-space. Fig. 2.3 and Movie S1 show a comparison of 2 Monte Carlo simulations where there are only 20 ligands present in the range of $K_D<10^{-7}$M, i.e., where the continuous Gaussian distribution is effectively zero. We find that random binding effects can lead to total loss of those 20 ligands, resulting in a very different evolution of the K_D distribution from cycle 12 onward in comparison with the case where only 2 of those ligands survive. SI, Fig. 2.S2 shows a distribution of the mean ligand K_D at cycle 20 obtained from 250 Monte Carlo simulations, confirming this enormous variability in outcomes, where the mean K_D value spans 3 orders of magnitude.

These results demonstrate the tremendous sensitivity of selection dynamics to both distribution shape and noise. They illustrate that selection pressures are parameterized not only by extrinsic environmental conditions given by the experimental setup, such as the tunable quantities Ks and T_{tot}, but just as importantly by inherently

uncertain intrinsic population parameters that govern relative competition between ligands of varying affinities.

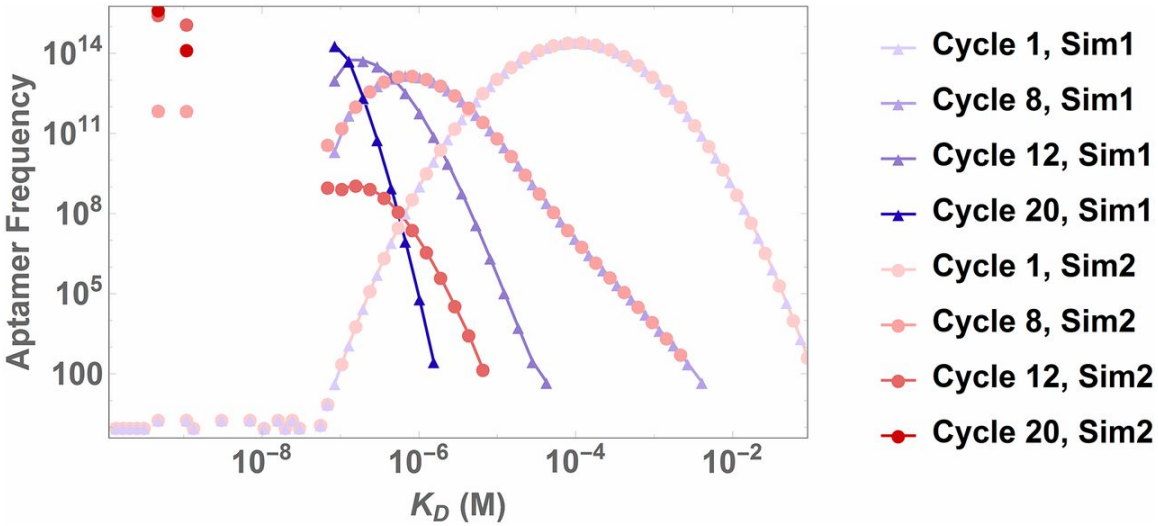

Figure 2.3: Noise affects SELEX dynamics.

We fix the experimental parameters, the initial Gaussian distribution N(−4,0.4) and the added noise of only 20 additional ligands initially present between $K_D=10^{-10}$M and 5×10^{-8}M. Two different Monte Carlo simulations from these identical initial conditions show dynamics of selection under random loss of the 20 strongest binders (blue triangles), versus dynamics when only two of those strong binders with affinities between 10^{-10} and 10^{-9}M are selected (red dots). In the latter case, these two high-affinity binders completely dominate the distribution from cycle 12 on and outcompete the remaining ligands with low affinities ($K_D>10^{-7}$M).

Revising Target Concentration

Optimization of the target concentration, T_{tot}, has long stood as a critical step in adjusting selection pressure based on experimental parameters (14–16). However, the results from the previous section now suggest that in addition to these experimental factors, the intrinsic affinity distribution of the initial ligand pool may have a significant influence on the impact T_{tot} exerts on the overall selection pressure. In light of this, we revisit the topic to study this impact by varying both $T_{tot}$and the initial distribution. Fig. 2.4 and Movie S2 first show the dramatic impact of target concentration on selection dynamics. The results indicate that $T_{tot}=10^{-4}$M (blue) provides optimal selection out of the three investigated target concentrations that use the initial Gaussian distribution $N(-4,0.4)$. To investigate the impact of T_{tot} more systematically, Fig. 2.5 shows the mean K_D value of ligands selected after 20 cycles as a function of T_{tot} for 9 different initial distributions. Note that as the mean K_D decreases, the average binding strength of the pool increases. Fig. 2.5 confirms that intermediate values of T_{tot} yield optimal selection. SI, Fig. 2.S7 A–C further shows that adding noise to the initial distributions introduces additional variability, but provides similar qualitative results. Interestingly, we find that different initial distributions can have very different optimal T_{tot}, stressing the importance of devising a strategy to mitigate this impact and thereby control the inherent uncertainty associated with the initial K_D distribution.

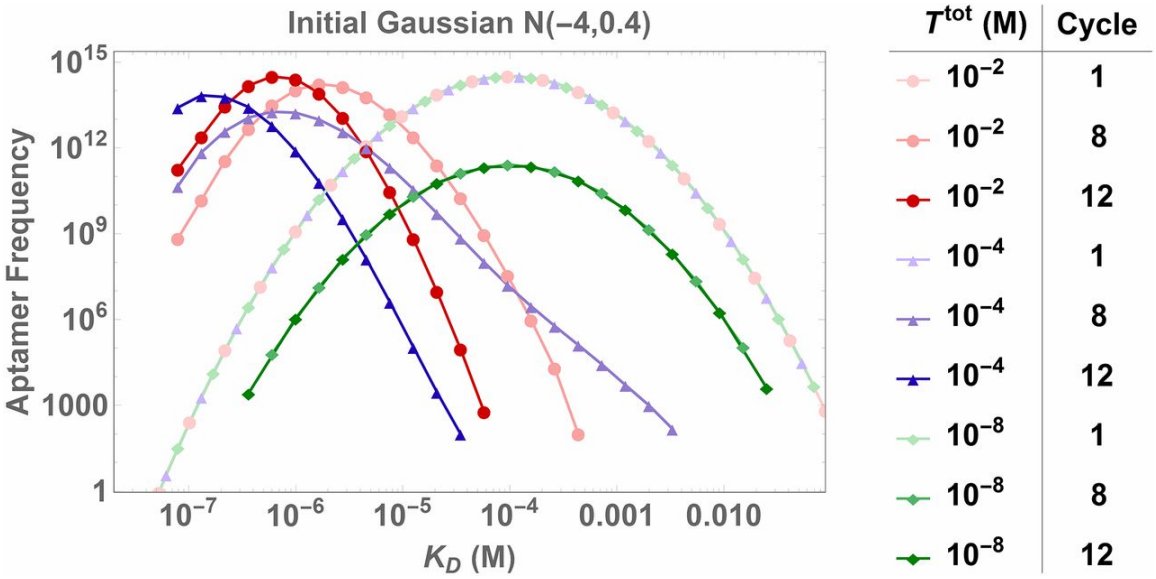

Figure 2.4: Impact of target concentration on SELEX dynamics.

Evolution of K_D distribution for three different values of the target concentrations is shown. Under a high target concentration of $T_{tot}=10^{-2}$M, the distribution shifts to the left and narrows, but does not skew toward high-affinity ligands. Additional skewing is achieved by reducing to $T_{tot}=10^{-4}$M, which increases selection pressure by intensifying ligand competition. However, further reduction to $T_{tot}=10^{-8}$M has the opposite effect and actually halts selection. In this case, the target concentration is so low that nonspecific ligand–substrate equilibria dominate selection dynamics and nullifies the selection pressure.

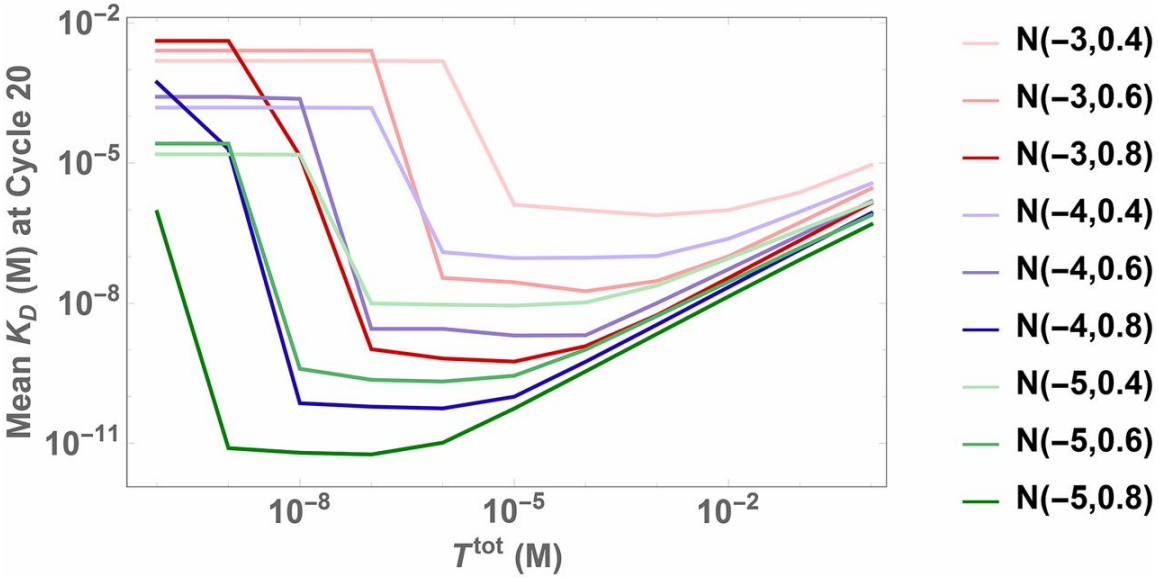

Figure 2.5: Optimal target concentrations strongly depend on assumed initial K_D distribution.

The plot shows the mean K_D as a measure of pool binding strength for the SELEX pool at cycle 20 using different constant target concentrations. Depending on the initial distribution of ligands, we find vastly different optimal target concentrations, i.e., concentrations with lower mean K_D.

K_S dependence and nonspecific selection

Our hybrid model has allowed us to explore the impact of the unknown initial K_D distribution and the target concentration T_{tot}, which are both present in all SELEX protocols. However, our model additionally introduces a ligand–substrate interaction that has never before been studied and offers a unique opportunity to apply it toward more recent selection schemes aimed at small-molecule aptamer development (26–28). We therefore extend our analysis to study uncertainties that govern an optimum K_S, and observe how changes in K_S impact selection dynamics for different K_D distributions.

Fig. 2.6 and Movie S3 show the evolution of a single initial K_D distribution for three different values of K_S, showing an optimal outcome for $K_S = 10^{-12}$M (blue). Noting these dynamics, we next vary K_S systematically and observe the mean K_D value of ligands present at cycle 20 for 9 different initial K_D distributions (Fig. 2.7 and SI, 2.S7 D–F). Similar to target concentration, we find an optimum in the intermediate ranges of K_S and a clear dependence on the initial distribution. However, contrary to target concentration, the mean K_D for smaller K_S is relatively insensitive. Thus, these results suggest that a lower value of $K_S = 10^{-16}$M would provide similar results across a multitude of initial distributions.

As it pertains to small-molecule selection schemes, these results provide useful insights into the impact that substrate binding affinity has on selection efficiency, and may offer some guidance in the appropriate selection of a substrate material. The results also provide general insights into the impact of partitioning efficiency and nonspecific binding on selection across various initial distributions and suggest that a given

partitioning efficiency or fraction of nonspecific selection can impact different initial distributions in vastly different ways.

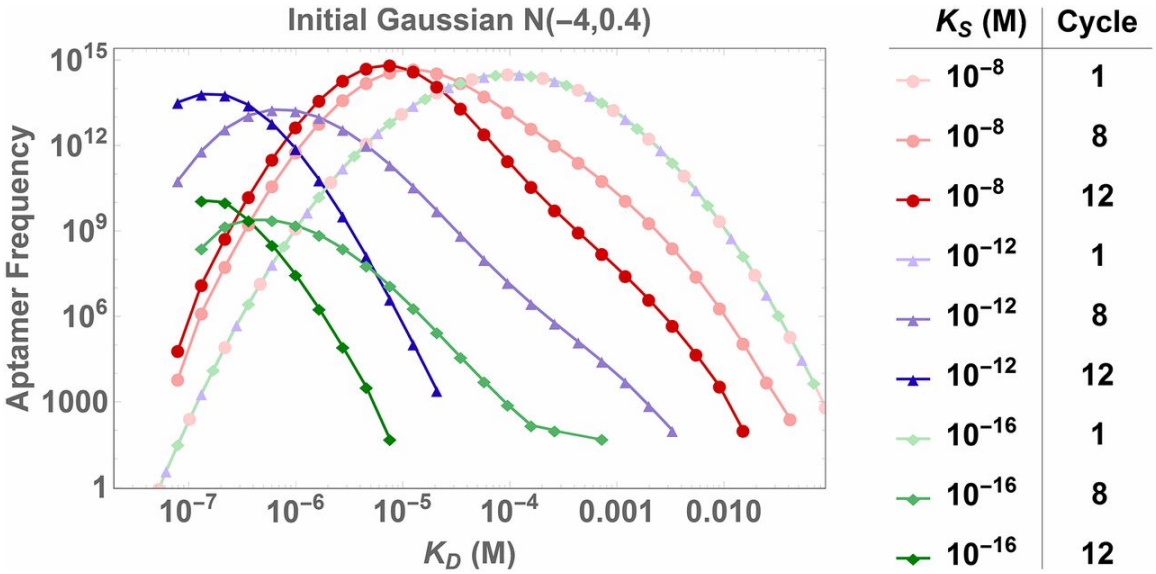

Figure 2.6: Impact of K_S on SELEX dynamics.

The plot shows the evolution of K_D distribution for three different values of K_S . Similar to target concentration, we find an optimal outcome in the middle range ($K_S = 10^{-12}$M, blue), but the outcome for low K_S is not as adverse as for low T_{tot}, because the distribution still shifts toward low K_D with increasing cycles.

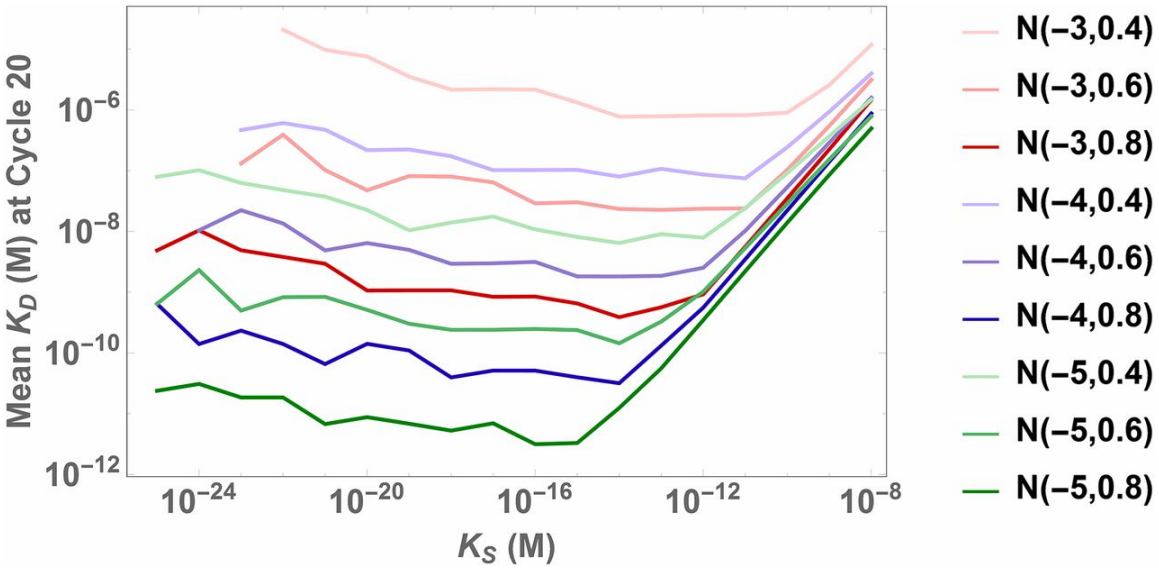

Figure 2.7: Optimal K_S depends on initial distribution.

Plot of mean K_D for the SELEX pool at cycle 20 using different values of K_S . Reducing K_S from its optimal value does not increase the mean K_D as strongly as a reduction of the target concentration from its optimum, as shown in Fig. 2.5.

Improving selection efficiency

We have shown that the initial K_D distribution has a tremendous impact on selection efficiency and plays a significant role in modulating the impact of experimental parameters such as T_{tot} and K_S. These results highlight that whereas established protocols are expected to perform well for some distributions, they may perform moderately for others. To address this variability in outcomes, we finally explore strategies to mitigate these impacts using only the experimental parameters T_{tot} and K_S. As a metric for our analysis, we introduce the quantity $\phi(c)$, which describes the fraction of ligands with K_D $<10^{-10}$M at cycle $c=\{1,\ldots,C\}$. Using this quantity, we further introduce two measures of efficiency: success probability $\Phi=\phi(C)$ and success speed SC defined as the cycle c at which $\phi(c)=0.5\phi(C)$.

We have seen that K_S and T_{tot} play distinct roles in the evolutionary dynamics of the K_D distribution. However, both parameters exhibit regimes of optimal selection that depend heavily on the initial distribution mean and width. Figs. 2.5 and 2.7 show that high values for T_{tot} and K_S have a similar impact across all distributions, and suggest a conservative approach of beginning at these high values for the initial cycles. This reduces the risk of eliminating high-affinity, low copy number ligands early on. As these high-affinity ligands are amplified in subsequent rounds, T_{tot} and K_S can be lowered to rapidly eliminate the remaining low-affinity ligands (SI, Figs. 2.S3 and 2.S4). Whereas ideas to lower the target concentrations have been discussed previously (26), our results indicate that other parameters such as K_S can be tuned simultaneously to improve outcome across a multitude of initial distributions and stochastic conditions. Fig. 2.8

shows Φ and SC obtained from 50 Monte Carlo simulations of an improved protocol where both T_{tot} and K_S are decreased over the cycles as described in SI Appendix, Table 2. These results are compared with the original protocol with constant values $T_{tot}=10^{-4}$M and $K_S=10^{-12}$M (26); SI, Fig. 2.S5 shows $\phi(c)$ including the SDs. Using six different initial Gaussian distributions with noise added similar to Fig. 2.3, we observe that the improved protocol with decreasing T_{tot} and K_S is faster and leads to a higher fraction of high-affinity binders than the original protocol. As an alternative metric of protocol performance, SI, Fig. 2.S8 shows the evolution of mean K_D across the cycles, and also introduces two alternative protocols where T_{tot} or K_S are decreased faster than in the improved protocol. The results indicate that whereas faster decreases can further improve performance for some distributions, they may also lead to adverse outcome for others.

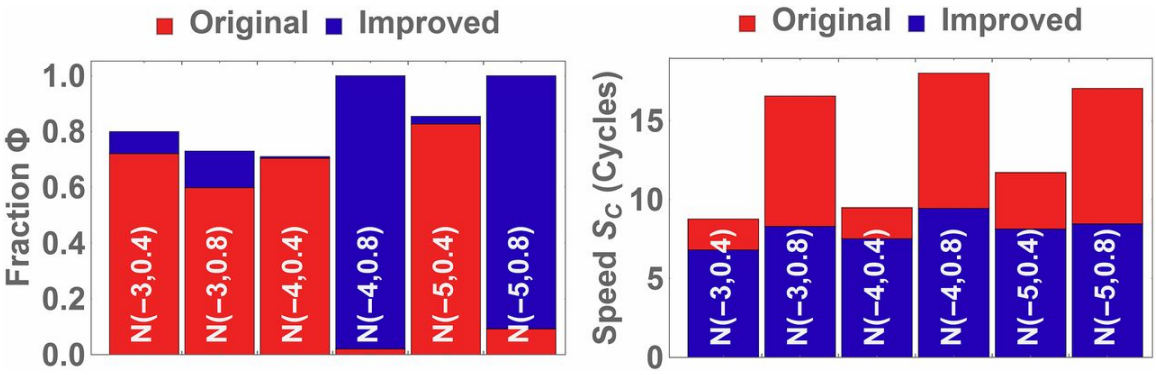

Figure 2.8: Plots comparing the fraction of high-affinity ligands Φ and speed of SELEX for six different K_D distributions.

The values are obtained from averaging 50 Monte Carlo simulations. We observe that decreasing T_{tot} and K_S over the rounds will lead to a higher fraction of strong binders (here with $K_D<10^{-10}$M) and will reach this fraction faster than when T_{tot} and Ks are kept constant.

Discussion

The results of our modeling draw striking parallels to outcomes in evolutionary biology, where environmental parameters define a fitness landscape and competition can change this landscape to influence survival and reproduction (31). Within SELEX, ligands compete for target molecules to ensure survival into the next cycle, whereas substrate binding traps the ligands and leads to their removal. Reduction of target concentration can increase competition, but when few target molecules are present, even high-affinity binders are unlikely to find a target. Similar to competition in limited resources scenarios, we find that the chance of survival for even the highest affinity ligand strongly depends on the strengths of the other ligands present in the population. Our surprising finding that a handful of high-affinity ligands can outcompete a pool of 10^{15} ligands is also seen in evolutionary biology, where highly advantageous traits can quickly spread in a population, given the right conditions. The model enables one to identify the parameters impacting selection, and can thus be used to improve selection efficiency. A further important component of evolution in biological systems is mutations. Mutations in SELEX can also appear during PCR amplification, but usually lead to reduced affinities of the strongest aptamers (30), so we ignored them in our current approach. However, for some SELEX protocols, mutations can be beneficial to expand the experimental sampling space (32), and it may be interesting to extend our model to those protocols.

In summary, our model provides a better understanding of the impact of the uncertainties in SELEX, and how experimental parameters can be tuned to improve outcome and speed of this expensive and time-consuming protocol. We have demonstrated how optimization of the parameters can enhance selection efficiency of one protocol dramatically, and we envisage that simple adaptations of our model can be used to improve the many other established protocols, as well as guide the design of novel protocols, which aim to limit the impact of uncertainties in selection methods.

Supplementary Information

Parameter	Symbol	Default Value
Number of Unique Aptamers	M^A	$4^{25} \approx 1.13 \times 10^{15}$
Number of Bins	M^B	100
Number of Cycles	C	20
Stochastic Model Threshold	Θ	100
Substrate Concentration Cycle 1	S^{tot}	$1.66 \times 10^{-6}M$
Substrate Concentration Cycle 2 Onward	S^{tot}	$1.66 \times 10^{-7}M$
Target Concentration	T^{tot}	$10^{-4}M$
Incubation Volume	V	$50\mu l$
Aptamer-Substrate Dissociation	K_S	$10^{-12}M$
PCR Amplification Factor	α_{PCR}	50

Table 2.S1: Default parameters.

Cycle Round	T^{tot}	K_S
1	$10^{-3}M$	$10^{-11}M$
2	$10^{-4}M$	$10^{-12}M$
3	$10^{-4}M$	$10^{-13}M$
4	$10^{-4}M$	$10^{-14}M$
5	$10^{-5}M$	$10^{-15}M$
6-10	$10^{-5}M$	$10^{-15}M$
11-20	$10^{-6}M$	$10^{-18}M$

Table 2.S2: The improved protocol.

Cycle Round	T^{tot}	K_S
1	$10^{-3}M$	$10^{-11}M$
2	$10^{-4}M$	$10^{-12}M$
3	$10^{-4}M$	$10^{-13}M$
4	$10^{-4}M$	$10^{-14}M$
5	$10^{-5}M$	$10^{-15}M$
6-10	$10^{-5}M$	$10^{-15}M$
11-20	$10^{-6}M$	$10^{-18}M$

Table 2.S3: Alternative protocols used in Fig. S8.

The fast K_S decrease protocol decreases Ttot similarly to the improved protocol, but K_S is decreased faster through the cycles. Likewise, the fast T_{tot} decrease protocol decreases K_S similarly to the improved protocol, but T_{tot} is decreased faster.

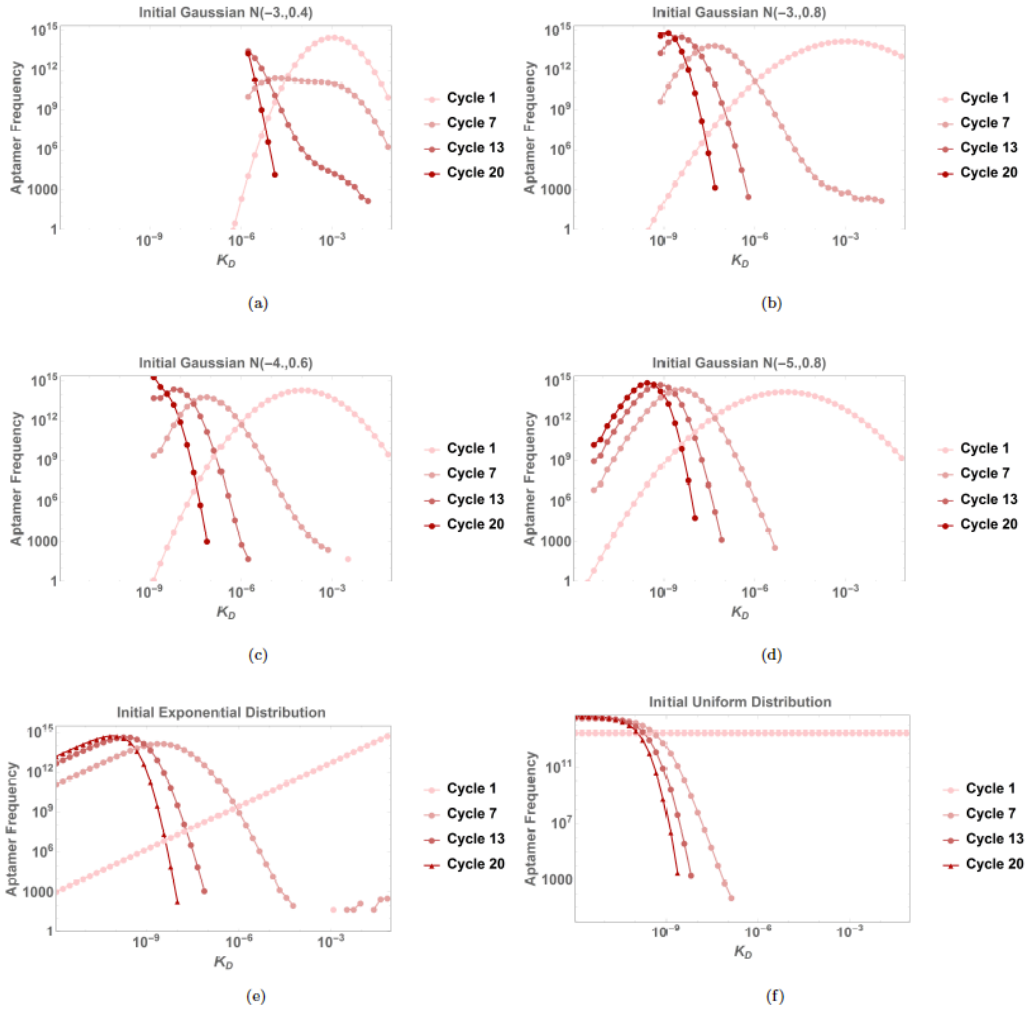

Figure 2.S1: SELEX dynamics over 20 cycles for six initial K_D distributions: four Gaussians with different means and standard deviations, an exponential distribution, and one uniform distribution.

While we certainly would not expect the real K_D distribution for targets of interest to be exponential or uniform, it is interesting to see the dynamics of SELEX for such distributions, and illustrates the point that the distribution has an important influence on selection efficiency. We see that the dynamics of evolution is quite different: in the uniform case, due to the large number of good binders, the bad ones are quickly removed. The exponential distribution (e) or the broad Gaussian (d) guarantee a sufficient number of good binders being present, but the protocol is not able to magnify the best binders (here, $K_D = 10^{-12}$M) and slightly worse binders still form the peak of the distribution. On the other hand, for the Gaussians (a)-(c), the protocol quickly selects the best binders present in the initial distribution.

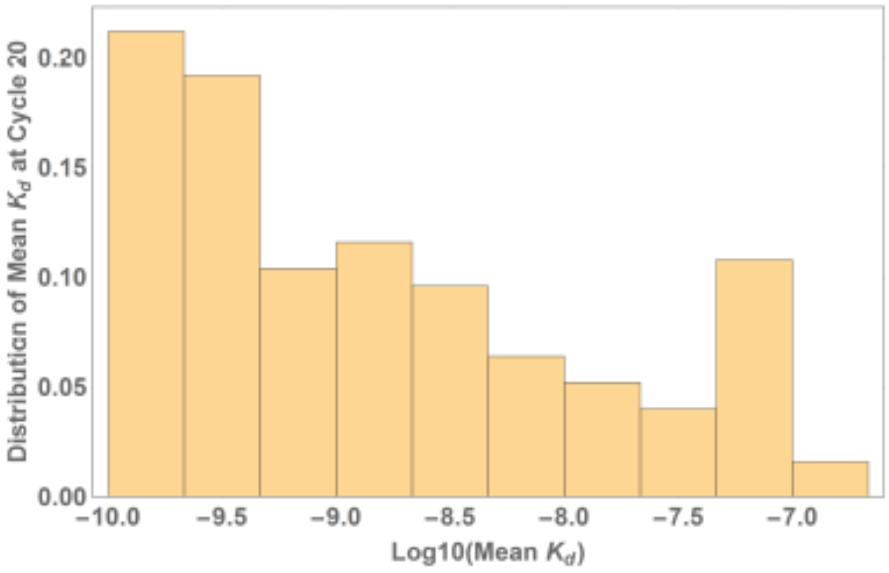

Figure 2.S2: Plot showing the distribution of the mean K_D of aptamers present after cycle 20 for the same experimental condition presented in Fig 2.3.

The distribution reflects results from 250 identical Monte Carlo simulations.

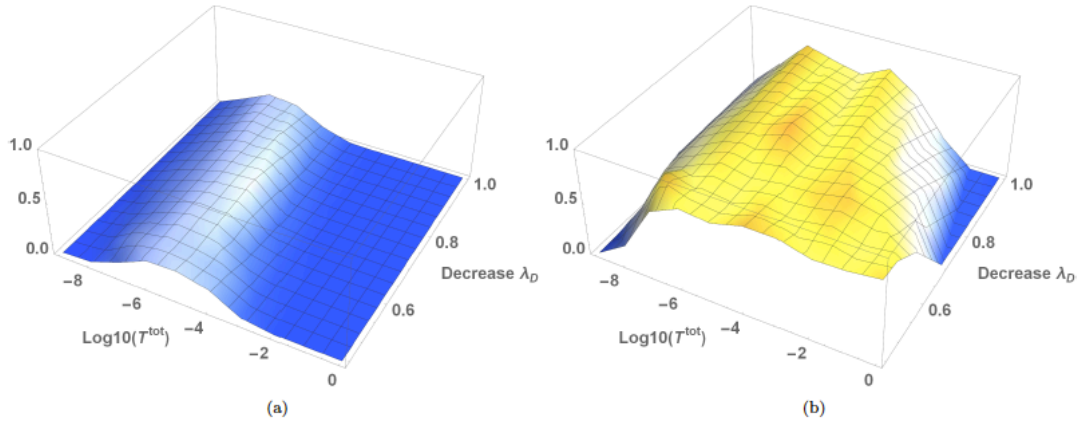

Figure 2.S3: Snapshots of the fraction of high-affinity aptamers with binding affinities stronger than $K_D = 10^{-10}$ M.

(a) At cycle 8, target concentrations close to 10^{-6} are the first to yield an increase of high affinity aptamers, and faster decreases broaden the range of target concentrations that lead to strong binders. (b) At cycle 20, a wide range of target concentrations leads to strong binders, unless the initial concentration is too low ($T_{tot}<10^{-7}$M). Very high

concentrations ($T_{tot}>10^{-1}M$)) can still lead to success, provided the concentration is decreased sufficiently fast.

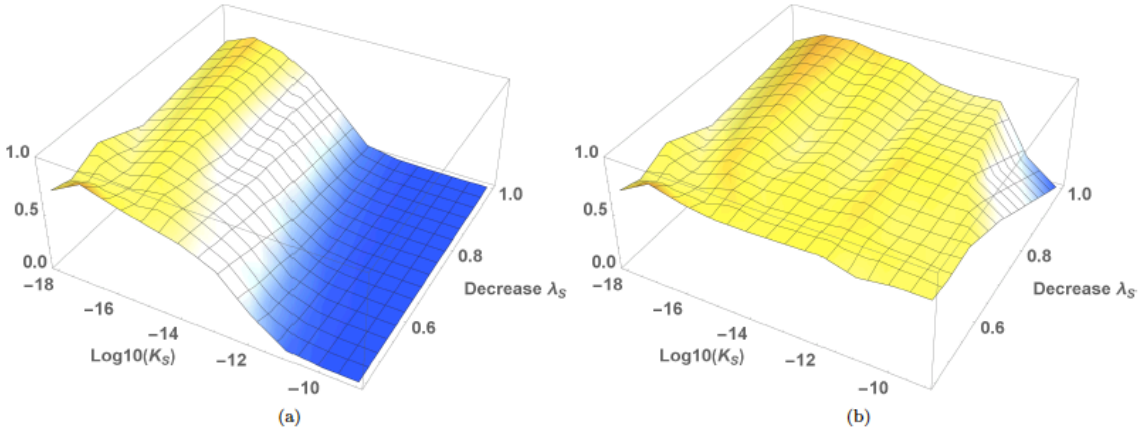

Figure 2.S4: Snapshots of the fraction of high-affinity aptamers with binding affinities stronger than $K_D = 10^{-10}$ M at two different cycles as a function of initial K_S.

(a) At cycle 8, lower initial values of K_S result in faster enrichment of high affinity aptamers. (b) At cycle 20, most initial values of K_S eventually lead to enrichment of high-affinity aptamers, provided the affinity is decreased sufficiently fast.

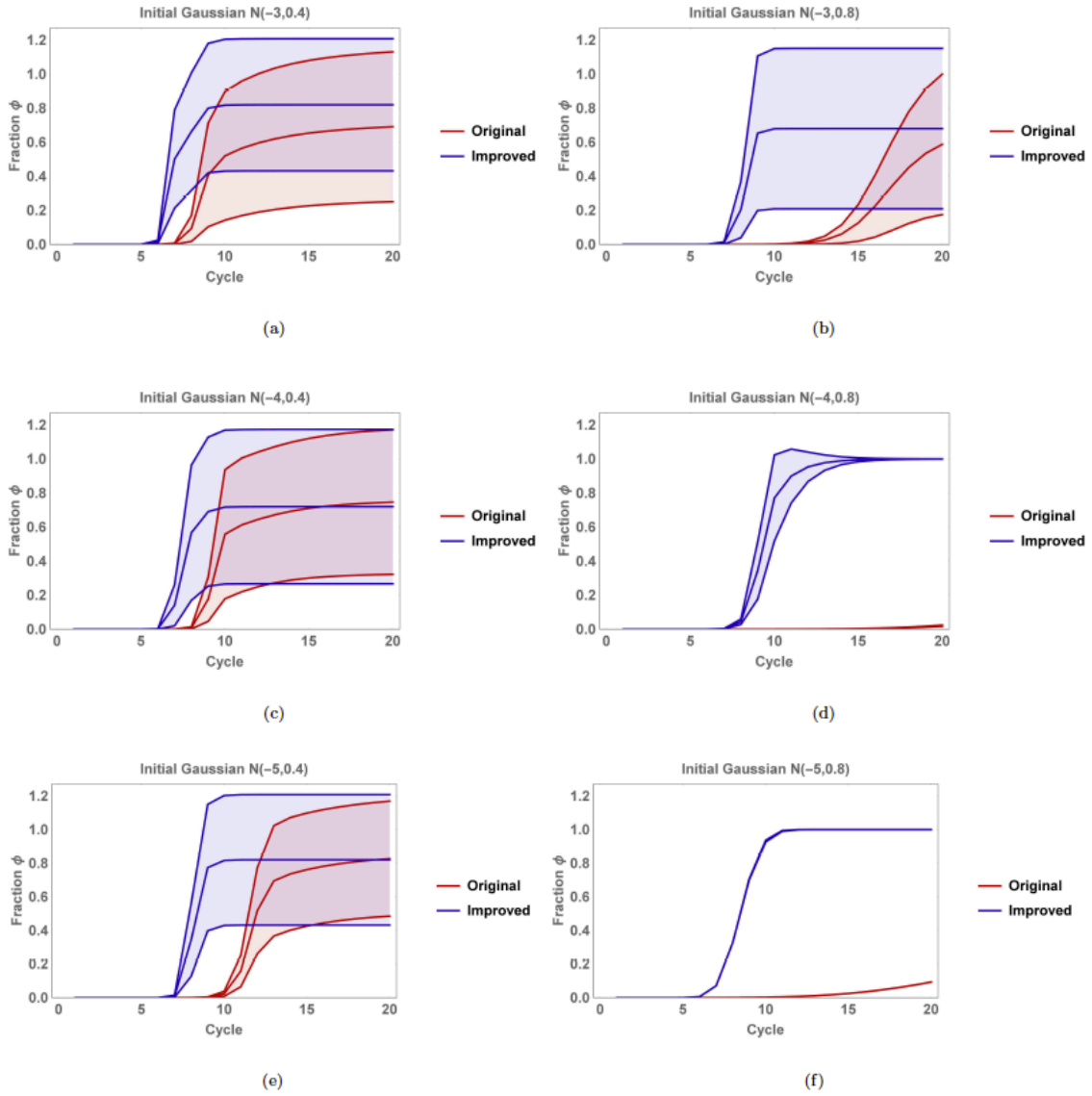

Figure 2.S5: Fraction of high affinity binders at each cycle.

Comparison of SELEX dynamics between the original SELEX protocol (Table S1 with constant T_{tot} and K_S, and the improved protocol with decreasing target concentration and K_S for six different Gaussian distributions with means -3,-4,-5 and standard deviations 0.4, 0.8. Plot shows fraction of good binders (binding stronger than 10^{-10} M over SELEX cycles and the standard deviation observed over 50 Monte Carlo simulations. We notice that the improved case reaches higher or equal plateaus as the constant protocol, and it reaches the plateau much faster. There is less variability in the success measures when the initial Gaussian is broader, as in those cases there is initially a large number of good binders present, so stochastic effects play only a small role

.

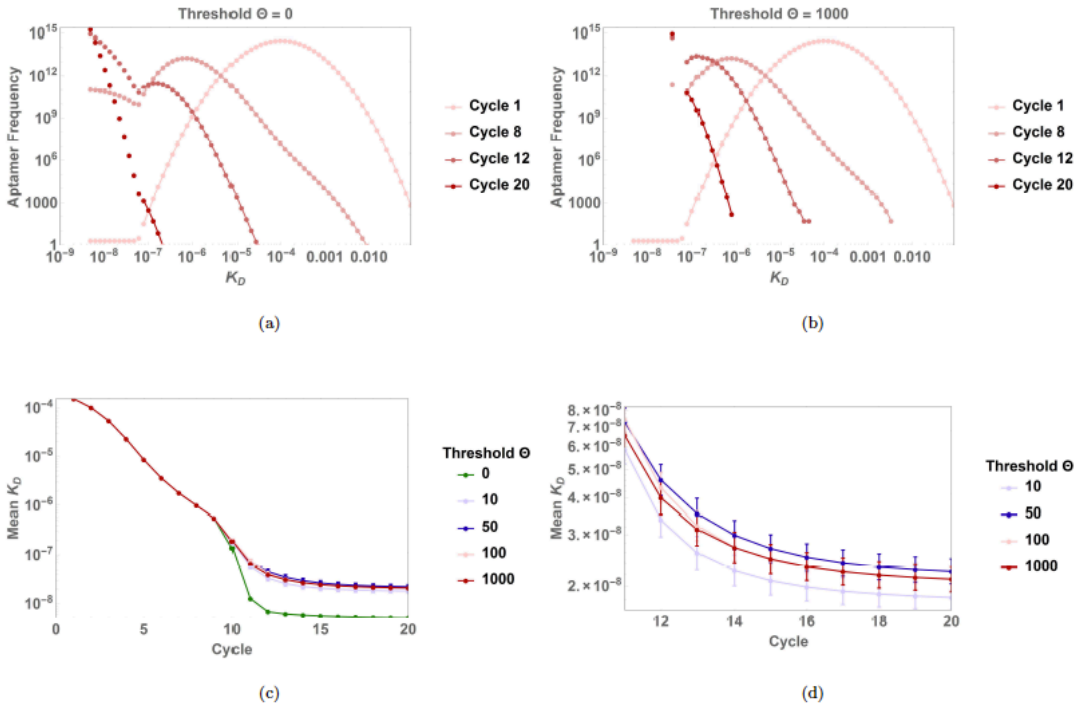

Figure 2.S6: Threshold dependence.

We show the dependence of simulation results on the threshold that defines when we use the stochastic or the deterministic model. In each case the initial distribution is a Gaussian N(-4,0.4) with added noise. (a) and (b) show sample realization for threshold=0 and threshold=1000. The case of threshold=0 means that we always use the deterministic model. Thus, there is no loss of molecular species, and the handful of aptamers in the low K_D range always outperform the ones with higher K_D. The case for threshold =1000 does appear qualitatively similar to the case threshold =100 used in the main text, so repeated runs are required to obtain statistical data. (c) and (d) show the dependence of the mean K_D value, as a measure of protocol performance, for different values of threhsold. Each graph is obtained from averaging 150 Monte Carlo simulations and shown with the corresponding error bars. In (c), we notice no visible differences between thresholds between threshold=0 and threshold=1000 before cycle 10. This is because in those initial cycles, the randomness seen in low K_D ligands does not affect the bulk of the ligand distribution, and thus does not affect the mean K_D significantly. From cycle 10 on, the results of the non-zero thresholds deviate from the case threshold=0, which predicts lower mean K_D values. This is because for deterministic dynamics, there is no loss of ligands possible throughout the cycles, and those high affinity ligands always take over the distribution after some time, as seen in (a). (d) shows the same data zoomed in, focusing on the non-zero thresholds from cycle 10 on. We see that from threshold =100 to threshold =1000 there is no visible difference, justifying the choice of threshold =100 in other simulations performed in this work.

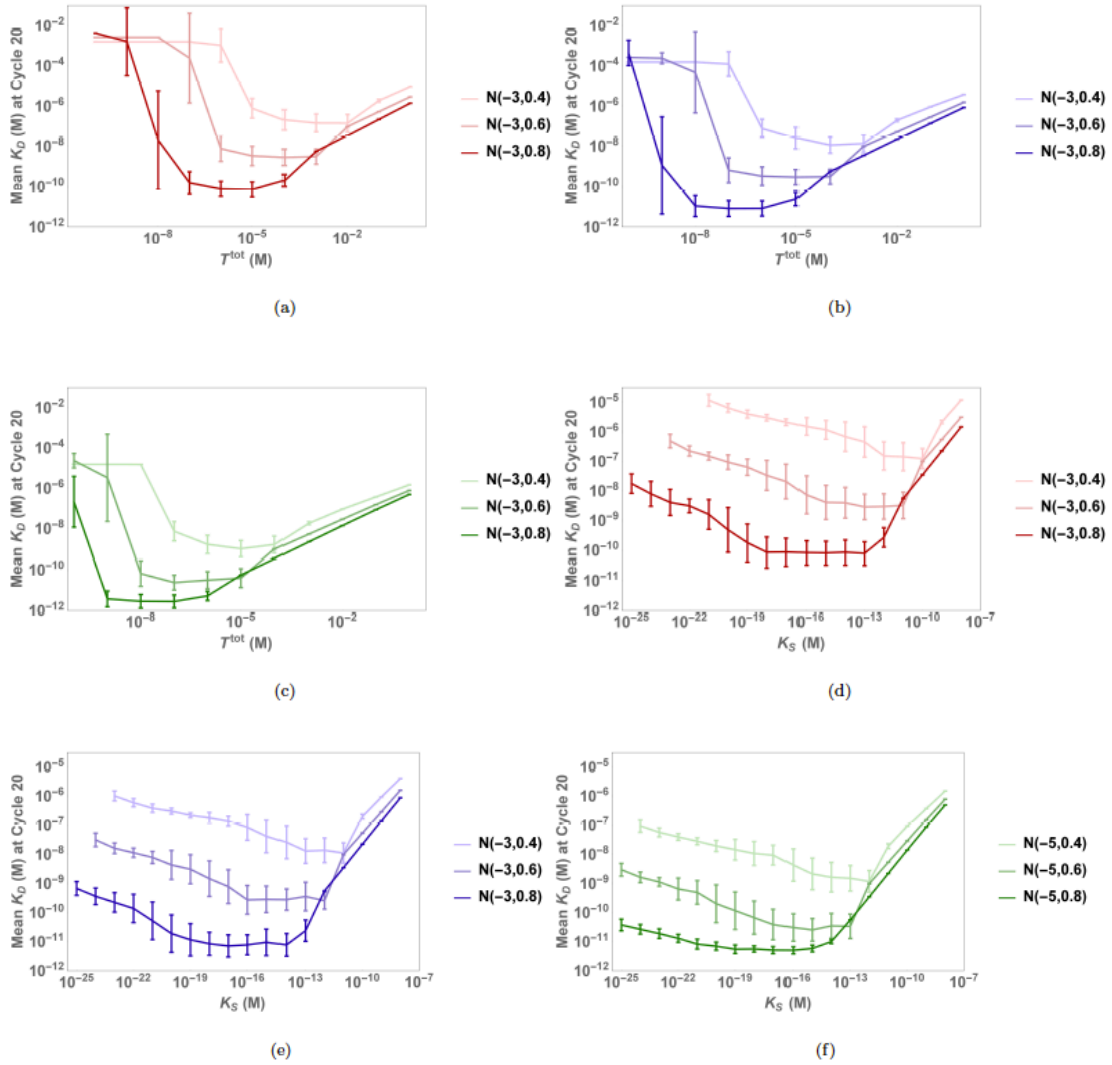

Figure 2.S7: The dependence of the mean K_D value on target concentration and substrate binding affinity is shown at cycle 20 for 9 different initial distributions of ligands.

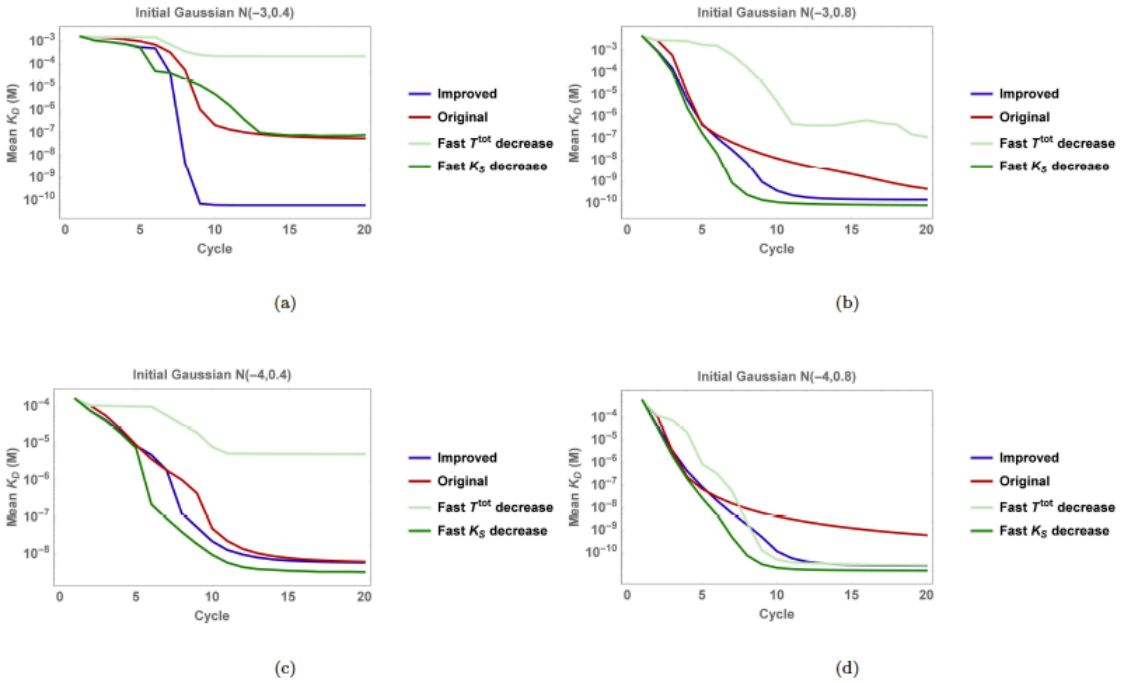

Figure 2.S8: The mean K_D of the distribution as a performance metric for the protocol is shown for 6 different initial Gaussian distributions with added noise, and 4 different protocols.

Chapter 2 References

1. Blind M & Blank M (2015) Aptamer selection technology and recent advances. *Molecular Therapy Nucleic Acids* 4(1): e223.

2. Bunka DH & Stockley PG (2006) Aptamers come of age--at last. *Nature Reviews Microbiology* 4(8): 588-596.

3. Chen C & Kuo T (2007) Simulations of SELEX against complex receptors with a condensed statistical model. *Computers & Chemical Engineering* 31(9): 1007-1019.

4. Chen C, Kuo T, Chan P & Lin L (2007) Subtractive SELEX against two heterogeneous target samples: Numerical simulations and analysis. *Computers in Biology and Medicine* 37(6): 750-759.

5. Cherney LT, Obrecht NM & Krylov SN (2013) Theoretical modeling of masking DNA application in aptamer-facilitated biomarker discovery. *Analytical Chemistry* 85(8): 4157-4164.

6. Cho M, *et al* (2013) Quantitative selection and parallel characterization of aptamers. *Proceedings of the National Academy of Sciences* 110(46): 18460-18465.

7. Ellington AD & Szostak JW (1990) In vitro selection of RNA molecules that bind specific ligands. *Nature* 346(6287): 818-822.

8. Farokhzad OC, *et al* (2006) Targeted nanoparticle-aptamer bioconjugates for cancer chemotherapy in vivo. *Proceedings of the National Academy of Sciences* 103(16): 6315-6320.

9. Ferguson BS, *et al* (2013) Real-time, aptamer-based tracking of circulating therapeutic agents in living animals. *Science Translational Medicine* 5(213): 213ra165-213ra165.

10. Gillespie DT, (2000) The chemical langevin equation. *Journal of Chemistry and Physics* 113: 297-306.

11. Gillespie DT (1976) A general method for numerically simulating the stochastic time evolution of coupled chemical reactions. *Journal of Computational Physics* 22(4): 403-434.

12. Gillespie DT, Hellander A & Petzold LR (2013) Perspective: Stochastic algorithms for chemical kinetics. *Journal of Chemistry and Physics* 138(17)

13. Hoinka J, *et al* (2015) Large scale analysis of the mutational landscape in HT-SELEX improves aptamer discovery. *Nucleic Acids Research* 43(12): 5699-5707.

14. Irvine D, Tuerk C & Gold L (1991) SELEXION: Systematic evolution of ligands by exponential enrichment with integrated optimization by non-linear analysis. *Journal of Molecular Biology* 222(3): 739-761.

15. Katilius E, Flores C & Woodbury NW (2007) Exploring the sequence space of a DNA aptamer using microarrays. *Nucleic Acids Research* 35(22): 7626-7635.

16. Keefe AD, Pai S & Ellington A (2010) Aptamers as therapeutics. *Nature Reviews Drug Discovery* 9(7): 537-550.

17. Levine HA & Nilsen-Hamilton M (2007) A mathematical analysis of SELEX. *Computational Biology and Chemistry* 31(1): 11-35.

18. Luo X., Pitre S., Dumontier M., Dehne F., Mckeague M., Derosa M.C., Golshani A.,Green J., (2010) Computational approaches toward the design of pools for the in vitro selection of complex aptamers. *Rna* 16(11): 2252-2262.

19. McKeague M & DeRosa MC (2012) Challenges and opportunities for small molecule aptamer development. *Journal of Nucleic Acids* 2012

20. Nguyen V, Kwon YS, Kim JH & Gu MB (2014) Multiple GO-SELEX for efficient screening of flexible aptamers. *Chemical Communications* 50(72): 10513-10516.

21. Nowak MA & Sigmund K (2004) Evolutionary dynamics of biological games. *Science* 303(5659): 793-799.

22. Park J, Tatavarty R, Kim DW, Jung H & Gu MB (2012) Immobilization-free screening of aptamers assisted by graphene oxide. *Chemical Communications* 48(15): 2071-2073.

23. Roh C, Kim SE & Jo S (2011) Label free inhibitor screening of hepatitis C virus (HCV) NS5B viral protein using RNA oligonucleotide. *Sensors* 11(7): 6685-6696.

24. Sefah K*, et al* (2014) In vitro selection with artificial expanded genetic information systems. *Proceedings of the National Academy of Sciences* 111(4): 1449-1454.

25. Seo Y, Nilsen-Hamilton M & Levine HA (2014) A computational study of alternate SELEX. *Bulletin of Mathematical Biology* 76(7): 1455-1521.

26. Shangguan D*, et al* (2006) Aptamers evolved from live cells as effective molecular probes for cancer study. *Proceedings of the National Academy of Sciences* 103(32): 11838-11843.

27. Stoltenburg R, Nikolaus N & Strehlitz B (2012) Capture-SELEX: Selection of DNA aptamers for aminoglycoside antibiotics. *Journal of Analytical Methods in Chemistry* 2012

28. Sun F, Galas D & Waterman MS (1996) A mathematical analysis of in vitro molecular selection-amplification. *Journal of Molecular Biology* 258(4): 650-660.

29. Tuerk C & Gold L (1990) Systematic evolution of ligands by exponential enrichment: RNA ligands to bacteriophage T4 DNA polymerase. *Science* 249(4968): 505-510.

30. Van Kampen NG (1992) *Stochastic Processes in Physics and Chemistry,* (North Holland.

31. Vant-Hull B, Payano-Baez A, Davis RH & Gold L (1998) The mathematics of SELEX against complex targets. *Journal of Molecular Biology* 278(3): 579-597.

32. Wang J, Rudzinski JF, Gong Q, Soh HT & Atzberger PJ (2012) Influence of target concentration and background binding on in vitro selection of affinity reagents. *PloS One* 7(8): e43940.

CHAPTER 3: Quantitative bioassay to identify antimicrobials through drug interaction fingerprint analysis

Published in the following manuscript:
Weinstein, Z.B. & Zaman, M.H. 2017, "Quantitative bioassay to identify antimicrobial drugs through drug interaction fingerprint analysis", *Scientific reports,* vol. 7, pp. 42644.

Abstract

Drug interaction analysis, which reports the extent to which the presence of one drug affects the efficacy of another, is a powerful tool to select potent combinatorial therapies and predict connectivity between cellular components. Combinatorial effects of drug pairs often vary even for drugs with similar mechanism of actions. Therefore, drug interaction fingerprinting may be harnessed to differentiate drug identities. We developed a method to analyze drug interactions for the application of identifying active pharmaceutical ingredients, an essential step to assess drug quality. We developed a novel approach towards the identification of active pharmaceutical ingredients by comparing drug interaction fingerprint similarity metrics such as correlation and Euclidean distance. To expedite this method, we used bioluminescent *E. coli* in a simplified checkerboard assay to generate unique drug interaction fingerprints of antimicrobial drugs. Of 30 antibiotics studied, 29 could be identified based on their drug interaction fingerprints. We present drug interaction fingerprint analysis as a cheap, sensitive and quantitative method towards substandard and counterfeit drug detection.

Introduction

Drug interactions for a given phenotype are defined as a combinatorial effect of two drugs that is different than expected(1). Drug interactions may be described as positive or negative depending on whether relatively more or less drug, respectively, is required to achieve a particular phenotype compared to single agents(1). Sensitive drug interaction testing is limited by the combinatorial explosion necessary to evaluate multiple doses of drugs. Traditional checkerboard testing involves isobologram analysis for a square matrix of increasing concentrations of two drugs on each axis. Berenbaum theorized a simplified method of testing for drug interactions in which approximately equi-inhibitory doses of two agents are combined, titrated and compared to single agent dose response curves(2).

Drug interaction analysis is a powerful tool to select potent combinatorial therapies(3), predict connectivity between cellular components(4) and drug mechanism of action(5). Drugs with similar mechanism of action tend to have similar but not identical drug interaction profiles(6). For instance, Yeh et al. report that the two 30S ribosome inhibitors doxycycline and tetracycline cluster together in a network analysis based on their drug interaction profiles. However, amongst the 21 antibiotics they are tested against, they show unique interactions with ampicillin and chloramphenicol suggesting these varied combinatorial responses may be used to create a unique interaction fingerprint for these agents. A study of antifungal drug interactions found that two ergosterol synthesis (ERG11) inhibitors fluconazole and miconazole varied in their tendency towards suppressive drug interactions(7). This suggests that drug interaction

fingerprinting may be possible for any active pharmaceutical ingredient (API) that imparts a quantifiable phenotype such as luminescence or growth inhibition.

A key feature of drug quality assessment is the detection of APIs. Current methods to detect APIs are of limited utility due to great expense (HPLC (8), NMR (9)), or low sensitivity/specificity (thin layer chromatography and colorimetric assays) of detection systems(10). These technologies are often of prohibitive cost, grid power and expertise to be of widespread use in low- and middle-income countries (LMICs). Biosensors may fill the gap for a fast drug detection system that transduces a change in growth phenotype to a specific change in luminescence output. Bacteria based biosensors are inherently reproducible and are low cost to maintain and propagate. The luminescence phenotype is especially desirable as it limits the possibility of false positives that may arise from contamination in assays evaluating turbidity. Previous bacterial biosensors have been used for the detection of antibiotic susceptibility in mycobacteria(11) and in drug mechanism of action studies by pharmaceutical companies(12).

Approximately 25% of medicines in LMICs are counterfeit or substandard, the majority of which are antimicrobial agents13. Substandard medicines may contain impurities such as synthetic byproducts and degradation products or the wrong dose of active ingredient14. A recent survey of thousands of antimalarials, anti-mycobacterials and other antibiotics found 40% of sampled drugs failed quality testing in some world regions(15). This is of particular concern due to the high global burden of malaria and tuberculosis. Tuberculosis alone accounts for 1.5 million deaths annually(16). Besides the

immediate concerns about treatment failures, substandard medicines are also hypothesized to contribute to the worldwide trend toward antimicrobial resistance (17,18). Successful treatment of tuberculosis requires months of medication, the mainstay of which is rifamycins (e.g., rifampicin, rifapentine, rifabutin), often in combination therapy with 2-3 other agents(19). Multidrug-resistant and extensively drug-resistant tuberculosis in particular necessitate prolonged combination therapy with up to 5 medications(20). In 2014, there were an estimated 9.6 million new cases of tuberculosis, and 190,000 deaths due to multi-drug resistant tuberculosis(16). Novel means to address the issue of substandard medicines may therefore decrease the health and financial burden associated with long-term treatment of all forms of tuberculosis.

In this study, we report a simplified checkerboard assay to quantify drug interactions between pairs of compounds in Escherichia coli expressing luciferase to expedite experiments. This methodology combines the sensitivity of larger checkerboard assays(1) to identify cellular response at varying levels of inhibition with the ease of setup of high throughput 2x2 drug interaction matrices by the Bliss independence model, which is a multiplicative model assuming drugs act independently. Using this method, we are able to generate unique profiles of bacterial response to varying combinations of drugs to create unique fingerprints for four anti-mycobacterial agents and a major rifampicin degradation product. By comparing drug interaction profile similarity metrics, we developed a novel approach towards the identification of APIs.

Results

Drug interaction profiling from a systematic screen of 25 antibiotics in E. coli

In order to determine the feasibility of drug interaction profiling for API identification, we first analyzed a previously published dataset and unpublished data (literature set) of all pairwise interactions among 25 antibacterial drugs in *E. coli* for unique drug interaction profiles(21). Figure 1a illustrates the experimental and analytical system for assessing drug interactions with the checkerboard method. In this paradigm, drug interactions are scored based on the concavity of isophenotypic contours. Concavity is determined by the logit function: log(x/(1-x)) - log(y/(1-y)); where x and y are normalized drug concentrations to achieve a similar level of inhibition. Figure 1b shows a subset of interaction scores for two drugs tested against a panel of 25 antibiotics in replicate. Drug interaction fingerprints (or profiles) are defined as a series of drug interaction scores for each query drug tested against a set of array drugs. Drug interaction fingerprints can be utilized for drug identification if the same drug tested against an array of other drugs is more similar to biological replicates than to the profile of other drugs. We used Spearman's correlation and Euclidean distance between profiles as a metric of similarity (Figure 3.1c).

To account for systematic experimental biases, we created 1,000 sets of profiles (25x25x1000, per set) with randomized replicate order from the literature set. The randomized profiles were then compared to identify drug identity based on minimal Euclidean distance and maximum correlation between interaction scores in replicate 2 vs. replicate 1, with each agent's replicate 1 interaction score iteratively compared to

replicate 2 scores of all 25 other agents. The most frequent replicate 2 ‘match’ of 1000 randomizations was compared to replicate 1 identity to assess successful identification of API. Distance metrics alone could identify up to 8/25 antibiotics using drug interaction scores with a single drug partner (Figure 3.1d). Kanamycin, fusidic acid and erythromycin had the greatest single agent identification value (8,7,6 correct identifications, respectively). Starting with kanamycin, each of the remaining drugs was iteratively added to the analysis based on rank of single drug identification success. With all agents considered, 22/25 drugs were identified by distance alone (Figure 3.1e). Considering the entire dataset, the Spearman’s correlation between replicate profiles successfully identified 23/25 agents. A combined analysis of correlation and distance scores allowed the successful identification of all but one of the 25 drugs (spectinomycin incorrectly identified as chloramphenicol). However, spectinomycin ranked as the second most likely agent by these metrics.

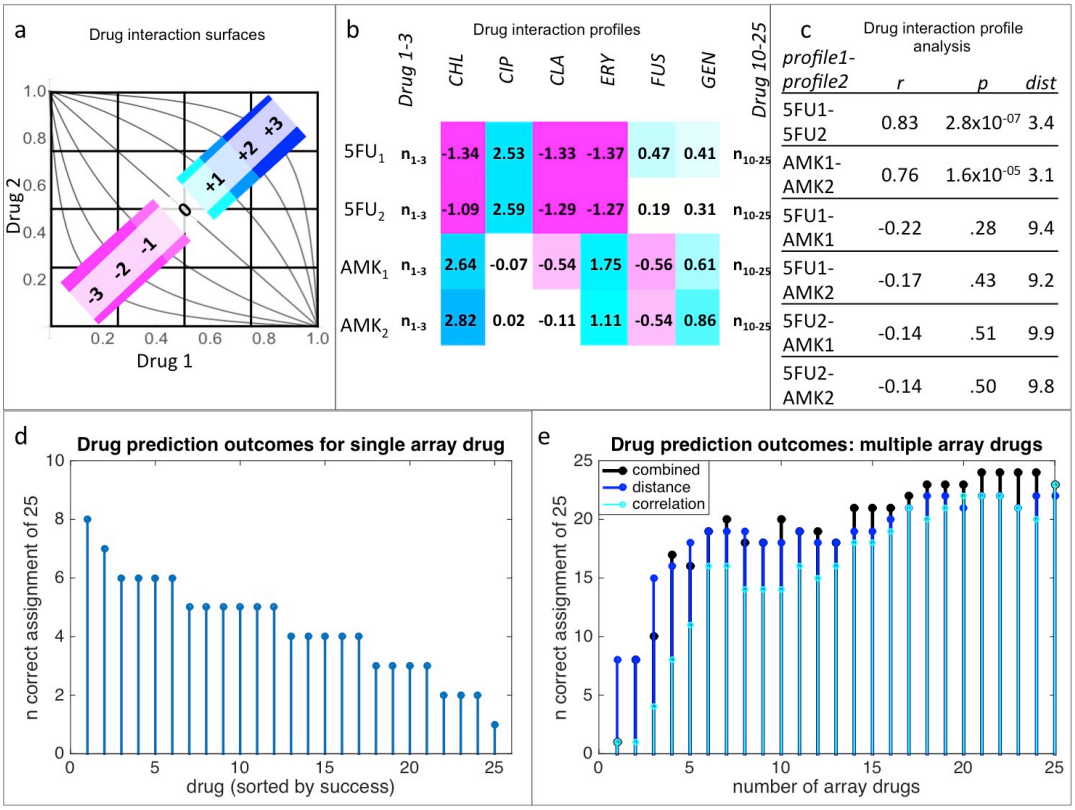

Figure 3.1: Drug interaction profile based identification of antibiotics

We first analyzed a previously published dataset of all pairwise interactions among 25 antibacterial drugs in *E. coli* for unique drug interaction profiles[21]. Drug interactions were approximated by the concavity of isophenotypic contours in a 2D grid of linearly increasing drug concentrations on each axis (a). Positive interactions are represented in blue, negative in magenta. A subset of interaction score replicates for query drugs, 5-fluorouracil and amikacin tested with array drugs chloramphenicol, ciprofloxacin, clarithromycin, erythromycin, fusidic acid and gentamicin (b). Drug interaction profiles are defined as a series of drug interaction scores for each query drug tested against a set of array drugs. Drug interaction profiles can be utilized for drug detection systems if the correlation of drug interaction profiles is greater for replicates than for comparison to other drug profiles (c). Alternatively, profile similarity may be based on minimum Euclidean distance between vectors of interaction. Euclidean distance between randomized replicates for query drugs against a single array drug could accurately identify 8/25 query drugs (d). Drugs were ranked based on their single agent identification value, serially added to the profile array and assessed for identification value based on Euclidean distance and/or rank correlation of profiles (e). Using the entire dataset, Euclidean distance, rank correlation and combined data could be used to correctly identify the vast majority of query drugs (22, 23, 24 correctly identified of 25, respectively).

A simplified sensitive method to assess drug interactions

To expedite the construction of novel drug interaction profiles, drugs were evaluated based on the inhibition of luminescence of a constitutively expressed luciferase plasmid in *E. coli*. We used a simplified approach to the classic 8x8 checkerboard method of drug interaction by sampling 24 concentrations of single or combined drugs (Figure 3.2a). An interaction score was computed based on the amount of drug mixture required to achieve 40% inhibition of luminescence compared to constituent drugs as single agents: $\log_2$(observed/expected dose) (Figure 3.2b). Positive and negative interactions indicate that relatively more or less drug respectively was required for the combination to achieve the same level of inhibition than expected based on constituent drugs and a score of zero indicates no interaction (Figure 3.2c).

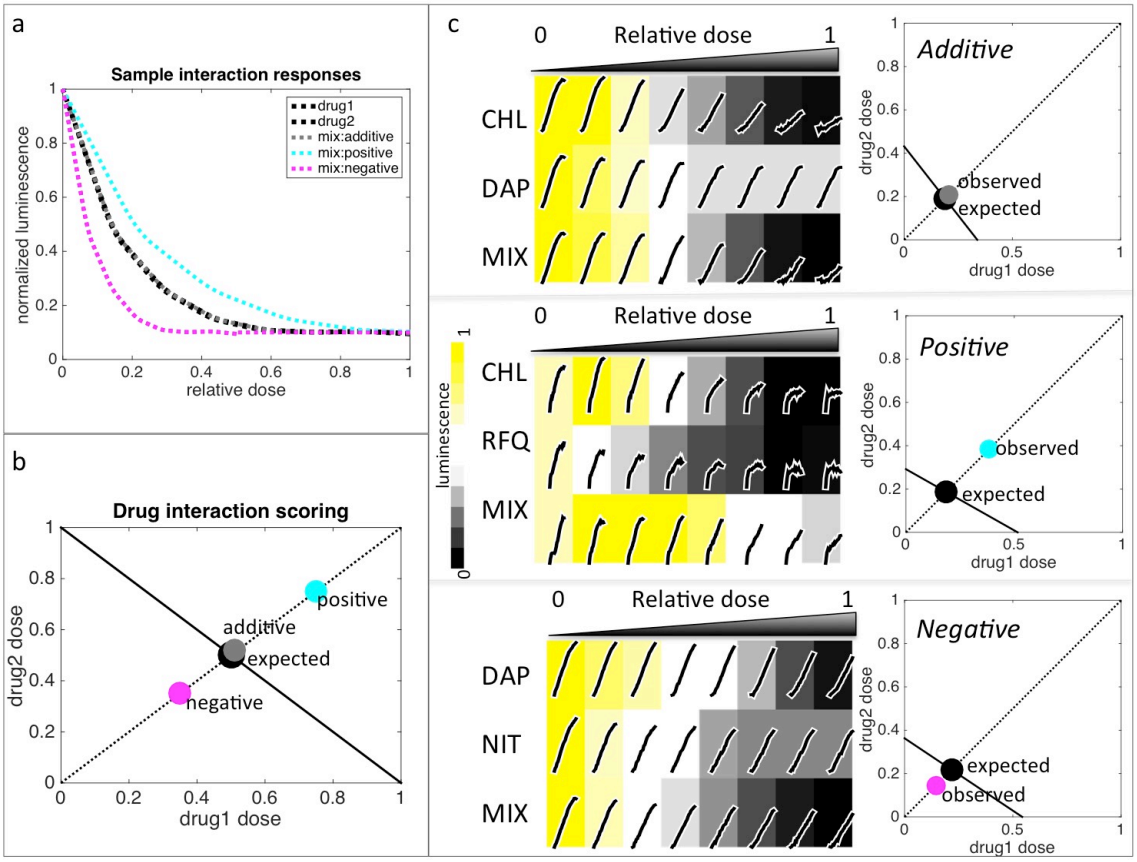

Figure 3.2: An expedited approach to drug interaction testing

We used a simplified, yet sensitive, approach to the classic 8x8 checkerboard method of drug interaction by sampling 24 concentrations of single or combined drugs for inhibition of *E. coli* luminescence (a). Drug interactions were assessed based on the amount of drug mixture (1/2 each drug 1 and drug 2, relative to individual drug dose) required to achieve the same inhibitory level as the constituent drugs (2) for 40% inhibition of luminescence (IC40). Doses are plotted in Cartesian coordinates with the x and y intercepts set to drug 1 and drug 2 IC40; the intersection of the line y=x and that connecting the two intercepts defines the expected IC40 of the combination (b). The interaction score is defined as $\log_2$(observed/expected distance from the origin). Deviations are classified as negative or positive interactions. Representative experiments for additive, positive and negative interactions (c upper, middle and lower panels, respectively). At left are plots of raw RLU over time superimposed on a heatmap of luminescence output. Luminescence output was defined as the area under the RLU curve normalized to the no drug condition. At right are plots illustrating expected (black dot) and observed (grey, cyan and magenta dots) doses of drug mixture required to achieve 40% inhibition of luminescence, based on drug 1 and drug 2 IC40 levels. CHL = chloramphenicol, DAP = dapsone, NIT = nitrofurantoin, RFQ = rifampicin quinone, MIX = mixture of drug 1 and drug 2.

We validated our method by assessing the pairwise interactions between 5 query drugs and 8 array drugs. The 5 query drugs contained 4 anti-mycobacterial agents [dapsone, rifampicin, rifabutin, rifapentine] and one major degradation product of rifampicin [rifampicin quinone]. The array drugs consisted of antibiotics of varying mechanisms of action [chloramphenicol, erythromycin, mupirocin, nalidixic acid, nitrofurantoin, oxacillin, streptomycin, and tetracycline]. The query drugs were selected based on their significance in tuberculosis treatment; array drugs were selected to provide a diverse range of interactions. All query drugs were also tested in combination with each other. Interaction score biological replicates were highly reproducible (Spearman's r = 0.87, $p = 5x10^{-16}$) (Figure 3.3a) and normally distributed (Figure 3.3b). Clustering analysis revealed that the rifampin related agents and degradation products had similar interaction profiles compared to the anti-folate agent dapsone (Figure 3.3c). Rifampin-related drugs were enriched for antagonistic interactions (mean interaction scores, 0.47 - 0.58) while dapsone was more likely to have negative or null interactions (mean interaction score, 0).

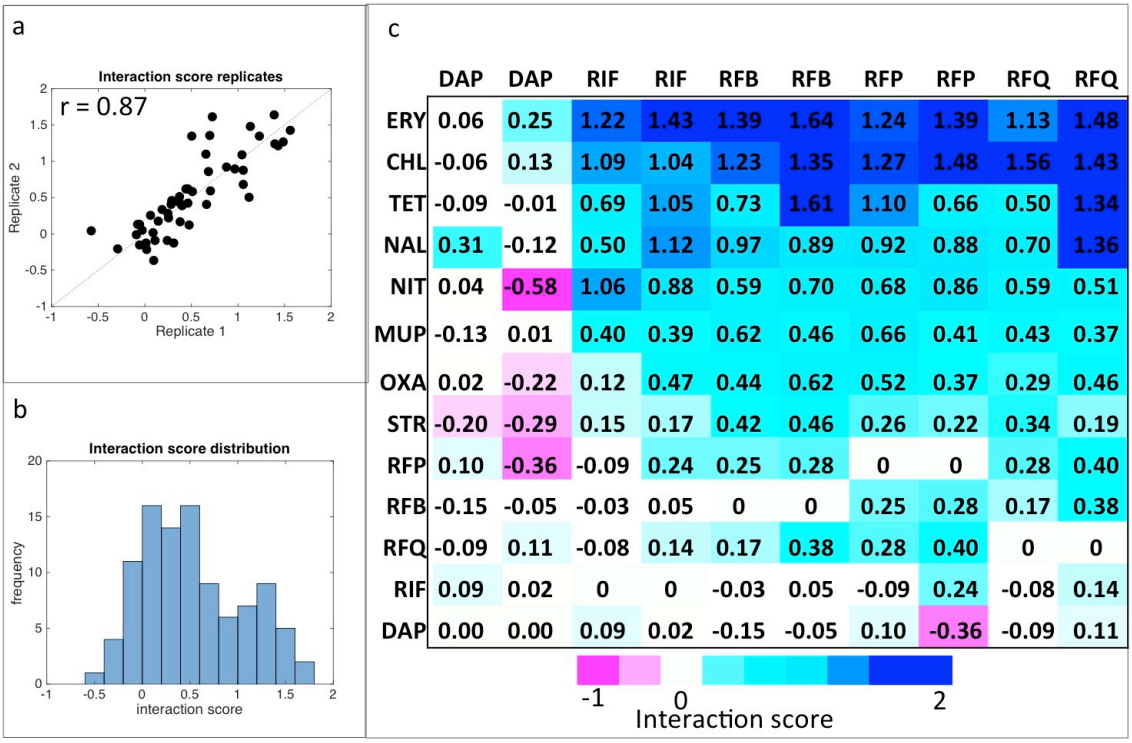

Figure 3.3: Interactions of pairwise combinations of anti-mycobacterial and antibiotic drugs are highly reproducible

Interaction score replicates for 50 drug pairs were highly reproducible (Spearman's r = 0.87, $p = 5x10^{-16}$) (a) and normally distributed based on the one-sample Kolmogorov-Smirnov test (b). The mean interaction score of all tested drug pairs (c). Clustering analysis reveals that dapsone had the most distinct interaction profile of all the query drugs, and rifapentine and rifabutin were most similar to each other. Of the rifampicin-related compounds, rifampicin quinone had the least similar correlation of interaction profiles, suggesting that drug interaction profiling may be used to differentiate rifampicin from its oxidation product.

Drug interaction profiling of anti-mycobacterial agents in E. coli

In accordance with the literature set, drug profile similarity of the bioluminescent set was initially assessed by examining correlation and distance between 1,000 sets of randomized profile replicates (13x5x1000, per set). Array drugs varied greatly in their identification power for query drugs (Figure 3.4a). When only single drug interaction scores were considered among the profile, streptomycin was the drug with the best identification power (4/5 drugs identified accurately for the majority of 1,000 randomizations). Nitrofurantoin and rifabutin had the next best identification power (3/5 drugs each). The remainder of agents could be used to accurately identify up to 2 of the 5 query drugs (Figure 3.4b). Dapsone, the only non-rifamycin agent tested, was unsurprisingly the simplest of the five query drugs to identify with 10/13 array drugs correctly identifying dapsone as single agents. For the majority of cases the rifampicin related drugs could be identified with 3-4 array drug data. In all, 4 array drugs were required to accurately discriminate between all 5 query drugs (Figure 3.4c). Perhaps due to the close relationship between the query drugs, correlation scores could at best identify 3/5 query drugs and weakened the identification overall when combined with distance scores.

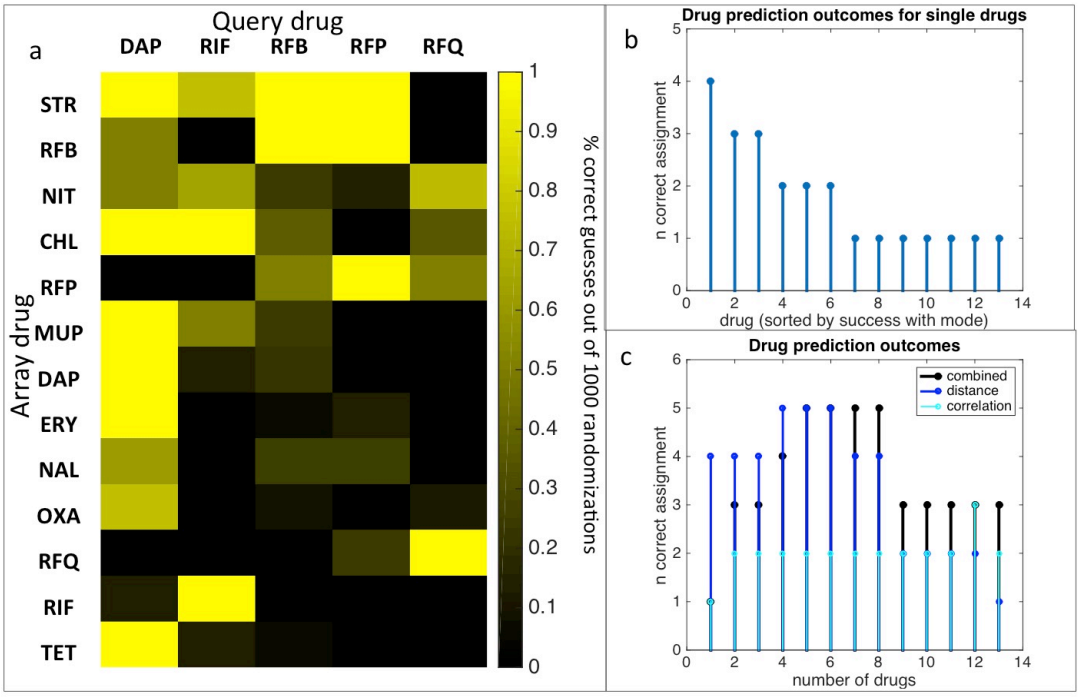

Figure 3.4: Drug identification success among the bioluminescent set of anti-mycobacterial agents

Drug profile similarity was assessed by examining correlation and distance between 1,000 sets of randomized profile replicates of the bioluminescent set. Array drugs varied greatly in their identification power for query drugs (a). Euclidean distance between randomized replicates for query drugs against a single array drug could accurately identify 4/5 query drugs (b) based on interactions with streptomycin alone. Drugs were ranked based on their single agent identification value, serially added to the profile array and assessed for identification value based on Euclidean distance and/or rank correlation of profiles (c). Using the entire dataset, Euclidean distance, rank correlation and combined data could be used to correctly identify all query drugs. Using more than 8 array drugs in the analysis weakened the number of correctly assigned query drugs.

Discussion

The World Health Organization has increasingly recognized the role of counterfeit and substandard medicines in the emergence and spread of antimicrobial resistant diseases (22). Assuring drug quality of anti-mycobacterial agents has the potential to improve outcomes for the millions of people suffering from tuberculosis in LMICs worldwide. The current challenges in cost, training and infrastructure to assess drug quality requires novel approaches to identifying active pharmaceutical ingredients. Here, we utilized differential responses to drug combinations to create unique fingerprints for anti-mycobacterial drugs.

We used bioluminescent *E. coli* to assess drug interactions between pairwise combinations of 5 anti-mycobacterial agents and 8 additional antibacterial drugs for a total of 50 drug pairs in replicate. Overall, this expedited approach to drug interaction testing was highly reproducible, retaining the ease of experimental setup normally associated with 2x2 dose combination matrices (6), while providing data for multiple levels of inhibition classically observable in checkerboard assays (23). The use of luminescence rather than turbidity as a proxy for cellular growth reduces experimental runtime from the typical 12-24 hours to one hour, which is more amenable to the quick assessment of drug quality.

Biosensors have previously been shown to relay broad drug mechanism of action such as nucleic acid, cell wall or protein inhibition using luciferase and GFP reporters for drug target expression(12,24). These biosensors have utility in drug discovery and environmental toxicology, but cannot distinguish between drugs with the same target.

Drug interaction profiling can further narrow drug mechanism as drugs within the same class tended to cluster together, and unique drug interactions within classes can distinguish individual compounds.

This technique should extend to any type of drug, so long as it elicits a quantifiable phenotype, such as luminescence. Although *E. coli* is in the phylum of Proteobacter while mycobacterium is in the phylum Actinobacteria, there is a large overlap in anti-mycobacterial agents and drugs that inhibit the growth of *E. coli*. In particular, RNA polymerase inhibiting drugs such as rifampicin, rifabutin and rifapentine are generally broad-spectrum antibiotics and therefore effective across a wide range of bacterial species (25,26). In our assay, *E. coli* are acting as a sensor and a one to one biological equivalent to mycobacteria is not essential for its utility in differentiating antimicrobial agents. However, not all anti-mycobacterial compounds affect *E. coli* growth. In such cases, the model organism *M. smegmatis* could be an alternative bacterium for creating drug interaction fingerprints (27).

The analyses above suggest that interaction testing with only four array drugs are required to successfully identify the majority of query drugs from the literature and bioluminescent sets. Therefore, several unknown compounds could be identified on a single 96-well plate of interaction assays. Of all thirty query drugs evaluated in the literature and bioluminescent sets, only one could not be accurately identified based on the analytical methods described herein. The misattribution of chloramphenicol as spectinomycin suggests a high similarity between these two ribosome inhibitors. Our method therefore allowed for near complete identification of a large subset of

antimicrobial agents, even for highly similar agents such as rifampicin, rifabutin and rifapentine. Furthermore, this method could differentiate rifampicin from rifampicin quinone, which indicates that drug interaction profiling can be used to detect the presence of drug degradation products.

A potential drawback of this approach may be the complexity of analyzing large drug-interaction datasets. This study used technologies such as a spectrophotometer and Matlab software for sensitive assessment of drug interactions. To convert this to a field test, photographic film may be used in lieu of a spectrophotometer to assess luminescence levels over time, and visual inspection can be used to verify if the drug interaction pattern matches the control drug. Alternatively, this assay could be adapted to a microfluidics based platform such as a lab in a suitcase (e.g., PharmaChk), which translates luminescence signal intensity to active pharmaceutical ingredient concentration (28).

While this study evaluated 100 drug interactions overall to find unique drug interaction patterns among 5 query drugs, we found that as few as 4 array drugs are needed to differentiate even the highly similar rifamycin related compounds. Currently, there are approximately one hundred antibiotics that are in clinical use. Our study presented a quantitative bioassay to identify 30 antimicrobial drugs, which is a large subset of available medicines. Further studies could expand the repertoire of drug fingerprints, with prioritization given to other essential medicines that are most likely to be counterfeit or substandard. Thus, quantitative drug interaction profiling has the capacity to transform ongoing efforts to reduce the harm due to substandard drugs.

Systematic drug interaction profiling has many potential applications in drug discovery, mechanism of action and underlying cellular component connectivity. This manuscript presents the possibility of utilizing new drug interaction fingerprints in order to improve drug identification with applications in the detection of substandard and counterfeit medicines. Compared to the gold standard detection system of HPLC, our approach presents a fast, inexpensive and scalable method to assess drug quality.

Materials and Methods

Experimental conditions

Experiments were conducted with wild-type strain *E. coli* K12 strain DL41 with luciferase expressing SC101 plasmid(29). Luciferase expression showed that luminescence output is highly reproducible (Replicates of area under the luminescence curve were highly correlated ($r = 0.99$, $p = 2x10^{-16}$) and well correlated with inoculum density ($r = 0.97$, $p = 8x10^{-7}$) (data not shown). All drugs were dissolved in DMSO and stored at −20°C. Bacterial cells were grown in LB liquid culture overnight and diluted 1/100 for 1 hour before final plating on 96-well plates at a final OD_{600} of 0.05 in LB with the desired drug concentrations controlled for final solvent concentration of 2% DMSO at 37°C. Plates were incubated in a temperature controlled microplate reader; with luminescence readings every 5 min. The following drugs were used in this study: chloramphenicol(CHL), dapsone (DAP), erythromycin (ERY), mupirocin (MUP), nalidixic acid (NAL), nitrofurantoin (NIT), oxacillin (OXA), rifabutin (RFB), rifapentine (RFP), rifampicin (RIF), rifampicin quinone (RFQ), streptomycin (STR), tetracycline (TET).

Drug interaction metrics

Dose response was assessed for each single drug and combination (a one to one mixture) with linear dilutions. Drug combinations are an equal mixture of single agents containing approximately one half minimal inhibitory concentration of each single agent. Dose-response curves were generated based on the area under the luminescence curve, standardized to the drug free condition, over a one-hour interval. All doses are adjusted to fraction of minimal inhibitory concentration from zero to one.

In Cartesian coordinates, the x and y intercepts are set to the concentration of drug 1 and drug 2 to reach 40% inhibition of luminescence. The interaction score is defined as $\log_2$(observed/expected dose) along the y=x axis; where the expected is determined by the intersection of y=x with the line connecting the x and y intercepts and the observed is the dose of the drug mixture required to reach 40 % inhibition of luminescence (Figure 2b). The same drug combined with itself is assumed to have zero interaction.

Drug identification metrics

Drug interaction score replicates were randomized to generate 1000 sets of replicates in order to limit systematic experimental bias in the data (Figure 5). This translates to 2 sets of matrices of 25 query drugs x 25 array drugs x 1000 randomizations for the literature set, and 2 sets of matrices of 5 query drugs x 13 array drugs x 1000 randomizations for the bioluminescent set. The Euclidean distance from each row of query drug data from set 1 to all other rows from set 2 was iteratively determined for all 1000 randomizations. Overall, this generated a matrix of 25x25x1000 comparisons of distance scores for the literature set and 5x5x1000 comparisons for the bioluminescent

set. A correct identification of the query drug was considered when the minimum Euclidean distance between each row in set 1 corresponded to the same row in set 2 (for example, rifabutin replicate 1 to rifabutin replicate 2). The same randomized datasets were assessed for the Spearman's correlation between each row of set 1 and all rows in set 2. In this setup, a correct identification of the query drug was considered when the maximum correlation between each row in set 1 corresponded to the same row in set 2 (for example, rifapentine replicate 1 to rifapentine replicate 2). Overall prediction success was determined by whether or not the correct query drug was identified by the mode of 1000 predictions for Euclidean distance and Spearman's correlation, respectively.

For the combined analysis, drug interaction score replicates were randomized to generate 1000 sets of replicates to limit systematic experimental bias in the replicates. Euclidean distance and Spearman's correlation were determined between all query drugs across replicates for all 1000 sets. For each set of replicates, the drug identification algorithm identified the query drug from replicate 1 with the minimum Euclidean distance as well as the maximum correlation with the query drug from replicate 2, for a total of 2000 predictions overall. A successful identification was based on whether the correct drug was selected by the mode of the 2000 predictions.

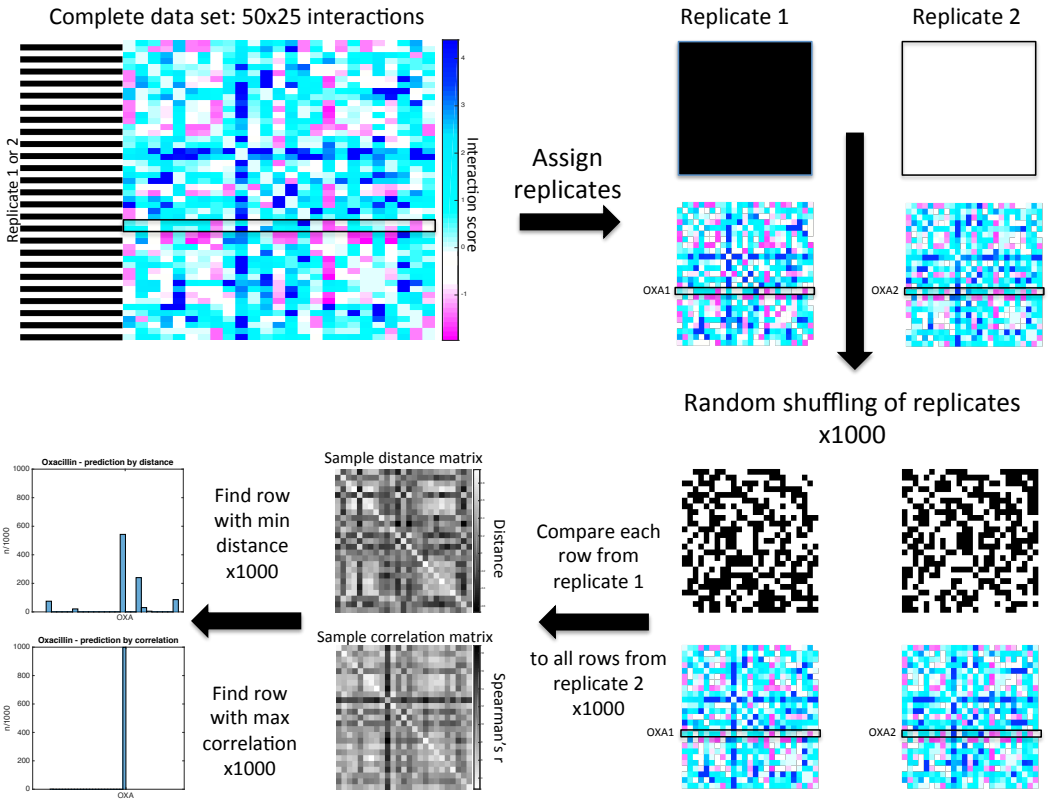

Figure 3.5: Workflow of drug interaction profile analysis.

The entire matrix of drug interactions (50x25 for the literature set) was assigned to replicate 1 or 2. To eliminate systematic bias, the replicates were randomized. This translates to 2 sets of matrices of 25 query drugs x 25 array drugs x 1000 randomizations for the literature set. The Euclidean distance from each row of data from set 1 to all other rows from set 2 was iteratively determined for all 1000 randomizations. A correct identification of the query drug was considered when the minimum Euclidean distance between each row in set 1 corresponded to the same row in set 2 (for example, oxacillin replicate 1 'OXA1' to oxacillin replicate 2 'OXA2'). The same randomized datasets were assessed for the Spearman's correlation between each row of set 1 and all rows in set 2. In this setup, a correct identification of the query drug was considered when the maximum correlation between each row in set 1 corresponded to the same row in set 2. Oxacillin was nearly always identified by its drug interaction similarity by the correlation metric, and was identified in the majority of cases by the distance metric.

Chapter 3 References

1. Greco, W. R., Bravo, G. & Parsons, J. C. The search for synergy: a critical review from a response surface perspective. *Pharmacology Reviews.* **47,** 331–385 (1995).

2. Berenbaum, M. C. A method for testing for synergy with any number of agents. *Journal of Infectious Diseases.* **137,** 122–130 (1978).

3. Zimmermann, G. R., Lehár, J. & Keith, C. T. Multi-target therapeutics: when the whole is greater than the sum of the parts. *Drug Discovery Today* **12,** 34–42 (2007).

4. Lehár, J. *et al.* Chemical combination effects predict connectivity in biological systems. *Molecular Systems Biology.* **3,** 80 (2007).

5. Farha, M. A. *et al.* Antagonism screen for inhibitors of bacterial cell wall biogenesis uncovers an inhibitor of undecaprenyl diphosphate synthase. *Proceedings of the National Academy of Sciences*. **112,** 11048–11053 (2015).

6. Yeh, P., Tschumi, A. I. & Kishony, R. Functional classification of drugs by properties of their pairwise interactions. *Nature Genetics.* **38,** 489–494 (2006).

7. Cokol, M. *et al.* Large-scale identification and analysis of suppressive drug interactions. *Chemistry and Biology.* **21,** 541–551 (2014).

8. Liu, J., Sun, J., Zhang, W., Gao, K. & He, Z. HPLC determination of rifampicin and related compounds in pharmaceuticals using monolithic column. *Journal of Pharmacology and Biomedical Analysis.* **46,** 405–409 (2008).

9. Salem, A. A., Mossa, H. A. & Barsoum, B. N. Quantitative determinations of levofloxacin and rifampicin in pharmaceutical and urine samples using nuclear magnetic resonance spectroscopy. *Spectrochimica Acta A Molecular and Biomolecular Spectroscopy.* **62,** 466–472 (2005).

10. World Health Organization (WHO). Survey of the quality of anti-tuberculosis medicines circulating in selected newly independent states of the former Soviet Union. (2013).

11. Riska, P. F. *et al.* Rapid film-based determination of antibiotic susceptibilities of Mycobacterium tuberculosis strains by using a luciferase reporter phage and the Bronx Box. *Journal of Clinical Microbiology.* **37,** 1144–1149 (1999).

12. Urban, A., Eckermann, S., Fast, B. & Metzger, S. Novel whole-cell antibiotic biosensors for compound discovery. *Applied Environmental Microbiology.* **20**, 6436–6443 (2007).

13. Pincock, S. WHO tries to tackle problem of counterfeit medicines in Asia. *British Medical Journal* **327,** 1126 (2003).

14. Johnston, A. & Holt, D. W. Substandard drugs: a potential crisis for public health. *British Journal of Clinical Pharmacology* **78,** 218–243 (2014).

15. Nayyar, G. M. L., Breman, J. G. & Herrington, J. E. The global pandemic of falsified medicines: laboratory and field innovations and policy perspectives. *American Journal of Tropical Medicine and Hygiene.* **92,** 2–7 (2015).

16. World Health Organization. Global tuberculosis report 2015. (2015).

17. Nayyar, G. M. L., Breman, J. G., Newton, P. N. & Herrington, J. Poor-quality antimalarial drugs in southeast Asia and sub-Saharan Africa. *Lancet Infectious Diseases.* **12,** 488–496 (2012).

18. Baker, S. Infectious disease. A return to the pre-antimicrobial era? *Science* **347,** 1064–1066 (2015).

19. Horsburgh, C. R., Barry, C. E. & Lange, C. Treatment of Tuberculosis. *New England Journal of Medicine.* **373,** 2149–2160 (2015).

20. World Health Organization. Companion handbook to the WHO guidelines for the programmatic management of drug-resistant tuberculosis. (2014).

21. Chandrasekaran, S. *et al.* Chemogenomics and orthology-based design of antibiotic combination therapies. *Molecular Systems Biology.* **12,** 872 (2016).

22. World Health Organization. The evolving threat of antimicrobial resistance: options for action: executive summary. (2012).

23. Cokol, M. *et al.* Systematic exploration of synergistic drug pairs. *Molecular Systems Biology.* **7,** 544 (2011).

24. Hong, H. & Park, W. TetR repressor-based bioreporters for the detection of doxycycline using Escherichia coli and Acinetobacter oleivorans. *Applied Microbiology and Biotechnology.* **98,** 5039–5050 (2014).

25. Zenkin N., Kulbachinskiy A., Bass I., Nikiforov V. Different rifampin sensitivities of Escherichia coli and Mycobacterium tuberculosis RNA polymerases are not explained by the difference in the beta-subunit rifampin regions I and II. *Antimicrobial Agents and Chemotherapy*. **4,** 1587-90 (2005).

26. Xu M., Zhou Y. N., Goldstein B.P., Jin D. J. Cross-resistance of Escherichia coli RNA polymerases conferring rifampin resistance to different antibiotics. *Journal of Bacteriology*. **8**, 2783-92 (2005).

27. Gordon S., Parish T., Roberts I. S., Andrew P. W. The application of luciferase as a reporter of environmental regulation of gene expression in mycobacteria. *Letters in Applied Microbiology*. **5,** 336-40 (1994).

28. Ho N. T., Desai D., Zaman M. H. Rapid and specific drug quality testing assay for artemisinin and its derivatives using a luminescent reaction and novel microfluidic technology. *American Journal of Tropical Medicine and Hygiene*. **6**, S24-30 (2015).

29. Kishony, R. & Leibler, S. Environmental stresses can alleviate the average deleterious effect of mutations. *Journal of Biology.* **2,** 14 (2003).

CHAPTER 4: Evolution of rifampicin resistance due to substandard medicines

Abstract

Poor-quality medicines undermine the treatment of infectious diseases such as tuberculosis, which requires months of treatment with rifampicin and other drugs. Rifampicin resistance is a critical concern for tuberculosis treatment. While sub-therapeutic doses of medicine are known to select for antibiotic resistance, the effect of degradation products on the evolution of resistance is unknown. Here, we demonstrate that substandard medicines select for gene alterations that confer resistance to standard medicines. We generated drug resistant *E. coli* and *M. smegmatis* strains by serially culturing bacteria in the degradation product of rifampicin, rifampicin quinone. Strains resistant to rifampicin quinone developed cross-resistance to the standard drug rifampicin, with some populations showing no growth inhibition at maximum concentrations of rifampicin. Sequencing of the rifampicin quinone treated strains indicated that they acquired mutations in the DNA-dependent RNA polymerase B subunit. These mutations were localized in the rifampicin resistance clusters, consistent with other reports of rifampicin resistant *E. coli* and Mycobacteria. Rifampicin quinone treated mycobacteria also had cross-resistance to other rifamycin class drugs: rifabutin and rifapentine. Our results strongly suggest that substandard may actively contribute to the development of resistance to standard medicines for rifamycin class drugs.

Introduction

The ability to treat infectious diseases such as tuberculosis is an ongoing global health issue. Tuberculosis has an incidence of approximately ten million people per year,

over 300,000 of which are rifampicin or multi-drug resistant (1). Poor quality medicines undermine the treatment of infectious diseases (2). Substandard medicines vary from standard drugs due to poor formulations associated with incorrect dose or bioavailability, or due to post manufacturing issues such as drug expiration and improper storage conditions (3, 4). Antimicrobial agents are among the most prevalent drugs to be counterfeit or substandard (3).

Drug degradation products may partially or fully replace the standard active pharmaceutical ingredient, resulting in a diminished dose to patients (5). Such under-dosing regimens are associated with the evolution of antimicrobial resistance (6). Therefore, substandard medicines are hypothesized to be a contributory factor in the worldwide trend towards antibiotic resistance. However, whether bacterial exposure to drug degradation products may cause the evolution of resistance to standard antibiotics has not been previously studied.

Rifampicin is a broad-spectrum rifamycin-derived antibiotic that is the basis of anti-tuberculosis monotherapy and combination treatment regimens (7). Of 10 million new TB cases in 2016, 600,000 were rifampicin resistant, necessitating the use of secondary treatments with increased toxicity (1, 8, 9). Rifampicin may also be used as a prophylaxis against staphylococcal and meningococcal infections, and has efficacy against a broad range of pathogens including *E. coli* and pseudomonas. Clinically, resistance may arise from drug regimen adherence issues and inappropriate treatments (10). *In vitro* studies demonstrate that subinhibitory doses of drugs may select for antibiotic resistant organisms (11).

The drug target of rifampicin is the rpoB subunit of DNA-dependent RNA polymerase (12). Resistance to rifampicin predominately arises due to mutations in the rpoB gene (13), resulting in a decreased affinity of rifampicin to its binding site (14). Three noncontiguous regions of the rpoB gene have been recognized as resistance clusters due to the high frequency of mutations at these sites in samples of drug resistant pathogens. Even single amino acid changes in the resistance clusters may confer a high degree of resistance.

Poorly synthesized or improperly stored rifampicin may contain impurities and degradation products (15). Rifampicin's main degradation product occurs from non-enzymatic auto-oxidation to form rifampicin quinone (16). The presence of rifampicin quinone in rifampicin containing tablets is a marker of poor quality (17). Rifampicin quinone may cause immunosuppression in animal models (18) and may underlie rifampicin-associated adverse drug interactions (19, 20).

The phenomenon of cross-resistance occurs when bacteria gain resistance to an antibiotic it has not been exposed to after gaining resistance to another antibiotic (21). Cross-resistance is common among antibiotics from similar classes; for example, Oz et al. reported cross-resistance between 3 DNA gyrase inhibitors in *E. coli* independently cultured under a single drug condition (22). Therefore, bacteria may be expected to acquire resistance to a standard antibiotic after exposure to a structurally similar drug degradation product.

As a model of substandard medicines, we examine rifampicin resistance arising from subtherapeutic doses and degradation products in two disparate bacterial species; *E.*

coli and *M. smegmatis*, the model organism for the study of *M. tuberculosis*. Here, we demonstrate that bacteria evolve resistance against both rifampicin and rifampicin quinone. Alarmingly, we found that bacteria that are resistant against the drug degradation product rifampicin quinone were also resistant to clinically relevant rifamycins. Our results strongly suggest that substandard medicines actively compound the worldwide antibiotic resistance problem by inducing the evolution of resistance to standard medicines.

Materials and Methods

Experimental conditions

Strains include wild type MG1655 *Escherichia coli* and MC(2) 155 *Mycobacterium smegmatis*, cultured at 37C in LB media or Middlebrook 7H9 with ADC supplement plus 0.2% glycerol, respectively. Bacteria were grown in 2-fold increments of RIF or RFQ (Sigma), with the maximum concentration at 400 ug/mL, and a final solvent concentration of 2% DMSO. We selected the bacteria in the well closest to MIC/2 to seed new bacterial cultures on the same dose series of RIF or RFQ after ~ 22 hours for *E. coli* and ~48 hours for *M. smegmatis*. Bacteria serially passaged in media plus 2% DMSO for the duration of the experiments served as the control groups.

Genotyping of RNA polymerase B rifampicin resistance clusters

Sequences were compared to the reference rpoB genes to for *E. coli* (NCBI gene ID: 948488) and *M. smegmatis* (NCBI gene ID: 4535217), using ApE plasmid editing software to identify mutations. RifRes and RfqRes populations were streaked on drug

free LB agar plates and incubated at 37C overnight to isolate colonies for sequencing. The rifampicin resistance clusters of the rpoB gene was assessed by Sanger Sequencing (QuintaraBio) using the following primers.

E. coli-rpoB-FWD 5'TCTCTGGGCGATCTGGATAC3'

E. coli-rpoB-REV 5'CAACAGCACGTTCCATACCA3'

M. smegmatis-rpoB-FWD 5'GCTGATCCAGAACCAGATCC

M. smegmatis-rpoB-REV 5'GATGACACCGGTCTTGTCG

Results

We developed an *in vitro* model to examine the role of substandard medicines in the acquisition of rifampicin resistance. Similar to previous resistance evolution studies, we grew bacteria in increasing doses of rifampicin (RIF) or rifampicin quinone (RFQ) over time. For the initial experimental setup, the maximum dose was greater than the minimal inhibitory concentration (MIC) for these compounds. We selected the bacteria in the well closest to MIC/2 to seed new bacterial cultures on the same dose series of RIF or RFQ (Methods). In such a setting, bacteria are expected to have a higher likelihood of resistance conferring mutation than in the drug free or very low drug condition, and the IC50 is expected to increase over time (22). We first studied *E. coli*, gram-negative bacteria with a short doubling time and evaluated its dose response to RIF or RFQ in 1-day cycles. We evolved resistance to RIF or RFQ, in three biological replicates. After only five cycles of selection, we observed resistance in all the strains, ranging from 2-fold to 14-fold for RIF and 32-fold to 64-fold for RFQ (Figure 4.1). We dubbed these strains

as RIF-res 1 to 3 and RFQ-res 1 to 3 and prepared glycerol stocks for further experimentation. These stocks were grown in cultures without selective pressure in drug-free media prior to follow up studies.

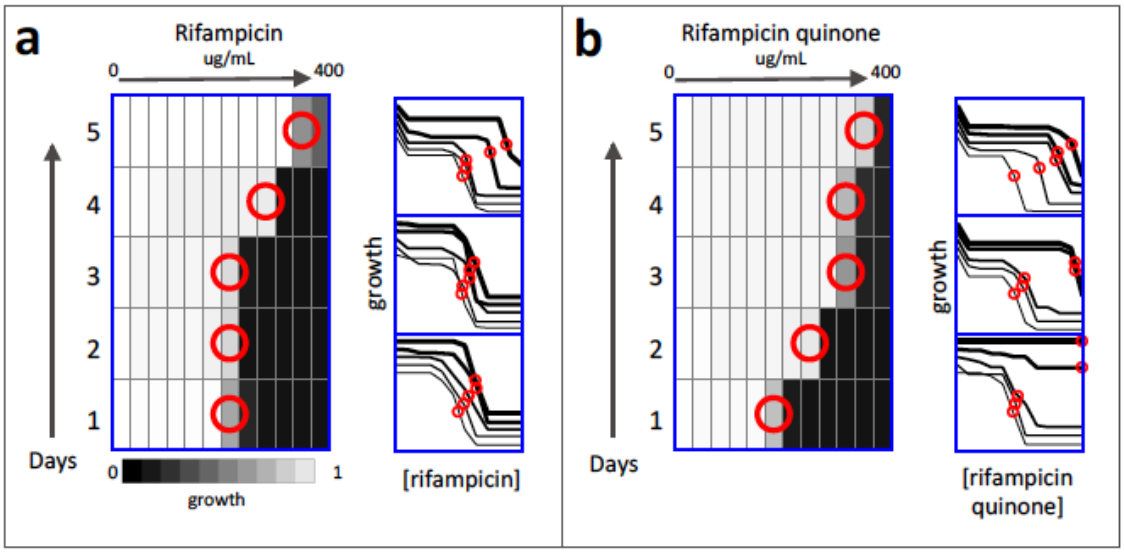

Figure 4.1: Evolution of resistance in *E. coli* exposed to rifampicin or the drug degradation product rifampicin quinone

E. coli are cultured in an array of concentrations of either rifampicin (a) or the drug degradation product rifampicin quinone (b) with 2-fold increments of doses. Each day, bacteria are selected from the dose at approximately one half the minimal inhibitory concentration (MIC/2) (red circles), diluted in fresh media and are aliquoted to a fresh array of drugs. All experiments were conducted in triplicate, with each heatmap corresponding to the top dose response curves in the subplots at right. The right shift in dose response curves over time demonstrates that *E. coli* acquire up to 14-fold increase in MIC after exposure to rifampicin (a) and 32-fold increase in MIC after exposure to rifampicin quinone (b).

RIF-resistant *E. coli* strains retained their increased MIC to RIF, confirming that these strains have acquired stable resistance (Figure 4.2a). Next, we wondered whether RFQ-resistant strains would be resistant to rifampicin. To answer this question, we grew our RFQ-res strains in increasing doses of RIF (Figure 4.2b). *E. coli* cultured in the drug degradation product rifampicin quinone reached up to 64-fold increase in resistance to rifampicin compared to solvent treated controls, despite no previous exposure to the standard drug. The level of rifampicin resistance was also higher in RFQ-res vs RIF-res. This result provides a proof of principle that substandard antibiotics may confer resistance to standard antibiotics.

We evaluated all three RIF-res and three RFQ-res populations for mutations in the rifampicin resistance cluster of the rpoB gene (Methods). Two of the RIF-res strains had non-synonymous mutations in rifampicin-resistance clusters (Figure 4.2c). Remarkably, all of the RFQ-res strains had mutations in the rifampicin-resistance clusters, explaining their resistance to rifampicin. The cluster I mutation N518D was found in both RIF-res and RFQ-res populations, and has previously been associated with rifampicin resistant Tb (23). RFQ-res populations also had S512F and D516G mutations that have been previously reported in rifampicin resistant *E. coli* and *Mycobacterium tuberculosis* samples (s512f: (24); d516G: PMID: (25), (26)). The results suggest that substandard antibiotics may cause the selection of resistance to standard antibiotics via well-defined mutations that confer resistance to the standard drug.

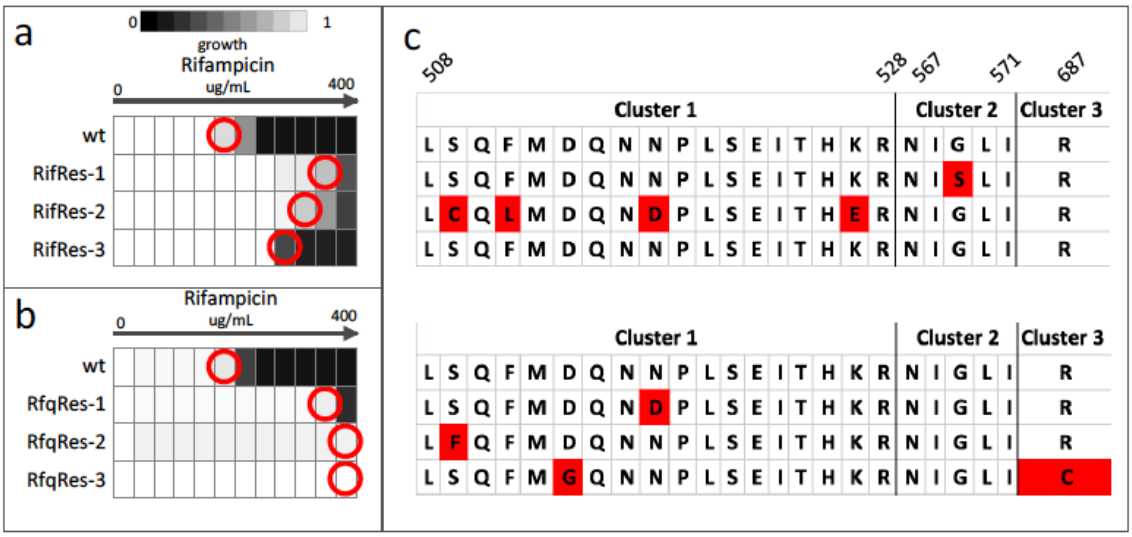

Figure 4.2: *E. coli* exposed to rifampicin or the drug degradation product rifampicin quinone show similar patterns of rifampicin resistance and genetic changes.

E. coli resistant to either rifampicin (RIF-Res) or the drug degradation product rifampicin quinone (RFQ-Res) over 5 days were assessed for stable increase in rifampicin minimal inhibitory concentration, compared to solvent treated controls (wt). RFQ-Respopulations showed cross-resistance to rifampicin with up to 64-fold increase in IC50 (red circles). Each population was assessed for genetic changes in the rifampicin resistance region of the rpoB gene. The majority of populations that acquired resistance to either rifampicin or rifampicin quinone acquired non-synonymous mutations in the rifampicin resistance clusters of the rpoB gene, as denoted by the highlighted red amino acid. These mutations are consistent with previous reports of rifampicin resistance due to rpoB mutations.

Rifampicin resistance is a critical concern for tuberculosis treatment. However, the long (~1 day) doubling time of Mycobacterium tuberculosis makes evolution experiments difficult to conduct. We therefore used *M. smegmatis*, a mycobacterium species with a shorter doubling time (2 hours), for our experiments. *M. smegmatis* cells were ~10-fold more sensitive to RIF and RFQ, compared to *E. coli*. Using the experimental setup described above, we evaluated *M. smegmatis* for the evolution of rifampicin resistance due to substandard medicines (Methods). We evolved six independent *M. smegmatis* strains resistant to RIF (names RIF-res1 to 6) and six strains resistant to RFQ (named RFQ-res1 to 6). Bacteria were selected from the dose that is closest to MIC/2, diluted in fresh media and aliquoted to a fresh array of drugs (Figure 4.3), every 48-hours, for 11 cycles. After 22 days of serial passages, *M. smegmatis* exposed to rifampicin quinone drugs evolved an increase in MIC compared to solvent-treated controls (t-test, $p = 0.03$), with population RFQ-res2 evolving up to 13-fold increase in MIC (Figure 4.3). We prepared glycerol stocks of all strains and used these stocks to grow cultures in drug-free media for further experimentation in *M. smegmatis*.

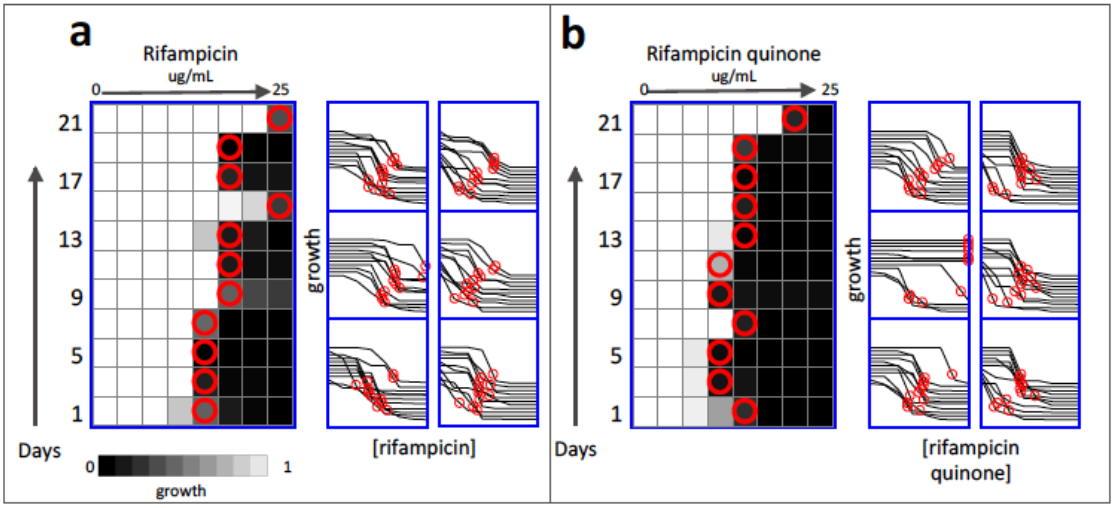

Figure 4.3: Evolution of resistance in Mycobacteria exposed to rifampicin and the drug degradation product rifampicin quinone.

M. smegmatis are cultured in an array of concentrations of either rifampicin (a) or the drug degradation product rifampicin quinone (b) with 2-fold increments of doses (n=6). Every 48 hours, bacteria are selected from the dose at approximately MIC/2 (red circles), diluted in fresh media and are aliquoted to a fresh array of drugs. Each heatmap corresponds to the upper left dose response curves. The right shift in dose response curves over time demonstrates that *M. smegmatis* acquired up to a 10-fold increase in MIC after exposure to rifampicin (b) and 13-fold increase in MIC after exposure to rifampicin quinone .describe plots in better consistency

As expected, RIF exposed- *M. smegmatis* strains maintained resistance to rifampicin after culture in selection-free media, with MIC fold increase of 4 to 64-fold compared to the parental population (Figure 4.4a). We next evaluated if RFQ exposed *M. smegmatis* strains acquired resistance to RIF. We observed strong rifampicin resistance in four of these six strains. RFQ-res2 population acquired 128-fold resistance to RIF, despite being only exposed to RFQ.

We assessed each population for genetic changes in the rifampicin resistance region of the rpoB gene. Three RIF-res populations and four RFQ-res populations acquired non-synonymous mutations in the rifampicin resistance clusters (Fig 4.4b). R529H (27), I572L (28) and P564L (29) mutations from RFQ-res *M. smegmatis* were previously reported in rifampicin resistant *E. coli* and mycobacteria. Therefore, we conclude that RFQ-exposure may select for genetic variants that are RIF-resistant in *M. smegmatis*.

Cross-resistance is common between structurally similar compounds. Rifampicin is in the rifamycin class of antibiotics, with closely related drugs rifabutin (RFB) and rifapentine (RFP). RIF-res and RFQ-res populations were further tested for cross-resistance to RFB and RFP (Fig 4.4c). Each of the RIF-resistant strains was resistant to both RFB and RFP, although resistance to RFB was only 2-fold in half of the populations. Half of the six RFQ-res populations had at least a 2-fold increase in the IC75 to both RFB and RFP, despite never having been exposed to either of the compounds. RFQ-res2 strain, which had very high resistance to RIF, also had high resistance to RFB (500-fold) and RFP (30-fold). These observations support the idea that strains exposed to

substandard medicines may acquire resistance to standard drugs with similar molecular structures.

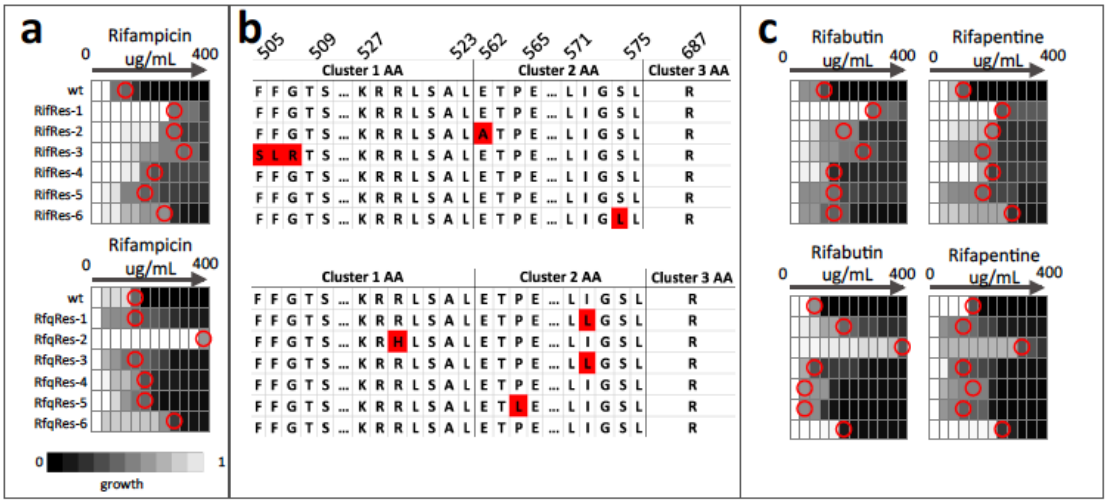

Figure 4.4: Mycobacteria exposed to rifampicin and the drug degradation product rifampicin quinone show similar patterns of rifampicin resistance and genetic changes.

M. smegmatis resistant to either rifampicin (RIF-Res) or the drug degradation product rifampicin quinone (RFQ-Res) over 21 days were assessed for stable increase in rifampicin minimal inhibitory concentration, compared to solvent treated controls (wt) (a). RFQ-Res populations showed cross-resistance to rifampicin with up to 128-fold increase in IC75 (red circles). Each population was assessed for genetic changes in the rifampicin resistance region of the rpoB gene (b). Amino acid sequences of the rifampicin resistance clusters 1,2 and 3 are displayed, with amino acids numbered using the *E. coli* mapping notation. The displayed clusters are truncated to include regions with mutations in the evolved populations. The majority of populations that acquired resistance to either rifampicin or rifampicin quinone acquired non-synonymous mutations in the rifampicin resistance clusters of the rpoB gene. These mutations were consistent with previous reports of rifampicin resistance in *M. tuberculosis* and *E. coli*. Rifampicin resistant Mycobacteria also showed cross-resistance to other rifamycin drugs, rifabutin and rifapentine (c). Two RFQ-Res populations (RFQ-Res1 and 3) that did not have resistance to rifampicin showed cross-resistance to rifabutin.

Discussion

According to the FDA, 10-25% of medicines worldwide are substandard (30), the majority of which are antimicrobial agents (2, 31). Up to one third of rifampicin containing medicines failed quality testing depending on world region (32-34). Despite these considerations, there has been no systematic study exploring the proximal and distal negative outcomes associated with substandard antimicrobial drugs. Apart from affecting the proximal treatment success of individual patients receiving subtherapeutic doses of medicine, it has been conjectured that substandard medicines affect treatment success in the future by promoting the evolution of resistance to standard medicines (35).

In our study, we demonstrate that substandard medicines promote drug resistance through exposure to an agent similar to the standard drug. Bacterial strains quickly evolved resistance to the drug degradation product RFQ, and these strains were resistant to the standard drug RIF and two similar antibiotics RFB and RFP, despite never being exposed to any of these drugs. Gene analysis indicated that resistance to the substandard drug RFQ was often associated with mutations in the rifampicin resistance cluster, explaining the convergent evolution in RIF and RFQ conditions. Interestingly, the two RFQ-res mycobacteria strains that did not acquire resistance to rifampicin (RFQ-res1 and RFQ-res3) had cross-resistance to rifabutin. These strains had the same I572L mutation in the rpoB gene. One of the RFQ treated mycobacterial populations became highly resistant to rifampicin, with only some growth inhibition at 100 times the wild type MIC.

E. coli acquired rifampicin resistance more quickly than *M. smegmatis*. This could be due to the differences in doubling time between the two organisms. *E. coli* populations double in approximately 20 minutes, while *M. smegmatis* populations double every 3 hours. This translates to approximately twice as many doubling times for *E. coli* than *M. smegmatis* for the duration of experiments (5 days * 3 doublings/hour *24 h/day ~360 doublings for *E. coli*. 21 days * 1 doubling/3 hours *24/day ~ 170 doublings for *M. smegmatis*).

Rifampicin resistant tuberculosis is classically thought to arise through factors such as transmission, poor treatment adherence and immune status (36). Substandard medicines contribute to these factors by hindering efforts to control disease, and undermining patient trust in the medical system (10). This study demonstrates a direct link between rifampicin drug quality and the acquisition of antimicrobial resistance in two disparate bacterial species. It remains to be seen how these observations will translate to other substandard medicines. However, our study provides a proof-of principle strongly suggesting that substandard antibiotics affect not only the current treatment success, but also the future treatments by selecting for mutations that confer resistance to standard antibiotics.

Chapter 4 References

1. World Health Organization (2017) *Global tuberculosis report 2017,* (World Health Organization, Geneva, Switzerland),

2. Pincock S (2003) WHO tries to tackle problem of counterfeit medicines in Asia. *British Medical Journal* 327(7424): 1126.

3. Johnston A & Holt DW (2014) Substandard drugs: A potential crisis for public health. *British Journal of Clinical Pharmacology* 78(2): 218-243.

4. van Crevel R*, et al* (2004) Bioavailability of rifampicin in indonesian subjects: A comparison of different local drug manufacturers. *International Journal of Tuberculosis and Lung Disease* 8(4): 500-503.

5. Hall Z, Allan EL, van Schalkwyk DA, van Wyk A & Kaur H (2016) Degradation of artemisinin-based combination therapies under tropical conditions. *American Journal of Tropical Medicine and Hygiene* 94(5): 993-1001.

6. Caminero JA (2008) Likelihood of generating MDR-TB and XDR-TB under adequate national tuberculosis control programme implementation. *International Journal of Tuberculosis and Lung Disease* 12(8): 869-877.

7. Horsburgh CR,Jr, Barry CE,3rd & Lange C (2015) Treatment of tuberculosis. *New England Journal of Medicine* 373(22): 2149-2160.

8. World Health Organization (2014) Companion handbook to the WHO guidelines for the programmatic management of drug-resistant tuberculosis.

9. van den Boogaard J, Kibiki GS, Kisanga ER, Boeree MJ & Aarnoutse RE (2009) New drugs against tuberculosis: Problems, progress, and evaluation of agents in clinical development. *Antimicrobial Agents and Chemotherapy* 53(3): 849-862.

10. Arnold A*, et al* (2017) Drug resistant TB: UK multicentre study (DRUMS): Treatment, management and outcomes in london and west midlands 2008-2014. *Journal of Infections* 74(3): 260-271.

11. Kohanski MA, DePristo MA & Collins JJ (2010) Sublethal antibiotic treatment leads to multidrug resistance via radical-induced mutagenesis. *Molecular Cell* 37(3): 311-320.

12. Campbell EA*, et al* (2001) Structural mechanism for rifampicin inhibition of bacterial rna polymerase. *Cell* 104(6): 901-912.

13. Farhat MR*, et al* (2013) Genomic analysis identifies targets of convergent positive selection in drug-resistant mycobacterium tuberculosis. *Nature Genetics* 45(10): 1183-1189.

14. Pang Y*, et al* (2013) Study of the rifampin monoresistance mechanism in mycobacterium tuberculosis. *Antimicrobial Agents and Chemotherapy* 57(2): 893-900.

15. Mohan B, Sharda N & Singh S (2003) Evaluation of the recently reported USP gradient HPLC method for analysis of anti-tuberculosis drugs for its ability to resolve

degradation products of rifampicin. *Journal of Pharmacology and Biomedical Analysis* 31(3): 607-612.

16. Bolt HM & Remmer H (1976) Implication of rifampicin-quinone in the irreversible binding of rifampicin to macromolecules. *Xenobiotica* 6(1): 21-32.

17. World Health Organization (2007) Rifampicin, isoniazid and pyrazinamide dispersible tablets. *WHO Drug Information.* 21(3): 232.

18. Konrad P & Stenberg P (1988) Rifampicin quinone is an immunosuppressant, but not rifampicin itself. *Clinical Immunology and Immunopathology* 46(1): 162-166.

19. Piriou A, Jacqueson A, Warnet JM & Claude JR (1983) Enzyme induction with high doses of rifampicin in wistar rats. *Toxicology Letters* 17(3-4): 301-306.

20. Shi F, Li X, Pan H & Ding L (2017) NQO1 and CYP450 reductase decrease the systemic exposure of rifampicin-quinone and mediate its redox cycle in rats. *Journal of Pharmacology and Biomedical Analysis* 132: 17-23.

21. Williams DL*, et al* (1998) Contribution of rpoB mutations to development of rifamycin cross-resistance in mycobacterium tuberculosis. *Antimicrobial Agents and Chemotherapy* 42(7): 1853-1857.

22. Oz T*, et al* (2014) Strength of selection pressure is an important parameter contributing to the complexity of antibiotic resistance evolution. *Molecular Biology and Evolution* 31(9): 2387-2401.

23. Andres S, Hillemann D, Rusch-Gerdes S & Richter E (2014) Occurrence of rpoB mutations in isoniazid-resistant but rifampin-susceptible mycobacterium tuberculosis isolates from Germany. *Antimicrobial Agents and Chemotherapy* 58(1): 590-592.

24. Durao P, Guleresi D, Proenca J & Gordo I (2016) Enhanced survival of rifampin- and streptomycin-resistant escherichia coli inside macrophages. *Antimicrobial Agents and Chemotherapy* 60(7): 4324-4332.

25. Tan Y*, et al* (2012) The beginning of the rpoB gene in addition to the rifampin resistance determination region might be needed for identifying rifampin/rifabutin cross-resistance in multidrug-resistant mycobacterium tuberculosis isolates from southern china. *Journal of Clinical Microbiology* 50(1): 81-85.

26. Jamieson FB*, et al* (2014) Profiling of rpoB mutations and MICs for rifampin and rifabutin in mycobacterium tuberculosis. *Journal of Clinical Microbiology* 52(6): 2157-2162.

27. Jin DJ & Gross CA (1988) Mapping and sequencing of mutations in the escherichia coli rpoB gene that lead to rifampicin resistance. *Journal of Molecular Biology* 202(1): 45-58.

28. McCammon MT*, et al* (2005) Detection of rpoB mutations associated with rifampin resistance in mycobacterium tuberculosis using denaturing gradient gel electrophoresis. *Journal of Clinical Microbiology* 49(6): 2200-2209.

29. Hauck Y, Fabre M, Vergnaud G, Soler C & Pourcel C (2009) Comparison of two commercial assays for the characterization of rpoB mutations in mycobacterium tuberculosis and description of new mutations conferring weak resistance to rifampicin. *Journal of Antimicrobial Chemotherapy* 64(2): 259-262.

30. World Health Organization (1999) Counterfeit drugs: Guidelines for the development of measures to combat counterfeit drugs

31. Nayyar GML, Breman JG, Newton PN & Herrington J (2012) Poor-quality antimalarial drugs in southeast asia and sub-saharan africa. *The Lancet.Infectious Diseases* 12(6): 488-496.

32. Kenyon TA*, et al* (1999) Detection of substandard fixed-dose combination tuberculosis drugs using thin-layer chromatography. *International Journal of Tuberculosis and Lung Disease* 3(11): 347-350.

33. Bate R, Jensen P, Hess K, Mooney L & Milligan J (2013) Substandard and falsified anti-tuberculosis drugs: A preliminary field analysis. *International Journal of Tuberculosis and Lung Disease* 17(3): 308-311.

34. Taylor RB*, et al* (2001) Pharmacopoeial quality of drugs supplied by Nigerian pharmacies. *Lancet* 357(9272): 1933-1936.

35. Newton PN, Green MD & Fernandez FM (2010) Impact of poor-quality medicines in the 'developing' world. *Trends in Pharmacological Science* 31(3): 99-101.

36. Koch A, Mizrahi V & Warner DF (2014) The impact of drug resistance on mycobacterium tuberculosis physiology: What can we learn from rifampicin?. *Emerging Microbes and Infections* 3(3): e17.

CHAPTER 5: Discussion

State of field before this work	State of field after this work
Computational models of aptamer selection strategies include varying drug target concentrations and partitioning efficiency	Computational models of aptamer selection strategies evaluate the influence of varying drug target concentration and partitioning efficiency in the context of varying aptamer library affinity distributions
Computational models of aptamer selection do not account for random loss of aptamers due to experimental conditions	Computational model of aptamer selection considers the influence of random loss of aptamer on the probability of successful aptamer selection
Biosensors can identify RNA polymerase targeting active pharmaceutical ingredients	Biosensors can distinguish between different RNA polymerase targeting active pharmaceutical ingredients
HPLC is required to resolve rifampicin from its degradation product rifampicin quinone	Drug interaction fingerprints can differentiate rifampicin from its degradation product rifampicin quinone
Subinhibitory doses of rifampicin are known to select for rifampicin resistance in Mycobacteria	A rifampicin degradation product is shown to select for rifampicin resistance in Mycobacteria

Table 5.1: State of the field before and after this dissertation

Among antimicrobial agents, anti-tuberculosis drugs such as rifampicin have a very high impact on global health given the annual incidence of tuberculosis is approximately ten million cases (1, 2). Antimicrobial resistance is a growing threat to the treatment of tuberculosis, with 200,000 deaths attributed to multidrug resistant tuberculosis each year. Poor quality anti-mycobacterial drugs undermine the treatment of

both drug sensitive and drug resistance tuberculosis. This dissertation presents novel methodologies for detecting active pharmaceutical ingredients for drug quality assurance. Here, a computational model optimized the selection of aptamers to active pharmaceutical ingredients. As an alternative strategy, a bioassay was developed to create unique fingerprints for the detection of rifamycin-based drugs and the rifampicin degradation product rifampicin quinone. Finally, the data presented herein demonstrated that the drug degradation product rifampicin quinone contributes to rifampicin resistance in *E. coli* and the TB model organism *Mycobacterium smegmatis* via genetic changes in the DNA dependent RNA polymerase B subunit.

Towards the aim of assessing selection strategies for DNA aptamers for small molecule drug detection, a computational model of SELEX was developed. This model provided a general framework that can be used to study the influence of experimental parameters on the probability of successful aptamer selection, including the affinity distribution of the aptamer library to the small molecule drug, affinity of the aptamer to the substrate used for partitioning drug-bound from drug-free aptamers, and concentration of small molecule drug target. This model also considered the influence of random events, which may lead to the loss of rare high affinity aptamers.

This model demonstrated that very high and very low small molecule target concentrations could be prohibitive for aptamer selection, which is consistent with previous studies (3). Under high target concentrations, selective pressure for a high affinity aptamer is low, so the affinity distribution changes little with each round of selection. While counterintuitive, very low target concentrations also impede the aptamer

selection process as non-specific binding events predominate over specific aptamer to target binding.

The probability of selecting a high affinity aptamer for a small molecule ligand is dependent on the initial K_D distribution of the aptamer library. However, the K_D distribution is uncertain. While many computational models for selection assume that the initial K_D distribution is log normal (4-6), this model examined selection efficiency using both Gaussian and non-Gaussian distributions. This model determined that the presence of as few as 20 high affinity aptamers out of 10^{15} candidate aptamers could strongly influence selection efficiency.

Similar to target concentration, intermediate ranges of affinity of aptamer to selection substrate are ideal for aptamer selection. Aptamer affinity to substrate may be tuned by increasing or decreasing the length of docking sequence for selection using capture oligonucleotides (7). Aptamer affinity to the selection substrate can also be altered by utilizing novel substrate materials such as graphene oxide, which binds via pi-pi interactions to single stranded DNA, and therefore preferentially adsorbs aptamers that are not bound to small molecule ligands (8). Contrary to the use of very low small molecule target concentrations, the use of very high affinity substrate was still associated with successful aptamer selection under our model. High partitioning efficiency should decrease the nonspecific selection of low affinity aptamers. This is consistent with the findings of other SELEX simulations (3, 4).

Consistent with the findings of other research groups, high selection efficiency and intermediate drug target concentrations were optimal for expediting aptamer

selection. While the initial affinity distribution of an aptamer library to a target is inherently unknown, previous studies tend to consider a single affinity distribution (3, 4). The data presented here therefore simulated the influence of experimental conditions using a variety of potential affinity distributions. Another advantage of this model is that it considered the random loss of high affinity aptamers due to experimental conditions such as washing steps, or transfer of materials, which is more realistic than models that assume no loss of aptamer candidates over this multi-step and often months long set of experiments (5). A limitation of this model is that it did not consider the impact of DNA mutations that may occur over rounds of selection on aptamer affinity to drug targets. Mutations may be detrimental if they eliminate high affinity aptamers. However they may be beneficial in increasing the diversity of aptamer candidates (9). Future versions of this model may therefore incorporate mutations to better understand its influence on the probability of selecting a high affinity aptamer.

To determine whether anti-mycobacterial drugs may be identified based on drug interaction profiles in *E. coli*, differential responses to drug combinations in *E. coli* were used to create unique fingerprints for anti-mycobacterial drugs (10). Novel drug interactions were assessed for 4 rifamycin based drugs and 1 drug degradation product against a panel of antibiotics with varying mechanism of action. By randomizing the data, de-identified vectors of drug interactions were compared to vectors of known drug interactions. The correct identification of active pharmaceutical ingredients was based on the similarity between drug interaction vectors, as measured by correlation and Euclidean distance between vectors.

Due to the high reproducibility of experiments and diversity of drug interactions, we were able to identify 29 of 30 antibiotics that were analyzed from both newly generated drug interaction profiles and from data obtained from the literature (11). By utilizing luminescence instead of turbidity as a proxy for growth, experimental run time was reduced from approximately 1 day to 1 hour (11, 12). Unlike HPLC, which is both resource and time intensive, many samples can be run in parallel for detection of active pharmaceutical ingredients. Furthermore, luminescence provides a simple signal for detection. While this study utilized a spectrophotometer, the method could be adapted for field-testing using photographic film and measurements of density or radius of signal as opposed to relative luminescence units (13).

In order to determine the fewest drug interaction experiments required to identify anti-mycobacterial query drugs, array drugs were ranked by their utility in distinguishing the five compounds of interest. Based on the interaction scores of streptomycin alone, four of the five query compounds could be confirmed. By adding in additional drug interaction data, all five compounds could be distinguished. As the remainder of drug interaction data was added to the analysis, the experimental noise among replicate interaction experiments was greater than the difference between query drugs; thereby weakening the ability to differentiate drugs by the fingerprinting method. This demonstrates that some of the array drugs serve as informers that are ideal for their distinct drug interactions among the query drugs.

The drug interaction fingerprinting method sampled the checkerboard assay was simple to setup and analyze; using parallel dose response testing of drugs and their

combination as opposed to 64 concentration combinations (14). The data analysis of this method is also relatively simple, by comparing relative doses to achieve different levels of inhibition as opposed to comparing the concavity of isophenotypic growth curves. By sampling several concentration combinations, this method is more robust than a 2x2 dose concentration setup that is sometimes used to measure drug combinatorial effect (15).

Systematic drug interaction profiling has many potential applications outside of drug quality assessment such as drug discovery and determination of mechanism of action (16, 17). Previous studies used luciferase expressing *B. subtilis* to couple the detection of RNA polymerase targeting drugs with a luminescence signal (16, 18). The advantage of our method is the ability to distinguish between different drugs of the same class; in this case multiple rifamycin-derived drugs. This method is also capable of differentiating rifampicin from its primary degradation product, rifampicin quinone. Future studies may apply drug interaction based biosensors to differentiate drugs with other mechanisms of action. A limitation of this model is that not all anti-mycobacterial compounds affect *E. coli* growth. To extend this work to such drugs, the model organism *M. smegmatis* could be an alternative bacterium for creating drug interaction fingerprints (19).

While this study provided predominately qualitative data on the presence or absence of a drug or degradation product, the data collected contains quantitative information on drug dose response. By simple adjustments to the drug-fingerprinting algorithm, query drug dose response could be compared to a reference drug dose response. Comparison of the apparent minimal inhibitory concentration would be applied

to the calculation of the query drug concentration. This bioassay could therefore provide expedited information on both drug identity and concentration.

A series of *in vitro* evolution experiments were conducted to determine whether exposure to rifampicin degradation products induces resistance to the standard antimicrobial rifampicin in *E. coli* and *M. smegmatis*. *E. coli* exposed to the degradation product rifampicin quinone developed over 50 fold resistance to rifampicin in under 1 week. The development of resistance coincided with non-synonymous mutations in the rifampicin resistance cluster of the rpoB gene. *M. smegmatis*, acquired up to 100 fold resistance to rifampicin after exposure to rifampicin quinone for 21 days. Mycobacteria that were cultured in rifampicin quinone also acquired cross-resistance to the rifamycin drugs rifabutin and rifapentine. Many, but not all, of the *M. smegmatis* populations acquired mutations in the rpoB gene.

A limitation of this study is that only the rifampicin resistance cluster region of the rpoB gene was sequenced. While no non-synonymous mutations were found between or flanking the clusters, it does not preclude mutations in other regions that may be associated with resistance. The vast majority of clinically derived rifampicin resistant mycobacterium tuberculosis strains have mutations in at least 1 of the 3 rifampicin resistance clusters, though mutations have also been reported in other regions of the gene (20, 21). Future studies may benefit from the sequencing of the entire rpoB gene. Whole genome sequencing would further allow for the detection of differential mutations under rifampicin quinone treatment.

Nearly all the *E. coli* populations in the experimental set developed mutations in the rpoB resistance clusters, while 7/12 *M. smegmatis* populations had similar mutations. *E. coli* acquired rifampicin resistance more quickly than *M. smegmatis*. This could be due to the differences in doubling time between the two organisms. *E. coli* populations double in approximately 20 minutes, while *M. smegmatis* populations double every 3 hours. This translates to approximately twice as many doubling times for *E. coli* than *M. smegmatis* for the duration of experiments (5 days * 3 doublings/hour *24 h/day ~360 doublings for *E. coli*. 21 days * 1 doubling/3 hours *24/day ~ 170 doublings for *M. smegmatis*). *E. coli* and *M. smegmatis* have a mutation rate on the same order of magnitude: approximately 10^{-10} mutations per nucleotide per generation (22, 23). Future experiments may extend the number of serial passages to allow for equivalent generation time between organisms. An alternative explanation for some of the difference in resistance acquisition is the variation in genome size between the two organisms (24). The *M. smegmatis* genome is approximately 1.5 times greater than *E. coli*'s genome with 6.99×10^6 and 4.64×10^6 base pairs respectively. Few drug resistant strains are reported in organisms with very small genomes such as Mycoplamsa (25).

A limitation of this study towards understanding the etiology of drug resistance in tuberculosis is that experiments were conducted *in vitro* with the model organism *M. smegmatis*. Repeating the experiments with *Mycobacterium tuberculosis* would be more clinically relevant, though laborious to conduct and requiring Biosafety Level 3 laboratories. *In vivo* testing in animal models may better recapitulate the etiology of rifampicin resistance acquisition through substandard medicines.

Isoniazid is another important first-line anti-mycobacterial drug. Fixed dose combination capsules may contain substandard isoniazid due to poor manufacturing practices. Exposure to light, heat or humidity; acidic conditions may accelerate drug degradation (26, 27). Isoniazid is a pro-drug that is activated by bacterial catalase-peroxidase 'KatG'. Isoniazid resistance is very common in clinical isolates and often associated with KatG of inhZ mutations (25, 28). Therefore, repeating this experimental setup using isoniazid and its degradation products is a logical follow up to better understand mycobacterial resistance to the most important tuberculosis treatments. Overall, this research provides the first demonstration of mycobacterial rifampicin resistance due to exposure to a degradation product and presents a simple model for the study of substandard medicines and their contribution to resistance.

Chapter 5 References

1. World Health Organization (2017) *Global tuberculosis report 2017,* (World Health Organization, Geneva, Switzerland).

2. World Health Organization (2014) Companion handbook to the WHO guidelines for the programmatic management of drug-resistant tuberculosis.

3. Wang J, Rudzinski JF, Gong Q, Soh HT & Atzberger PJ (2012) Influence of target concentration and background binding on in vitro selection of affinity reagents. *PLoS One* 7(8): e43940.

4. Chen C & Kuo T (2007) Simulations of SELEX against complex receptors with a condensed statistical model. *Computers & Chemical Engineering* 31(9): 1007-1019.

5. Levine HA & Nilsen-Hamilton M (2007) A mathematical analysis of SELEX. *Computational Biology and Chemistry* 31(1): 11-35.

6. Pressman A, Moretti JE, Campbell GW, Muller UF & Chen IA (2017) Analysis of in vitro evolution reveals the underlying distribution of catalytic activity among random sequences. *Nucleic Acids Research* 45(14): 8167-8179.

7. Stoltenburg R, Nikolaus N & Strehlitz B (2012) Capture-SELEX: Selection of DNA aptamers for aminoglycoside antibiotics. *Journal of Analytical Methods in Chemistry* 2012: 415697.

8. Nguyen VT, Kwon YS, Kim JH & Gu MB (2014) Multiple GO-SELEX for efficient screening of flexible aptamers. *Chemical Communications (Cambridge)* 50(72): 10513-10516.

9. Hoinka J*, et al* (2015) Large scale analysis of the mutational landscape in HT-SELEX improves aptamer discovery. *Nucleic Acids Research* 43(12): 5699-5707.

10. Weinstein ZB & Zaman MH (2017) Quantitative bioassay to identify antimicrobial drugs through drug interaction fingerprint analysis. *Scientific Reports* 7: 42644.

11. Chandrasekaran S*, et al* (2016) Chemogenomics and orthology-based design of antibiotic combination therapies. *Molecular Systems Biology* 12(5): 872.

12. Farha MA & Brown ED (2010) Chemical probes of escherichia coli uncovered through chemical-chemical interaction profiling with compounds of known biological activity. *Chemistry and Biology* 17(8): 852-862.

13. Riska PF*, et al* (1999) Rapid film-based determination of antibiotic susceptibilities of mycobacterium tuberculosis strains by using a luciferase reporter phage and the bronx box. *Journal of Clinical Microbiology* 37(4): 1144-1149.

14. Cokol M*, et al* (2014) Large-scale identification and analysis of suppressive drug interactions. *Chemistry and Biology* 21(4): 541-551.

15. Yeh P, Tschumi AI & Kishony R (2006) Functional classification of drugs by properties of their pairwise interactions. *Nature Genetics* 38(4): 489-494.

16. Urban A*, et al* (2007) Novel whole-cell antibiotic biosensors for compound discovery. *Applied Environmental Microbiology* 73(20): 6436-6443.

17. Lehar J*, et al* (2007) Chemical combination effects predict connectivity in biological systems. *Molecular Systems Biology* 3: 80.

18. Mariner KR, Ooi N, Roebuck D, O'Neill AJ & Chopra I (2011) Further characterization of bacillus subtilis antibiotic biosensors and their use for antibacterial mode-of-action studies. *Antimicrobial Agents and Chemotherapy* 55(4): 1784-1786.

19. Gordon S, Parish T, Roberts IS & Andrew PW (1994) The application of luciferase as a reporter of environmental regulation of gene expression in mycobacteria. *Letters in Applied Microbiology* 19(5): 336-340.

20. Campbell EA*, et al* (2001) Structural mechanism for rifampicin inhibition of bacterial rna polymerase. *Cell* 104(6): 901-912.

21. Siu GK*, et al* (2011) Mutations outside the rifampicin resistance-determining region associated with rifampicin resistance in mycobacterium tuberculosis. *Journal of Antimicrobial Chemotherapy* 66(4): 730-733.

22. Lee H, Popodi E, Tang H & Foster PL (2012) Rate and molecular spectrum of spontaneous mutations in the bacterium escherichia coli as determined by whole-genome sequencing. *Proceedings of the National Academy of Sciences of the United States of America* 109(41): E2774-83.

23. Rock JM*, et al* (2015) DNA replication fidelity in mycobacterium tuberculosis is mediated by an ancestral prokaryotic proofreader. *Nature Genetics* 47(6): 677-681.

24. Levy SB (2008) Genome size and antibiotic resistance. *Antimicrobial Agents and Chemotherapy* 52(7): 2696-07.

25. Projan SJ (2007) (Genome) size matters. *Antimicrobial Agents and Chemotherapy* 51(4): 1133-1134.

26. Singh, S., Mariappan, T.T., Sharda, N.,Singh, B., (2000) Degradation of rifampicin, isoniazid and pyrazinamide from prepared mixtures and marketed single and combination products under acid conditions. *Pharmacy and Pharmacology Communications Pharmacy and Pharmacology Communications* 6(11): 491-494.

27. Bhutani H, Mariappan TT & Singh S (2004) The physical and chemical stability of anti-tuberculosis fixed-dose combination products under accelerated climatic conditions. *The international journal of tuberculosis and lung disease* 8(9): 1073-1080.

28. Banerjee A*, et al* (1994) inhA, a gene encoding a target for isoniazid and ethionamide in mycobacterium tuberculosis. *Science* 263(5144): 227-230.

BIBLIOGRAPHY

Agrawal, S., Ashokraj, Y., Bharatam, P.V., Pillai, O. & Panchagnula, R. 2004, "Solid-state characterization of rifampicin samples and its biopharmaceutic relevance", *European journal of pharmaceutical sciences : official journal of the European Federation for Pharmaceutical Sciences,* vol. 22, no. 2-3, pp. 127-144.

Andres, S., Hillemann, D., Rusch-Gerdes, S. & Richter, E. 2014, "Occurrence of rpoB mutations in isoniazid-resistant but rifampin-susceptible Mycobacterium tuberculosis isolates from Germany", *Antimicrobial Agents and Chemotherapy,* vol. 58, no. 1, pp. 590-592.

Arnold, A., Cooke, G.S., Kon, O.M., Dedicoat, M., Lipman, M., Loyse, A., Butcher, P.D., Ster, I.C. & Harrison, T.S. 2017, "Drug resistant TB: UK multicentre study (DRUMS): Treatment, management and outcomes in London and West Midlands 2008-2014", *The Journal of infection,* vol. 74, no. 3, pp. 260-271.

Asaumi, R., Toshimoto, K., Tobe, Y., Hashizume, K., Nunoya, K.I., Imawaka, H., Lee, W. & Sugiyama, Y. 2018, "Comprehensive PBPK Model of Rifampicin for Quantitative Prediction of Complex Drug-Drug Interactions: CYP3A/2C9 Induction and OATP Inhibition Effects", *CPT: pharmacometrics & systems pharmacology,* .

Ashokraj, Y., Kohli, G., Kaul, C.L. & Panchagnula, R. 2005, "Quality control of anti-tuberculosis FDC formulations in the global market: part II-accelerated stability studies", *The international journal of tuberculosis and lung disease : the official journal of the International Union against Tuberculosis and Lung Disease,* vol. 9, no. 11, pp. 1266-1272.

Baker, S. 2015, "Infectious disease. A return to the pre-antimicrobial era?", *Science,* vol. 347, no. 6226, pp. 1064-1066.

Ballereau, F., Prazuck, T., Schrive, I., Lafleuriel, M.T., Rozec, D., Fisch, A. & Lafaix, C. 1997, "Stability of essential drugs in the field: results of a study conducted over a two-year period in Burkina Faso", *The American Journal of Tropical Medicine and Hygiene,* vol. 57, no. 1, pp. 31-36.

Banerjee, A., Dubnau, E., Quemard, A., Balasubramanian, V., Um, K.S., Wilson, T., Collins, D., de Lisle, G. & Jacobs, W.R.,Jr 1994, "inhA, a gene encoding a target for isoniazid and ethionamide in Mycobacterium tuberculosis", *Science (New York, N.Y.),* vol. 263, no. 5144, pp. 227-230.

Basco, L.K., Ringwald, P., Manene, A.B. & Chandenier, J. 1997, "False chloroquine resistance in Africa", *Lancet (London, England),* vol. 350, no. 9072, pp. 224-6736(05)62397-5.

Bate, R., Jensen, P., Hess, K., Mooney, L. & Milligan, J. 2013, "Substandard and falsified anti-tuberculosis drugs: a preliminary field analysis", *The international journal of tuberculosis and lung disease : the official journal of the International Union against Tuberculosis and Lung Disease,* vol. 17, no. 3, pp. 308-311.

Berenbaum, M.C. 1978, "A method for testing for synergy with any number of agents", *The Journal of infectious diseases,* vol. 137, no. 2, pp. 122-130.

Berens, C., Thain, A. & Schroeder, R. 2001, "A tetracycline-binding RNA aptamer", *Bioorganic & medicinal chemistry,* vol. 9, no. 10, pp. 2549-2556.

Bhutani, H., Mariappan, T.T. & Singh, S. 2004, "The physical and chemical stability of anti-tuberculosis fixed-dose combination products under accelerated climatic conditions", *The international journal of tuberculosis and lung disease : the official journal of the International Union against Tuberculosis and Lung Disease,* vol. 8, no. 9, pp. 1073-1080.

Bhutani, H., Singh, S., Jindal, K.C. & Chakraborti, A.K. 2005, "Mechanistic explanation to the catalysis by pyrazinamide and ethambutol of reaction between rifampicin and isoniazid in anti-TB FDCs", *Journal of pharmaceutical and biomedical analysis,* vol. 39, no. 5, pp. 892-899.

Blix, H.S., Viktil, K.K., Moger, T.A. & Reikvam, A. 2010, "Drugs with narrow therapeutic index as indicators in the risk management of hospitalised patients", *Pharmacy practice,* vol. 8, no. 1, pp. 50-55.

Bolt, H.M. & Remmer, H. 1976, "Implication of rifampicin-quinone in the irreversible binding of rifampicin to macromolecules", *Xenobiotica; the fate of foreign compounds in biological systems,* vol. 6, no. 1, pp. 21-32.

Caminero, J.A. 2008, "Likelihood of generating MDR-TB and XDR-TB under adequate National Tuberculosis Control Programme implementation", *The international journal of tuberculosis and lung disease : the official journal of the International Union against Tuberculosis and Lung Disease,* vol. 12, no. 8, pp. 869-877.

Campbell, E.A., Korzheva, N., Mustaev, A., Murakami, K., Nair, S., Goldfarb, A. & Darst, S.A. 2001, "Structural mechanism for rifampicin inhibition of bacterial rna polymerase", *Cell,* vol. 104, no. 6, pp. 901-912.

Castan, P., de Pablo, A., Fernandez-Romero, N., Rubio, J.M., Cobb, B.D., Mingorance, J. & Toro, C. 2014, "Point-of-care system for detection of Mycobacterium tuberculosis and rifampin resistance in sputum samples", *Journal of clinical microbiology,* vol. 52, no. 2, pp. 502-507.

Chandrasekaran, S., Cokol-Cakmak, M., Sahin, N., Yilancioglu, K., Kazan, H., Collins, J.J. & Cokol, M. 2016, "Chemogenomics and orthology-based design of antibiotic combination therapies", *Molecular systems biology,* vol. 12, no. 5, pp. 872.

Chen, C. & Kuo, T. 2007, "Simulations of SELEX against complex receptors with a condensed statistical model", *Computers & chemical engineering,* vol. 31, no. 9, pp. 1007-1019.

Cherney, L.T., Obrecht, N.M. & Krylov, S.N. 2013, "Theoretical modeling of masking DNA application in aptamer-facilitated biomarker discovery.", *Analytical Chemistry,* vol. 85, no. 8, pp. 4157-4164.

Coker, C., Zhao, H. & Mobley, H.L. 2002, "Green fluorescent protein urea sensors. Uropathogenic Proteus mirabilis", *Methods in molecular biology (Clifton, N.J.),* vol. 183, pp. 287-293.

Cokol, M., Chua, H.N., Tasan, M., Mutlu, B., Weinstein, Z.B., Suzuki, Y., Nergiz, M.E., Costanzo, M., Baryshnikova, A., Giaever, G., Nislow, C., Myers, C.L., Andrews, B.J., Boone, C. & Roth, F.P. 2011, "Systematic exploration of synergistic drug pairs", *Molecular systems biology,* vol. 7, pp. 544.

Cokol, M., Weinstein, Z.B., Yilancioglu, K., Tasan, M., Doak, A., Cansever, D., Mutlu, B., Li, S., Rodriguez-Esteban, R., Akhmedov, M., Guvenek, A., Cokol, M., Cetiner, S., Giaever, G., Iossifov, I., Nislow, C., Shoichet, B. & Roth, F.P. 2014, "Large-scale identification and analysis of suppressive drug interactions", *Chemistry & biology,* vol. 21, no. 4, pp. 541-551.

David, H.L. 1970, "Probability distribution of drug-resistant mutants in unselected populations of Mycobacterium tuberculosis", *Applied Microbiology,* vol. 20, no. 5, pp. 810-814.

Durao, P., Guleresi, D., Proenca, J. & Gordo, I. 2016, "Enhanced Survival of Rifampin- and Streptomycin-Resistant Escherichia coli Inside Macrophages", *Antimicrobial Agents and Chemotherapy,* vol. 60, no. 7, pp. 4324-4332.

Ellington, A.D. & Szostak, J.W. 1990, "In vitro selection of RNA molecules that bind specific ligands", *Nature,* vol. 346, no. 6287, pp. 818-822.

Fan, J., de Jonge, B.L., MacCormack, K., Sriram, S., McLaughlin, R.E., Plant, H., Preston, M., Fleming, P.R., Albert, R., Foulk, M. & Mills, S.D. 2014, "A novel high-throughput cell-based assay aimed at identifying inhibitors of DNA metabolism in bacteria", *Antimicrobial Agents and Chemotherapy,* vol. 58, no. 12, pp. 7264-7272.

Farha, M.A. & Brown, E.D. 2010, "Chemical probes of Escherichia coli uncovered through chemical-chemical interaction profiling with compounds of known biological activity", *Chemistry & biology,* vol. 17, no. 8, pp. 852-862.

Farha, M.A., Czarny, T.L., Myers, C.L., Worrall, L.J., French, S., Conrady, D.G., Wang, Y., Oldfield, E., Strynadka, N.C. & Brown, E.D. 2015, "Antagonism screen for inhibitors of bacterial cell wall biogenesis uncovers an inhibitor of undecaprenyl diphosphate synthase", *Proceedings of the National Academy of Sciences of the United States of America,* vol. 112, no. 35, pp. 11048-11053.

Farhat, M.R., Shapiro, B.J., Kieser, K.J., Sultana, R., Jacobson, K.R., Victor, T.C., Warren, R.M., Streicher, E.M., Calver, A., Sloutsky, A., Kaur, D., Posey, J.E., Plikaytis, B., Oggioni, M.R., Gardy, J.L., Johnston, J.C., Rodrigues, M., Tang, P.K., Kato-Maeda, M., Borowsky, M.L., Muddukrishna, B., Kreiswirth, B.N., Kurepina, N., Galagan, J., Gagneux, S., Birren, B., Rubin, E.J., Lander, E.S., Sabeti, P.C. & Murray, M. 2013, "Genomic analysis identifies targets of convergent positive selection in drug-resistant Mycobacterium tuberculosis", *Nature genetics,* vol. 45, no. 10, pp. 1183-1189.

Frost, N.R., McKeague, M., Falcioni, D. & DeRosa, M.C. 2015, "An in solution assay for interrogation of affinity and rational minimer design for small molecule-binding aptamers", *The Analyst,* vol. 140, no. 19, pp. 6643-6651.

Gordon, S., Parish, T., Roberts, I.S. & Andrew, P.W. 1994, "The application of luciferase as a reporter of environmental regulation of gene expression in mycobacteria", *Letters in applied microbiology,* vol. 19, no. 5, pp. 336-340.

Gotrik, M., Sekhon, G., Saurabh, S., Nakamoto, M., Eisenstein, M. & Soh, H.T. 2018, "Direct Selection of Fluorescence-Enhancing RNA Aptamers", *Journal of the American Chemical Society,* vol. 140, no. 10, pp. 3583-3591.

Greco, W.R., Bravo, G. & Parsons, J.C. 1995, "The search for synergy: a critical review from a response surface perspective.", *Pharmacological reviews,* vol. 47, no. 2, pp. 331-385.

Hall, Z., Allan, E.L., van Schalkwyk, D.A., van Wyk, A. & Kaur, H. 2016, "Degradation of Artemisinin-Based Combination Therapies Under Tropical Conditions", *The American Journal of Tropical Medicine and Hygiene,* vol. 94, no. 5, pp. 993-1001.

Hansen, L.H. & Sorensen, S.J. 2000, "Detection and quantification of tetracyclines by whole cell biosensors", *FEMS microbiology letters,* vol. 190, no. 2, pp. 273-278.

Hauck, Y., Fabre, M., Vergnaud, G., Soler, C. & Pourcel, C. 2009, "Comparison of two commercial assays for the characterization of rpoB mutations in Mycobacterium tuberculosis and description of new mutations conferring weak resistance to rifampicin", *The Journal of antimicrobial chemotherapy,* vol. 64, no. 2, pp. 259-262.

Ho, N.T., Desai, D. & Zaman, M.H. 2015, "Rapid and specific drug quality testing assay for artemisinin and its derivatives using a luminescent reaction and novel microfluidic technology", *The American Journal of Tropical Medicine and Hygiene,* vol. 92, no. 6 Suppl, pp. 24-30.

Hoinka, J., Berezhnoy, A., Dao, P., Sauna, Z.E., Gilboa, E. & Przytycka, T.M. 2015, "Large scale analysis of the mutational landscape in HT-SELEX improves aptamer discovery", *Nucleic acids research,* vol. 43, no. 12, pp. 5699-5707.

Hong, H. & Park, W. 2014, "TetR repressor-based bioreporters for the detection of doxycycline using Escherichia coli and Acinetobacter oleivorans", *Applied Microbiology and Biotechnology,* vol. 98, no. 11, pp. 5039-5050.

Horsburgh, C.R.,Jr, Barry, C.E.,3rd & Lange, C. 2015, "Treatment of Tuberculosis", *The New England journal of medicine,* vol. 373, no. 22, pp. 2149-2160.

Ivask, A., Rolova, T. & Kahru, A. 2009, "A suite of recombinant luminescent bacterial strains for the quantification of bioavailable heavy metals and toxicity testing", *BMC biotechnology,* vol. 9, pp. 41-6750-9-41.

Jähnke, R. & Dwornik, K. 2018, *A concise quality control guide on essential drugs and other medicines: Supplement 2018 to Volume II on thin layer chromatography tests,* GPHF, Frankfurt am Main, Germany.

Jamieson, F.B., Guthrie, J.L., Neemuchwala, A., Lastovetska, O., Melano, R.G. & Mehaffy, C. 2014, "Profiling of rpoB mutations and MICs for rifampin and rifabutin in Mycobacterium tuberculosis", *Journal of clinical microbiology,* vol. 52, no. 6, pp. 2157-2162.

Jin, D.J. & Gross, C.A. 1988, "Mapping and sequencing of mutations in the Escherichia coli rpoB gene that lead to rifampicin resistance", *Journal of Molecular Biology,* vol. 202, no. 1, pp. 45-58.

Johnston, A. & Holt, D.W. 2014, "Substandard drugs: a potential crisis for public health.", *British journal of clinical pharmacology,* vol. 78, no. 2, pp. 218-243.

Kelesidis, T. & Falagas, M.E. 2015, "Substandard/counterfeit antimicrobial drugs", *Clinical microbiology reviews,* vol. 28, no. 2, pp. 443-464.

Kenyon, T.A., Kenyon, A.S., Kgarebe, B.V., Mothibedi, D., Binkin, N.J. & Layloff, T.P. 1999, "Detection of substandard fixed-dose combination tuberculosis drugs using thin-layer chromatography", *The international journal of tuberculosis and lung disease : the official journal of the International Union against Tuberculosis and Lung Disease,* vol. 3, no. 11, pp. 347-350.

Kim, Y.S., Kim, J.H., Kim, I.A., Lee, S.J., Jurng, J. & Gu, M.B. 2010, "A novel colorimetric aptasensor using gold nanoparticle for a highly sensitive and specific detection of oxytetracycline", *Biosensors & bioelectronics,* vol. 26, no. 4, pp. 1644-1649.

Kishony, R. & Leibler, S. 2003, "Environmental stresses can alleviate the average deleterious effect of mutations", *Journal of biology,* vol. 2, no. 2, pp. 14-4924-2-14. Epub 2003 May 29.

Koch, A., Mizrahi, V. & Warner, D.F. 2014, "The impact of drug resistance on Mycobacterium tuberculosis physiology: what can we learn from rifampicin?", *Emerging microbes & infections,* vol. 3, no. 3, pp. e17.

Kohanski, M.A., DePristo, M.A. & Collins, J.J. 2010, "Sublethal antibiotic treatment leads to multidrug resistance via radical-induced mutagenesis.", *Molecular cell,* vol. 37, no. 3, pp. 311-320.

Konrad, P. & Stenberg, P. 1988, "Rifampicin quinone is an immunosuppressant, but not rifampicin itself", *Clinical immunology and immunopathology,* vol. 46, no. 1, pp. 162-166.

Kruse, A.J., Peerdeman, S.M., Bet, P.M. & Debets-Ossenkopp, Y.J. 2006, "Successful treatment with linezolid and rifampicin of meningitis due to methicillin-resistant Staphylococcus epidermidis refractory to vancomycin treatment", *European journal of clinical microbiology & infectious diseases : official publication of the European Society of Clinical Microbiology,* vol. 25, no. 2, pp. 135-137.

Laserson, K.F., Kenyon, A.S., Kenyon, T.A., Layloff, T. & Binkin, N.J. 2001, "Substandard tuberculosis drugs on the global market and their simple detection", *The international journal of tuberculosis and lung disease : the official journal of the International Union against Tuberculosis and Lung Disease,* vol. 5, no. 5, pp. 448-454.

Lee, H., Popodi, E., Tang, H. & Foster, P.L. 2012, "Rate and molecular spectrum of spontaneous mutations in the bacterium Escherichia coli as determined by whole-genome sequencing", *Proceedings of the National Academy of Sciences of the United States of America,* vol. 109, no. 41, pp. E2774-83.

Lehár, J., Zimmermann, G.R., Krueger, A.S., Molnar, R.A., Ledell, J.T., Heilbut, A.M., Short, G.F., Giusti, L.C., Nolan, G.P., Magid, O.A., Lee, M.S., Borisy, A.A., Stockwell, B.R. & Keith, C.T. 2007, "Chemical combination effects predict connectivity in biological systems.", *Molecular systems biology,* vol. 3, pp. 80.

Levine, H.A. & Nilsen-Hamilton, M. 2007, "A mathematical analysis of SELEX", *Computational biology and chemistry,* vol. 31, no. 1, pp. 11-35.

Levy, S.B. 2008, "Genome size and antibiotic resistance", *Antimicrobial Agents and Chemotherapy,* vol. 52, no. 7, pp. 2696-07.

Liu, J., Sun, J., Zhang, W., Gao, K. & He, Z. 2008, "HPLC determination of rifampicin and related compounds in pharmaceuticals using monolithic column", *Journal of pharmaceutical and biomedical analysis,* vol. 46, no. 2, pp. 405-409.

Mariappan, T.T., Jindal, K.C. & Singh, S. 2004, "Overestimation of rifampicin during colorimetric analysis of anti-tuberculosis products containing isoniazid due to formation of isonicotinyl hydrazone", *Journal of pharmaceutical and biomedical analysis,* vol. 36, no. 4, pp. 905-908.

Mariner, K.R., Ooi, N., Roebuck, D., O'Neill, A.J. & Chopra, I. 2011, "Further characterization of Bacillus subtilis antibiotic biosensors and their use for antibacterial mode-of-action studies", *Antimicrobial Agents and Chemotherapy,* vol. 55, no. 4, pp. 1784-1786.

McCammon, M.T., Gillette, J.S., Thomas, D.P., Ramaswamy, S.V., Graviss, E.A., Kreiswirth, B.N., Vijg, J. & Quitugua, T.N. 2005, "Detection of rpoB mutations associated with rifampin resistance in Mycobacterium tuberculosis using denaturing gradient gel electrophoresis", *Antimicrobial Agents and Chemotherapy,* vol. 49, no. 6, pp. 2200-2209.

Mikalauskas, A., Parkins, M.D. & Poole, K. 2017, "Rifampicin potentiation of aminoglycoside activity against cystic fibrosis isolates of Pseudomonas aeruginosa", *The Journal of antimicrobial chemotherapy,* vol. 72, no. 12, pp. 3349-3352.

Mohan, B., Sharda, N. & Singh, S. 2003, "Evaluation of the recently reported USP gradient HPLC method for analysis of anti-tuberculosis drugs for its ability to

resolve degradation products of rifampicin", *Journal of pharmaceutical and biomedical analysis,* vol. 31, no. 3, pp. 607-612.

Nayyar, G.M.L., Breman, J.G. & Herrington, J.E. 2015, "The global pandemic of falsified medicines: laboratory and field innovations and policy perspectives", *The American Journal of Tropical Medicine and Hygiene,* vol. 92, no. 6 Suppl, pp. 2-7.

Nayyar, G.M.L., Breman, J.G., Newton, P.N. & Herrington, J. 2012, "Poor-quality antimalarial drugs in southeast Asia and sub-Saharan Africa.", *The Lancet.Infectious diseases,* vol. 12, no. 6, pp. 488-496.

Newton, P.N., Green, M.D. & Fernandez, F.M. 2010, "Impact of poor-quality medicines in the 'developing' world", *Trends in pharmacological sciences,* vol. 31, no. 3, pp. 99-101.

Nguyen, V.T., Kwon, Y.S., Kim, J.H. & Gu, M.B. 2014, "Multiple GO-SELEX for efficient screening of flexible aptamers", *Chemical communications (Cambridge, England),* vol. 50, no. 72, pp. 10513-10516.

Norval, P.Y., Blomberg, B., Kitler, M.E., Dye, C. & Spinaci, S. 1999, "Estimate of the global market for rifampicin-containing fixed-dose combination tablets", *The international journal of tuberculosis and lung disease : the official journal of the International Union against Tuberculosis and Lung Disease,* vol. 3, no. 11, pp. 292-300.

Okeke, I.N., Lamikanra, A. & Edelman, R. 1999, "Socioeconomic and behavioral factors leading to acquired bacterial resistance to antibiotics in developing countries", *Emerging infectious diseases,* vol. 5, no. 1, pp. 18-27.

Oz, T., Guvenek, A., Yildiz, S., Karaboga, E., Tamer, Y.T., Mumcuyan, N., Ozan, V.B., Senturk, G.H., Cokol, M., Yeh, P. & Toprak, E. 2014, "Strength of selection pressure is an important parameter contributing to the complexity of antibiotic resistance evolution.", *Molecular biology and evolution,* vol. 31, no. 9, pp. 2387-2401.

Pang, Y., Lu, J., Wang, Y., Song, Y., Wang, S. & Zhao, Y. 2013, "Study of the rifampin monoresistance mechanism in Mycobacterium tuberculosis", *Antimicrobial Agents and Chemotherapy,* vol. 57, no. 2, pp. 893-900.

Pecoul, B., Chirac, P., Trouiller, P. & Pinel, J. 1999, "Access to essential drugs in poor countries: a lost battle?", *JAMA,* vol. 281, no. 4, pp. 361-367.

Pincock, S. 2003, "WHO tries to tackle problem of counterfeit medicines in Asia.", *British Medical Journal,* vol. 327, no. 7424, pp. 1126.

Piriou, A., Jacqueson, A., Warnet, J.M. & Claude, J.R. 1983, "Enzyme induction with high doses of rifampicin in Wistar rats", *Toxicology letters,* vol. 17, no. 3-4, pp. 301-306.

Prankerd, Richard J., Walters, John M., Parnes,Joel H., 1992, "Kinetics for degradation of rifampicin, an azomethine-containing drug which exhibits reversible hydrolysis in acidic solutions", *International Journal of Pharmaceutics,* vol. 78, no. 1, pp. 59-67.

Pressman, A., Moretti, J.E., Campbell, G.W., Muller, U.F. & Chen, I.A. 2017, "Analysis of in vitro evolution reveals the underlying distribution of catalytic activity among random sequences", *Nucleic acids research,* vol. 45, no. 14, pp. 8167-8179.

Projan, S.J. 2007, "(Genome) size matters", *Antimicrobial Agents and Chemotherapy,* vol. 51, no. 4, pp. 1133-1134.

Qi, Y., Xiu, F.R., Zheng, M. & Li, B. 2016, "A simple and rapid chemiluminescence aptasensor for acetamiprid in contaminated samples: Sensitivity, selectivity and mechanism", *Biosensors & bioelectronics,* vol. 83, pp. 243-249.

Ramachandran, G., Chandrasekaran, V., Hemanth Kumar, A.K., Dewan, P., Swaminathan, S. & Thomas, A. 2013, "Estimation of content of anti-TB drugs supplied at centres of the Revised National TB Control Programme in Tamil Nadu, India", *Tropical medicine & international health : TM & IH,* vol. 18, no. 9, pp. 1141-1144.

Reisbig, Richard R., Woody, A. Young M., Woody,Robert W., 1982, "Rifampicin as a spectroscopic probe of the mechanism of RNA polymerase from *E. coli*", *Biochemistry Biochemistry,* vol. 21, no. 1, pp. 196-200.

Risha, P.G., Msuya, Z., Clark, M., Johnson, K., Ndomondo-Sigonda, M. & Layloff, T. 2008, "The use of Minilabs to improve the testing capacity of regulatory authorities in resource limited settings: Tanzanian experience", *Health policy (Amsterdam, Netherlands),* vol. 87, no. 2, pp. 217-222.

Riska, P.F., Su, Y., Bardarov, S., Freundlich, L., Sarkis, G., Hatfull, G., Carriere, C., Kumar, V., Chan, J. & Jacobs, W.R.,Jr 1999, "Rapid film-based determination of antibiotic susceptibilities of Mycobacterium tuberculosis strains by using a luciferase reporter phage and the Bronx Box", *Journal of clinical microbiology,* vol. 37, no. 4, pp. 1144-1149.

Rock, J.M., Lang, U.F., Chase, M.R., Ford, C.B., Gerrick, E.R., Gawande, R., Coscolla, M., Gagneux, S., Fortune, S.M. & Lamers, M.H. 2015, "DNA replication fidelity in

Mycobacterium tuberculosis is mediated by an ancestral prokaryotic proofreader", *Nature genetics,* vol. 47, no. 6, pp. 677-681.

Roger, B. & Boateng, K. 2007, "Bad medicine in the market", *World hospitals and health services : the official journal of the International Hospital Federation,* vol. 43, no. 3, pp. 17-21.

Salem, A.A., Mossa, H.A. & Barsoum, B.N. 2005, "Quantitative determinations of levofloxacin and rifampicin in pharmaceutical and urine samples using nuclear magnetic resonance spectroscopy", *Spectrochimica acta.Part A, Molecular and biomolecular spectroscopy,* vol. 62, no. 1-3, pp. 466-472.

Santos, L., Medeiros, M.A., Santos, S., Costa, M.C., Tavares, R. & Curto, M.J.M. 2001, *NMR studies of some rifamycins*.

Sassanfar, M. & Szostak, J.W. 1993, "An RNA motif that binds ATP", *Nature,* vol. 364, no. 6437, pp. 550-553.

Seo, Y., Nilsen-Hamilton, M. & Levine, H.A. 2014, "A computational study of alternate SELEX.", *Bulletin of mathematical biology,* vol. 76, no. 7, pp. 1455-1521.

Shakoor, O., Taylor, R.B. & Behrens, R.H. 1997, "Assessment of the incidence of substandard drugs in developing countries", *Tropical medicine & international health : TM & IH,* vol. 2, no. 9, pp. 839-845.

Shewiyo, D.H., Kaale, E., Risha, P.G., Dejaegher, B., Smeyers-Verbeke, J. & Vander Heyden, Y. 2012, "Optimization of a reversed-phase-high-performance thin-layer chromatography method for the separation of isoniazid, ethambutol, rifampicin and pyrazinamide in fixed-dose combination antituberculosis tablets", *Journal of chromatography.A,* vol. 1260, pp. 232-238.

Shi, F., Li, X., Pan, H. & Ding, L. 2017, "NQO1 and CYP450 reductase decrease the systemic exposure of rifampicin-quinone and mediate its redox cycle in rats", *Journal of pharmaceutical and biomedical analysis,* vol. 132, pp. 17-23.

Shishoo, C.J., Shah, S.A., Rathod, I.S., Savale, S.S. & Vora, M.J. 2001, "Impaired bioavailability of rifampicin in presence of isoniazid from fixed dose combination (FDC) formulation", *International journal of pharmaceutics,* vol. 228, no. 1-2, pp. 53-67.

Singh, S., Mariappan, T.T., Sharda, N.,Singh, B., 2000, "Degradation of Rifampicin, Isoniazid and Pyrazinamide from Prepared Mixtures and Marketed Single and

Combination Products Under Acid Conditions", *Pharmacy and Pharmacology Communications Pharmacy and Pharmacology Communications,* vol. 6, no. 11, pp. 491-494.

Siu, G.K., Zhang, Y., Lau, T.C., Lau, R.W., Ho, P.L., Yew, W.W., Tsui, S.K., Cheng, V.C., Yuen, K.Y. & Yam, W.C. 2011, "Mutations outside the rifampicin resistance-determining region associated with rifampicin resistance in Mycobacterium tuberculosis", *The Journal of antimicrobial chemotherapy,* vol. 66, no. 4, pp. 730-733.

Smirnov, I. & Shafer, R.H. 2000, "Effect of loop sequence and size on DNA aptamer stability", *Biochemistry,* vol. 39, no. 6, pp. 1462-1468.

Spill, F., Weinstein, Z.B., Irani Shemirani, A., Ho, N., Desai, D. & Zaman, M.H. 2016, "Controlling uncertainty in aptamer selection", *Proceedings of the National Academy of Sciences of the United States of America,* vol. 113, no. 43, pp. 12076-12081.

Stoltenburg, R., Nikolaus, N. & Strehlitz, B. 2012, "Capture-SELEX: Selection of DNA Aptamers for Aminoglycoside Antibiotics", *Journal of analytical methods in chemistry,* vol. 2012, pp. 415697.

Suarez, J., Ranguelova, K., Jarzecki, A.A., Manzerova, J., Krymov, V., Zhao, X., Yu, S., Metlitsky, L., Gerfen, G.J. & Magliozzo, R.S. 2009, "An oxyferrous heme/protein-based radical intermediate is catalytically competent in the catalase reaction of Mycobacterium tuberculosis catalase-peroxidase (KatG)", *The Journal of biological chemistry,* vol. 284, no. 11, pp. 7017-7029.

Tan, Y., Hu, Z., Zhao, Y., Cai, X., Luo, C., Zou, C. & Liu, X. 2012, "The beginning of the rpoB gene in addition to the rifampin resistance determination region might be needed for identifying rifampin/rifabutin cross-resistance in multidrug-resistant Mycobacterium tuberculosis isolates from Southern China", *Journal of clinical microbiology,* vol. 50, no. 1, pp. 81-85.

Taylor, R.B., Shakoor, O., Behrens, R.H., Everard, M., Low, A.S., Wangboonskul, J., Reid, R.G. & Kolawole, J.A. 2001, "Pharmacopoeial quality of drugs supplied by Nigerian pharmacies", *Lancet (London, England),* vol. 357, no. 9272, pp. 1933-1936.

Tuerk, C., MacDougal, S. & Gold, L. 1992, "RNA pseudoknots that inhibit human immunodeficiency virus type 1 reverse transcriptase", *Proceedings of the National Academy of Sciences of the United States of America,* vol. 89, no. 15, pp. 6988-6992.

Urban, A., Eckermann, S., Fast, B., Metzger, S., Gehling, M., Ziegelbauer, K., Rubsamen-Waigmann, H. & Freiberg, C. 2007, "Novel whole-cell antibiotic biosensors for compound discovery", *Applied and Environmental Microbiology,* vol. 73, no. 20, pp. 6436-6443.

van Crevel, R., Nelwan, R.H., Borst, F., Sahiratmadja, E., Cox, J., van der Meij, W., de Graaff, M., Alisjahbana, B., de Lange, W.C. & Burger, D. 2004, "Bioavailability of rifampicin in Indonesian subjects: a comparison of different local drug manufacturers", *The international journal of tuberculosis and lung disease : the official journal of the International Union against Tuberculosis and Lung Disease,* vol. 8, no. 4, pp. 500-503.

van den Boogaard, J., Kibiki, G.S., Kisanga, E.R., Boeree, M.J. & Aarnoutse, R.E. 2009, "New drugs against tuberculosis: problems, progress, and evaluation of agents in clinical development", *Antimicrobial Agents and Chemotherapy,* vol. 53, no. 3, pp. 849-862.

van der Werf, M.J., Langendam, M.W., Huitric, E. & Manissero, D. 2012, "Multidrug resistance after inappropriate tuberculosis treatment: a meta-analysis", *The European respiratory journal,* vol. 39, no. 6, pp. 1511-1519.

Visser, B.J., Meerveld-Gerrits, J., Kroon, D., Mougoula, J., Vingerling, R., Bache, E., Boersma, J., van Vugt, M., Agnandji, S.T., Kaur, H. & Grobusch, M.P. 2015, "Assessing the quality of anti-malarial drugs from Gabonese pharmacies using the MiniLab(R): a field study", *Malaria journal,* vol. 14, pp. 273-015-0795-z.

Wang, J., Rudzinski, J.F., Gong, Q., Soh, H.T. & Atzberger, P.J. 2012, "Influence of target concentration and background binding on in vitro selection of affinity reagents", *PloS one,* vol. 7, no. 8, pp. e43940.

Weaver, A.A., Reiser, H., Barstis, T., Benvenuti, M., Ghosh, D., Hunckler, M., Joy, B., Koenig, L., Raddell, K. & Lieberman, M. 2013, "Paper analytical devices for fast field screening of beta lactam antibiotics and antituberculosis pharmaceuticals", *Analytical Chemistry,* vol. 85, no. 13, pp. 6453-6460.

Webb, A.J., Kelwick, R. & Freemont, P.S. 2017, "Opportunities for applying whole-cell bioreporters towards parasite detection", *Microbial biotechnology,* vol. 10, no. 2, pp. 244-249.

Weinstein, Z.B. & Zaman, M.H. 2017, "Quantitative bioassay to identify antimicrobial drugs through drug interaction fingerprint analysis", *Scientific reports,* vol. 7, pp. 42644.

Williams, D.L., Spring, L., Collins, L., Miller, L.P., Heifets, L.B., Gangadharam, P.R. & Gillis, T.P. 1998, "Contribution of rpoB mutations to development of rifamycin cross-resistance in Mycobacterium tuberculosis", *Antimicrobial Agents and Chemotherapy,* vol. 42, no. 7, pp. 1853-1857.

Williams, K.P., Liu, X.H., Schumacher, T.N., Lin, H.Y., Ausiello, D.A., Kim, P.S. & Bartel, D.P. 1997, "Bioactive and nuclease-resistant L-DNA ligand of vasopressin", *Proceedings of the National Academy of Sciences of the United States of America,* vol. 94, no. 21, pp. 11285-11290.

World Health Organization, 2015, *Global tuberculosis report 2015*.

World Health Organization, 2014, *Companion handbook to the WHO guidelines for the programmatic management of drug-resistant tuberculosis.*

World Health Organization, 2012, *The evolving threat of antimicrobial resistance: options for action*.

World Health Organization, 2011, *Survey of the quality of anti-tuberculosis medicines circulating in selected newly independent states of the former Soviet Union*.

World Health Organization, 2011, *Survey of the quality of selected antimalarial medicines circulating in six countries of sub-Saharan Africa*.

World Health Organization, 2007, "Rifampicin, isoniazid and pyrazinamide dispersible tablets", *WHO drug information.* vol. 21, no. 3, pp. 232.

World Health Organization, 1999, "Counterfeit Drugs: Guidelines for the development of measures to combat counterfeit drugs".

Xu, M., Zhou, Y.N., Goldstein, B.P. & Jin, D.J. 2005, "Cross-resistance of Escherichia coli RNA polymerases conferring rifampin resistance to different antibiotics", *Journal of Bacteriology,* vol. 187, no. 8, pp. 2783-2792.

Yeh, P., Tschumi, A.I. & Kishony, R. 2006, "Functional classification of drugs by properties of their pairwise interactions.", *Nature genetics,* vol. 38, no. 4, pp. 489-494.

Zenkin, N., Kulbachinskiy, A., Bass, I. & Nikiforov, V. 2005, "Different rifampin sensitivities of Escherichia coli and Mycobacterium tuberculosis RNA polymerases are not explained by the difference in the beta-subunit rifampin regions I and II", *Antimicrobial Agents and Chemotherapy,* vol. 49, no. 4, pp. 1587-1590.

Zhao, W., Sachsenmeier, K., Zhang, L., Sult, E., Hollingsworth, R.E. & Yang, H. 2014, "A New Bliss Independence Model to Analyze Drug Combination Data.", *Journal of biomolecular screening,* vol. 19, no. 5, pp. 817-821.

Zhou, Q., Xia, X., Luo, Z., Liang, H. & Shakhnovich, E. 2015, "Searching the Sequence Space for Potent Aptamers Using SELEX in Silico", *Journal of chemical theory and computation,* vol. 11, no. 12, pp. 5939-5946.

Zimmermann, G.R., Lehar, J. & Keith, C.T. 2007, "Multi-target therapeutics: when the whole is greater than the sum of the parts", *Drug discovery today,* vol. 12, no. 1-2, pp. 34-42.

CURRICULUM VITAE